GRADUATE AERONAUTICAL LABORATORIES
CALIFORNIA INSTITUTE OF TECHNOLOGY

1985 AFOSR/ONR CONTRACTORS MEETING

ON TURBULENT COMBUSTION

23-25 JULY 1985

Firestone Flight Sciences Laboratory

Guggenheim Aeronautical Laboratory

Karman Laboratory of Fluid Mechanics and Jet Propulsion

Pasadena

Unclassified

SECURITY CLASSIFICATION OF THIS PAGE

REPORT DOCUMENTATION PAGE

1a. REPORT SECURITY CLASSIFICATION	1b. RESTRICTIVE MARKINGS
2a. SECURITY CLASSIFICATION AUTHORITY	3. DISTRIBUTION/AVAILABILITY OF REPORT
2b. DECLASSIFICATION/DOWNGRADING SCHEDULE	Unlimited
4. PERFORMING ORGANIZATION REPORT NUMBER(S)	5. MONITORING ORGANIZATION REPORT NUMBER(S)
6a. NAME OF PERFORMING ORGANIZATION: California Institute of Technology; 6b. OFFICE SYMBOL (If applicable)	7a. NAME OF MONITORING ORGANIZATION: AFOSR
6c. ADDRESS (City, State and ZIP Code): 1201 E. California Blvd. Pasadena, CA 91125	7b. ADDRESS (City, State and ZIP Code)
8a. NAME OF FUNDING/SPONSORING ORGANIZATION: AFOSR; 8b. OFFICE SYMBOL (If applicable)	9. PROCUREMENT INSTRUMENT IDENTIFICATION NUMBER
8c. ADDRESS (City, State and ZIP Code)	10. SOURCE OF FUNDING NOS.

PROGRAM ELEMENT NO.	PROJECT NO.	TASK NO.	WORK UNIT NO.
ONR			

11. TITLE (Include Security Classification): Abstracts: 1985 AFOSR/ONR Contractors Meeting on Turbulent Combustion

12. PERSONAL AUTHOR(S): Editor: Paul E. Dimotakis

13a. TYPE OF REPORT	13b. TIME COVERED FROM ____ TO ____	14. DATE OF REPORT (Yr., Mo., Day)	15. PAGE COUNT
		23 July 1985	151

16. SUPPLEMENTARY NOTATION

17. COSATI CODES			18. SUBJECT TERMS (Continue on reverse if necessary and identify by block number)
FIELD	GROUP	SUB. GR.	

19. ABSTRACT (Continue on reverse if necessary and identify by block number)

This report consists of a collection of expanded abstracts of the numerous research progress reports given by AFOSR/ONR supported contractors and grantees on the Air Force and Navy basic research program on Turbulent Combustion and of invited papers from other governmental agencies and contractors.

20. DISTRIBUTION/AVAILABILITY OF ABSTRACT	21. ABSTRACT SECURITY CLASSIFICATION
UNCLASSIFIED/UNLIMITED ☐ SAME AS RPT. ☐ DTIC USERS ☐	

22a. NAME OF RESPONSIBLE INDIVIDUAL	22b. TELEPHONE NUMBER (Include Area Code)	22c. OFFICE SYMBOL

DD FORM 1473, 83 APR EDITION OF 1 JAN 73 IS OBSOLETE.

Unclassified

SECURITY CLASSIFICATION OF THIS PAGE

AGENDA

1985 AFOSR/ONR CONTRACTORS MEETING ON TURBULENT COMBUSTION

23-25 July 1985

Baxter Lecture Hall
California Institute of Technology
Pasadena, CA

Monday, 22 July

5:00 - 7:00 PM	Early Registration - Pasadena Holiday Inn

Tuesday, 23 July

8:00 - 8:50 AM	Official Registration - Baxter Lecture Hall Lounge
8:50 - 9:00	Opening Remarks and Welcome J. M. TISHKOFF AFOSR Program Manager and Meeting Coordinator
Session Topic: Chairman:	Experiments L. E. WILSON, AFWL
9:00 - 9:45 AM	Chemical Reactions in Turbulent Mixing Flows H. W. LIEPMANN, J. E. BROADWELL and P. E. DIMOTAKIS California Institute of Technology (AFOSR)
9:45 - 10:15	Structure and Mixing in Turbulent Shear Flows A. ROSHKO California Institute of Technology (ONR)
10:15 - 10:45	BREAK
10:45 - 11:15	An Investigation of Flow Structure, Mixing and Chemical Reaction in Combusting Turbulent Flows C. T. BOWMAN and B. J. CANTWELL Stanford University (AFOSR)
11:15 - 11:45	Chemical Laser Research L. E. WILSON AFWL/ARDC
11:45 - 12:05 PM	Turbulence Scales and Their Effect on Turbulent Premixed Flame Structure D. A. SANTAVICCA Pennsylvania State University (AFOSR)
12:05 - 1:15	LUNCH

Session Topic:	Numerical Simulations
Chairman:	W. M. ROQUEMORE, AFWAL
1:15 - 1:45	Direct Numerical Simulation of an Unpremixed Turbulent Jet Flame W-H. JOU, R. W. METCALFE and P. GIVI Flow Industries (AFOSR)
1:45 - 2:30	Numerical Simulations of Transition from Laminar to Turbulent Flows E. S. ORAN, J. P. BORIS, J. H. GARDNER and K. KAILASANATH Naval Research Laboratory
2:30 - 3:00	Time-Dependent Simulation of Turbulent Combustion H. R. BAUM and R. G. REHM National Bureau of Standards (AFOSR)
3:00 - 3:30	BREAK
3:30 - 4:00	Numerical Experiments on Turbulent Mixing S. B. POPE Cornell University (AFOSR)
4:00 - 4:30	Numerical Simulation of Turbulent Flames Using Vortex Methods A. F. GHONIEM Massachusetts Institute of Technology (AFOSR)
4:30 - 5:00	Evaluation of Experimental Data for Validation of Numerical Predictions for Turbulent Combustion W. C. STRAHLE Georgia Institute of Technology (AFOSR)
5:00	ADJOURN

Wednesday, 24 July

Session Topic:	Experiments and Predictions of Turbulence and Combustion Instability
Chairman:	M. K. ELLINGSWORTH, ONR
8:30 - 9:15 AM	Research on Mechanisms of Exciting Pressure Oscillations in Ramjet Engines F. E. C. CULICK, F. E. MARBLE and E. E. ZUKOSKI California Institute of Technology (AFOSR)

9:15 - 9:45	Numerical Simulations of Shear Layer/Acoustic Wave Interactions in a Ramjet Combustor W-H. JOU and S. MENON Flow Industries (ONR)
9:45 - 10:15	BREAK
10:15 - 10:45	Experimental and Numerical Characterization of Ramjet Combustor Flowfields A. S. NEJAD, R. R. CRAIG, P. L. BUCKLEY, F. D. STULL and S. P. VANKA AFWAL/PORT
10:45 - 11:15	Aerodynamic and Kinetic Processes in Flames C. K. LAW University of California, Davis (AFOSR)
11:15 - 11:45	Combustion Research Using Laser Sheet Lighting, AFOSR Summer Faculty Research Program at APL R. S. TANKIN, Northwestern University; H. H. CHIU, University of Chicago; S. A. LOTTES, University of Chicago; and W. M. ROQUEMORE, AFWAL/POSF
11:45 - 1:00 PM	LUNCH

Government Presentations

1:00 - 1:15	M. J. SALKIND, AFOSR
1:15 - 1:45	AFOSR Sponsored Research in Airbreathing Combustion J. M. TISHKOFF, AFOSR
1:45 - 2:15	BREAK
2:15 - 2:45	R. E. WHITEHEAD, ONR
2:45 - 3:15	Combustion Research for Aeropropulsion Systems E. J. MULARZ, NASA Lewis Research Center
3:15 - 3:45	Turbulent Combustion Research at Sandia National Laboratories S. C. JOHNSTON, Sandia National Laboratories
3:15 - 4:30	BUSINESS MEETING - AFOSR CONTRACTORS ONLY
6:30 - 7:30	NO HOST BAR
7:30 PM	BANQUET Invited Speaker: H. W. LIEPMANN

Thursday, 25 July

Session Topic:	Experiments
Chairman:	F. D. STULL, AFWAL
8:30 - 9:00 AM	Research in Turbulent and Unsteady Flows J. M. MCMICHAEL AFOSR
9:00 - 9:30	Carbon Monoxide and Turbulence-Chemistry Interactions: Blow Off and Extinction of Turbulent Jet Diffusion Flames M. C. DRAKE and S. M. CORREA G. E. Corporate R & D Center (AFOSR)
9:30 - 10:00	Chemically Reacting Turbulent Flow W. M. PITTS and T. KASHIWAGI NBS (AFOSR)
10:00 - 10:30	BREAK
10:30 - 11:00	Characterization of Density Fluctuations in a Premixed Turbulent V-Shaped Flame M. NAMAZIAN, I. G. SHEPHERD and L. TALBOT University of California, Berkeley (AFOSR)
11:00 - 11:30	Turbulence-Combustion Interactions -- Theory and Experiments T-Y. TOONG Massachusetts Institute of Technology (AFOSR)
11:30 - 12:00	Laser Tomography for Investigation of Turbulent Flames H. G. SEMERJIAN and S. R. RAY NBS (AFOSR)
12:00 - 1:30 PM	LUNCH
1:30 - 3:30	Caltech Laboratory Facilities Tour
3:30	MEETING ADJOURNMENT

LIST OF ABSTRACTS

1985 AFOSR/ONR CONTRACTORS MEETING ON TURBULENT COMBUSTION

23-25 July 1985

Baxter Lecture Hall
California Institute of Technology
Pasadena, CA

Page Abstract

Page Abstract

TITLE: TIME DEPENDENT SIMULATION OF TURBULENT COMBUSTION

AFOSR Grant/Contract No. AFOSR-ISSA-85-0026

Principal Investigator(s): Howard R. Baum and Ronald G. Rehm

National Bureau of Standards
Gaithersburg, MD 20899

SUMMARY/OVERVIEW:

A mathematical model of the transient diffusion controlled combustion of a gaseous blob of fuel imbedded in an oxidizing atmosphere is presented. It is intended ultimately as a computational "molecule" to be imbedded in direct simulations of larger scale reacting flows. The model consists of an interacting three-dimensional strain vortex field which exactly satisfies the Navier-Stokes equations, an analytically determined Lagrangian representation of the mixing process, and reaction-diffusion equations in Lagrangian coordinates. Results are shown for the flow pattern, mixing, and a simple model of bulk aerosol coagulation. The combination of geometry-specific large scale simulations and local solutions to idealized small scale combustion problems whose parameters are determined by requiring consistency between scales could lead to global turbulent combustion calculations based solely on the equations governing the physical processes of interest.

TECHNICAL DISCUSSION

It is assumed that a three dimensional time dependent simulation resolving the largest scales of the relevant phenomena is being performed. At the resolution limits of this computation, in a frame of reference moving with the large scale flow, a "local ambient state" can be determined. This state is characterized by a vorticity and strain, together with values for temperature, density, and oxidizer mass fraction. If the dimensions of the fuel blob are below the resolution limit, then its initial state is prescribed. If it is macroscopically resolveable, then the concentration of fuel is also part of the "local ambient state." In this latter case the fuel-oxidizer material interface is taken to be planar initially. The objective of the calculation is to determine the local rate of heat release and consumption of fuel as a function of the local ambient state parameters and time.

The first step in the solution process is to obtain a tractable representation of the local velocity field consistent with prescribed strain and initial vorticity fields. An exact solution to the Navier-Stokes equations consistent with these objectives is shown in Fig. 1. It includes local effects of vortex stretching, advection, and diffusion in a transition from a delta function initial distribution to the final steady state as a Burgers vortex. It is in fact the Greens function for any prescribed symmetric vorticity distribution. The evolution of any such distribution would also satisfy the Navier-Stokes equations for a constant property fluid.

The next step is to use this solution to generate an analytic representation of the Lagrangian coordinates of this flow field. The existence of such a

representation allows the transient "engulfing" and inviscid mixing of reactants to be readily calculated for any initially simple spatial configuration of fuel and oxidizer. Figures 2 thru 5 show the evolution of the material coordinates of two species initially separated by a planar interface asymmetrically placed with respect to the center of the initial ring of concentrated vorticity described by the delta function distribution. The Lagrangian coordinates are also a convenient framework for the analysis of both instantaneous and time averaged calculations of bulk reactions. A practical example to be discussed briefly is smoke aerosol coagulation, a process for which the neglect of molecular diffusion between smoke aerosol and clear gas is a good approximation.

Finally, the diffusion-controlled reaction can be formulated in this coordinate system without loss of accuracy. The next phase of the investigation will focus on analyzing and solving the equations for the Schvab-Zeldovich variables describing the combustion processes. This analysis will be carried out for a variable property fluid in three dimensions. The three dimensional aspect of the transformation is a straight forward modification of the present methodology, since the basic solutions define a three-dimensional flow field. Thus, efforts will be concentrated on generating a sufficiently wide class of results for the reaction-diffusion equations to permit a set of approximate recipes for rates of heat release to be obtained.

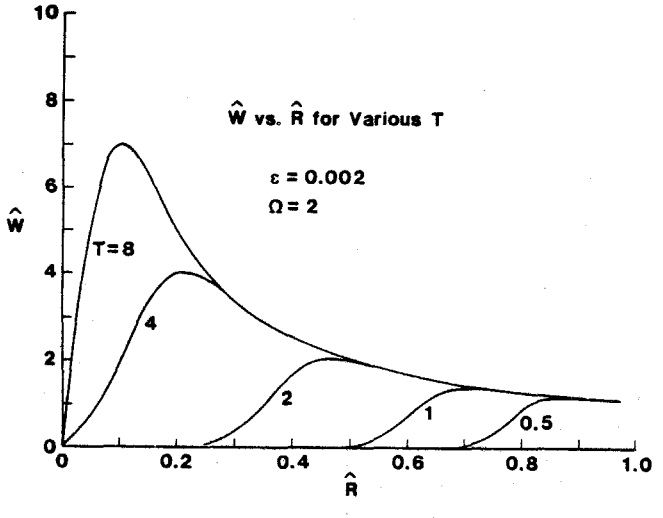

Fig. 1 - Swirl component of velocity profiles showing vortex evolution; local Reynolds number 500.

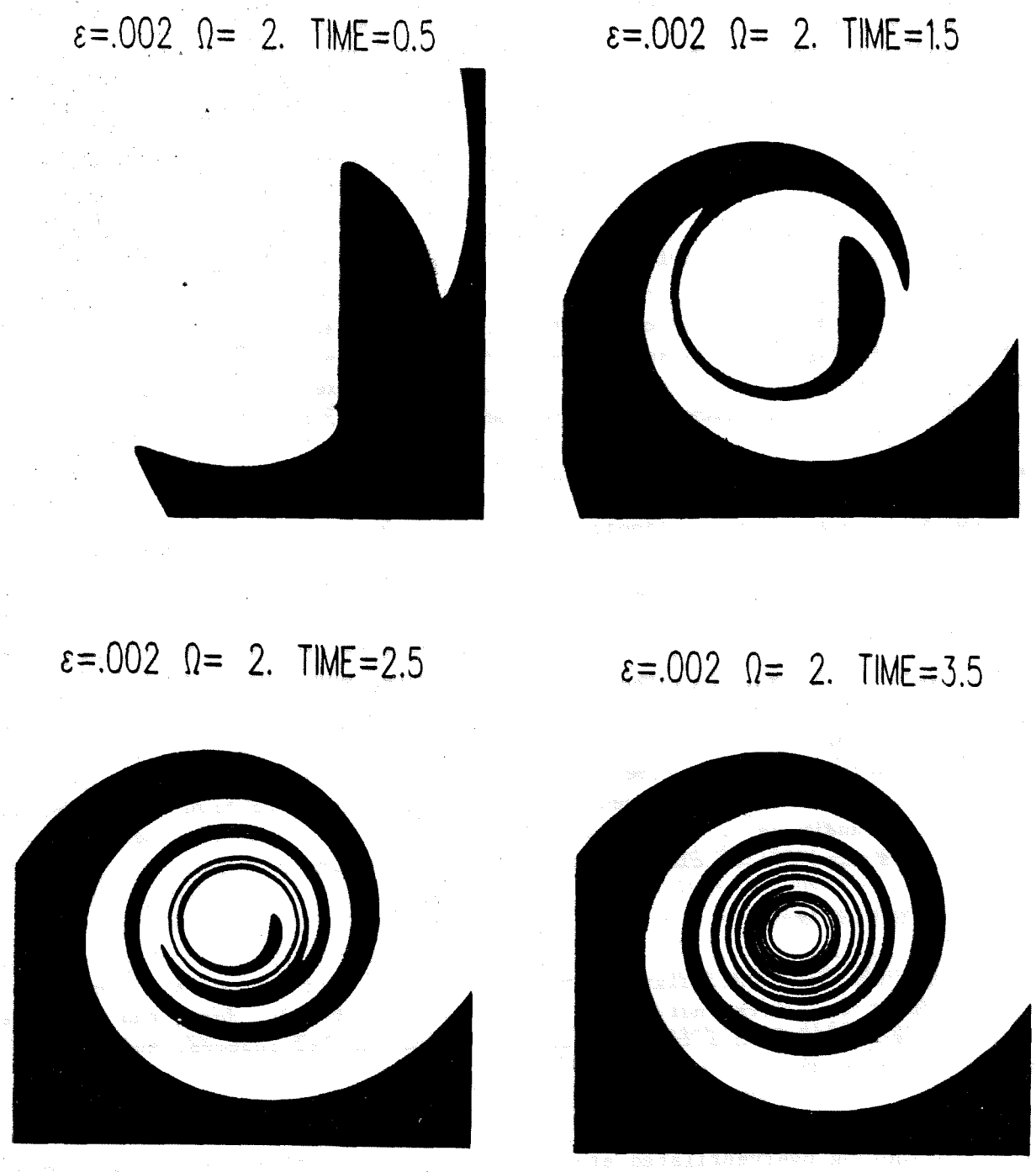

Fig. 2-5 - Deformation of initially plane material surfaces displaced one half initial vortex radius from symmetry plane.

FUEL ADDITIVE EFFECTS IN SOOTING FLAMES

(AFOSR Contract No. F49620-83-C-0113)*

Principal Investigator: P. A. Bonczyk

United Technologies Research Center
East Hartford, CT 06108

SUMMARY/OVERVIEW

Soot is, in almost every circumstance, an undesirable product of combustion. A relatively straightforward and yet effective way to minimize or eliminate soot formation is by using fuel additives. This has been executed successfully in both laboratory and practical combustion media. Since, however, the mechanism of additive behavior is not understood at present, criteria for the selection and evaluation of specific additives are not available, which has hindered their more frequent use.

The aim of this experimental research program is to seek to clarify the nature of the mechanisms responsible for fuel additive suppression of soot in well-defined laboratory flames. Departing from past qualitative approaches, this research stresses the use of spatially precise nonperturbing laser/optical techniques such as: soot size, number density and volume fraction, with and without additives, from elastic (Mie) light scattering; additive species concentrations from optical absorption and/or laser-induced fluorescence; temperature from spectroscopic measurements. Experiments are carried out in gaseous- or prevaporized liquid-fueled diffusion flames seeded with alkaline-earth and iron additives, respectively. Analysis of the interrelations among soot, additive species and temperature is expected to clarify additive mechanisms.

TECHNICAL DISCUSSION

During this past year, significant progress has been made in a number of areas pertinent to understanding additive behavior (Ref. 1). Here, the technical discussion is confined to a few developments of particular interest and significance.

Temperature Measurements: Spatially precise temperature measurements have been made for a sooting overventilated ethylene/air diffusion flame emanating from a Wolfhard-Parker burner. The burner has a central 5 x 45 mm fuel slot, two adjacent and symmetrically located 10 x 45 mm air slots, and provision for a sur-

---

*Co-funded by AFOSR and AF Engineering and Services Center, Tyndall AFB, Fla.

rounding flow of shroud air or nitrogen. Horizontal temperature profiles were measured at 5 mm vertical intervals, with 10^{-2} cm precision, using standard sodium line reversal methods. A representative portion of this data is shown in Fig. 1. In order to relate temperature to soot and additive effectiveness thereon, three different temperatures have been defined in Fig. 2 and their vertical dependences given. T_{max} is the maximum flame temperature and, for example, corresponds to either peak of the two lobes for the z = 8 mm profile in Fig. 1. $T_{f_v(max)}$ is appropriate to the horizontal position for which the soot volume fraction is a maximum. Finally, $T_{x=0}$ is the temperature at the burner center. The significance of these temperatures is as follows. In past work at UTRC, the effectiveness of a barium (Ba) fuel additive was measured at points in the flame coincident with those for $T_{f_v(max)}$ and $T_{x=0}$ in Fig. 2. At $f_v(max)$, the Ba effectiveness decreased with distance from the flame apex, while at x = 0 the decrease was similar but significantly more rapid. Since in Fig. 2 $T_{f_v(max)} < T_{x=0}$ with respect to the vertical departure of the two temperatures from T_{max}, the spatial dependence of Ba effectiveness is correlated with excursion of the measurement position from that corresponding to T_{max}. Accordingly, a strong link is indicated between additive effectiveness and flame temperature.

Data which support the argument above are given in Fig. 3. In it, the horizontal dependence of the effectiveness of strontium (Sr), a species closely related to Ba, is given at 23 mm height. Within the luminous flame at this height, the temperature minimum is at x = 0, whereas the maxima are at x = ± 2.5 mm. Note that similar to Ba above, the Sr effectiveness increases in the direction of increasing temperature. (f_v/f_v^o) data much beyond $f_v(max)$ are difficult to obtain due to rapidly decreasing light scattering signal intensities.

Soot Measurements: Data for additive effectiveness on soot have been obtained for alkaline-earth metals other than Ba. The measurements as a whole demonstrate that Ba > Sr > Ca as regards the effect which the metals have on soot. The dependence of soot reduction on additive molarity for the latter metals is given in Fig. 4; related results have been obtained for soot size and number density. Data like those in Fig. 4 are relevant to comprehending Ba mechanisms for this reason. Although alkaline-earth salts are similar chemically in that for the different metals similar species of the type M, MO, MOH, etc. (M = Ba, Sr or Ca) occur in seeded flames, the relative concentrations of M or MO, for example, are not the same. This is so since the species participate in reactions of the type, $M + OH \rightleftarrows MO + H$, and others, which have different equilibrium constants for dissimilar M. Accordingly, then, by combining data like that in Fig. 4 with species concentration measurements, it should be possible to relate one or more of M, MO, etc. to soot suppression.

Species Concentrations: As mentioned, additive species concentrations are important since one or more of the species may be related to soot suppression. An example of concentration measurement is given in Fig. 5. In it, the near saturated fluorescence intensity of SrOH is shown as a function of horizontal position. Due to near saturation, it may be shown that the fluorescence is approximately proportional to concentration; hence, Fig. 5 gives the lateral variation

of SrOH concentration. Since the concentration peaks in the vicinity of T_{max}, the species is implicated, per the discussion above, as a possible soot suppresant. This conclusion is tentative pending, for example, related Sr and SrO measurements which are currently in progress.

The fluorescence of SrOH as a function of laser energy is shown in Fig. 6. Saturation sets in near 10^{-5} Joules since for this and higher laser energies the dependence of fluorescence on energy is no longer linear. The data in Fig. 5 were taken at 10^{-2} Joules laser energy. In addition to its relation to understanding soot suppression, Fig. 6 has a further significance since to our knowledge the saturated fluorescence of a triatomic flame species has never been observed previously.

Prevaporized Liquid Fuels: Detailed Mie scattering measurements of soot parameters have been started using a prevaporized liquid fuel burner which supports an axisymmetric hydrocarbon/air diffusion flame. The fuel is preheated up to about 250°C at all points along the fuel tube, which is sufficient to completely vaporize a toluene/iso-octane mixture containing a dissolved ferrocene (dicyclopentadienyl iron) additive. In Fig. 7, the effect of ferrocene on light scattering at 50° is shown as a function of axial position in the flame. Since to first approximation the scattered intensity is proportional to the soot volume fraction, the data give soot suppression as a function of additive concentration and measurement position. In the 10 to 20 mm vertical interval, other data not included here show that the soot size progressively increases. Since ferrocene is not effective in this interval, the data in Fig. 7 tentatively indicate that ferrocene does not affect early stages of soot formation and that fuel structure effects are not important. On the other hand, the apparent action of ferrocene is to accelerate the oxidative burnout of soot at late combustion stages. More detailed measurements of the preceding type are currently underway.

NEAR TERM PLANS

For the ethylene/air flame, additional concentration measurements of the type made for SrOH are required in order to clarify Ba (or Sr) soot suppressing mechanisms. For the toluene flame, more detailed Mie/soot scattering data are required, as well as flame temperature and additive species concentrations.

REFERENCES

1. Bonczyk, P. A.: 20th Symposium (Int'l) on Combustion, Ann Arbor, Mich., 12-17 August 1984; Particulate Emission Technology Meeting, Monterey, Calif., 16-18 April 1985; Annual Scientific Report(s), AFOSR Contract No. F49620-83-C-0113, 3 June 1985 (and 25 May 1984).

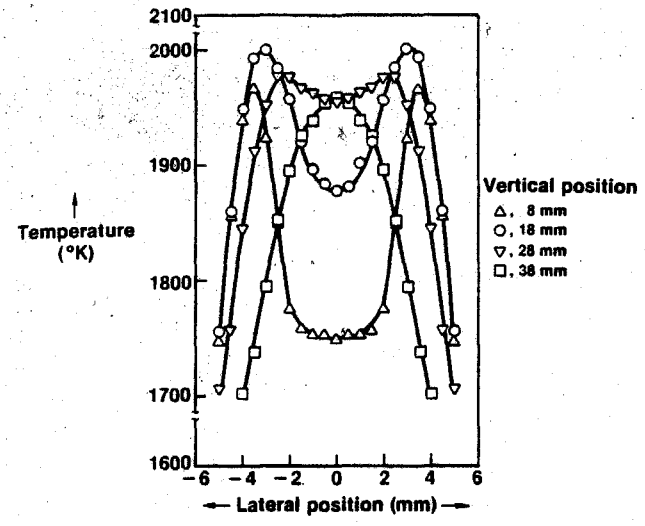

Fig. 1. Spatial Temperature Profiles

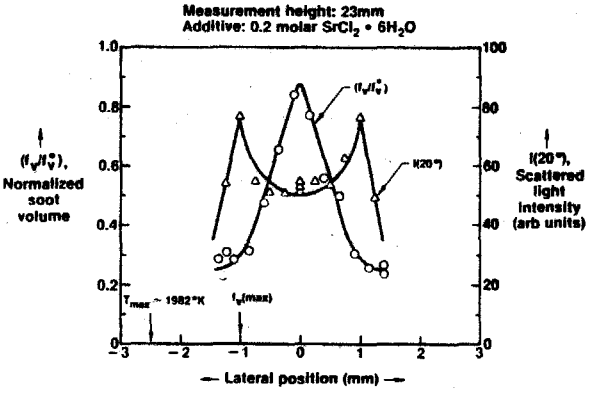

Fig. 3. Lateral Dependence of Additive Effectiveness

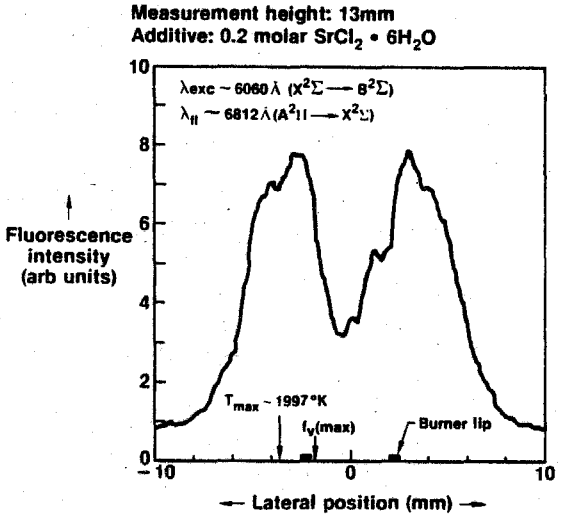

Fig. 5. Laser Excited SrOH Flame Fluorescence

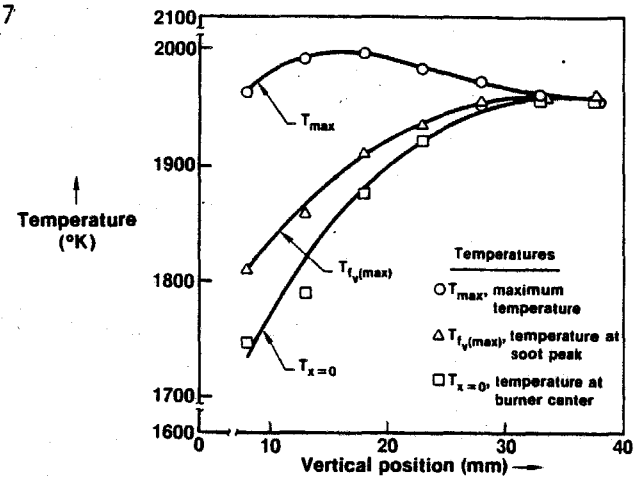

Fig. 2. Vertical Variations of Significant Flame Temperatures

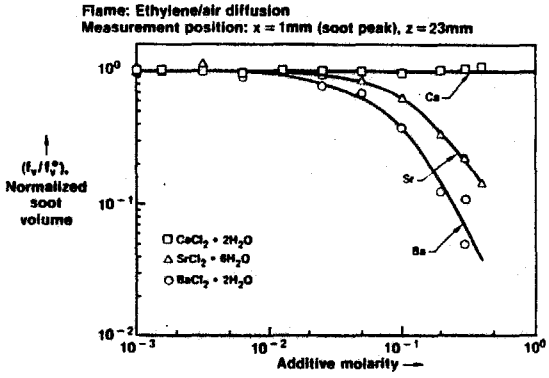

Fig. 4. Soot Volume Dependence on Additive Concentration

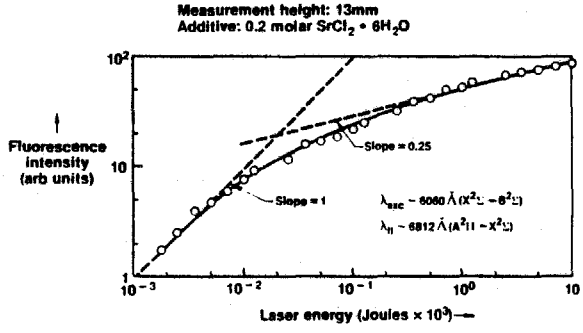

Fig. 6. Saturated Laser Excited SrOH Fluorescence

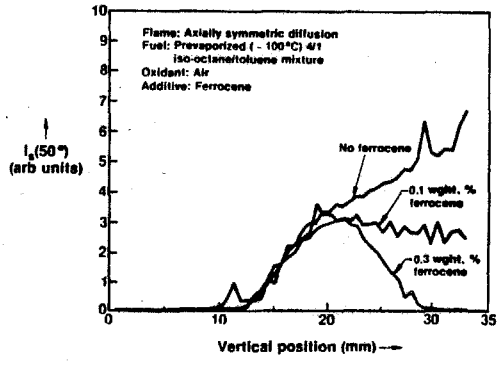

Fig. 7. Light Scattering Dependence on Vertical Position and Additive Concentration

An Investigation of Flow Structure, Mixing and Chemical Reaction in Combusting Turbulent Flows

AFOSR Grant Number 84–0373

Craig T. Bowman and Brian J. Cantwell

Department of Mechanical Engineering
Stanford University
Stanford, California 94305

Summary

An experimental investigation of the relationship between flow structure, and chemical reaction structure in a combusting turbulent flow has been initiated. The objective is to study the spatial structure of the unsteady reaction process as it relates to the spatial structure of the unsteady velocity field. The method of approach involves the use of laser–induced fluorescence techniques to locate intermediate species (C_2, CH) which are present only in the reaction zone. Measurements of velocity will be carried out using Laser Doppler Velocimetry. Results for the unsteady reaction field will be overlaid on ensemble averaged measurements of the velocity field to produce a picture of the unsteady mixing and reaction process. It is expected that the work will lead to an improved understanding of the sequence of flow events involving entrainment of free stream reactants and combustion in chemically active zones subjected to flow straining. Information of this type will contribute to improved models of combustion.

Technical Discussion

Recent research in turbulent combustion has focused on establishing appropriate models for the interaction between turbulence structure and flame chemistry. Although there has been a considerable increase in our understanding of the physics of mixing and combustion, there are as yet no data which directly reveal the coupling between the unsteady velocity field and the unsteady reaction field in a combusting flow. The objective of the present work is to combine time–resolved field measurements of velocity and of the concen-

tration of short lived species in a time–dependent hydrocarbon–air flame. Interpretation of the results will employ topological methods which have been used to characterize the structure of non–reacting flows. This methodology provides a unified approach for characterizing various strain and rotation fields which can occur in turbulent flows. The results from this study can be used to address the following important question: how much detail of the physics of the flame–turbulence interaction is required for the development of models for a given level of prediction?

The research makes use of a variable pressure facility designed to permit the study of chemically reacting flows for pressures in the range from 0.1 to 10.0 atmospheres and free stream velocities up to 10.0 meters per second. The variable pressure feature of the facility allows the flow Reynolds number and Grashof number to be varied while overall velocities and length scales are held fixed. The configuration investigated in this study is a co–flowing non–premixed jet flame, with methane in the core flow and air in the surrounding flow. The methane passes through a small chamber containing a loudspeaker which can be used to add a velocity perturbation to the core flow at various frequencies and amplitudes. The test section is equipped with Schlieren quality windows on all four sides to provide access for a variety of optical measurements.

Initial experiments were conducted at low Reynolds number with the aim of documenting the conditions under which we could generate a controlled flow. By forcing the jet in a range of frequencies encompassing its unforced natural frequency it was possible to produce a very periodic and controllable flow which is suitable for making conditionally sampled measurements of the unsteady velocity and reaction fields. Figure 1 shows a visualization of the structure of these periodically driven flames. In these pictures the luminous image of the flame is superimposed on the Schlieren image. The jet exit velocity and freestream velocity are fixed while the excitation frequency is varied. The leftmost photograph depicts the unforced case. The rightmost photograph depicts the case where

the forcing is at a relatively high frequency compared to the natural frequency of the flow. In these cases a double flame structure is observed with two distinct wavelengths. The luminous core exhibits an instability with a perturbation wavelength which is substantially longer than the wavelength of the outer hot gas envelope. The middle photograph depicts the case where the forcing is at a relatively low frequency. In this case the flow is excited at a frequency which causes the luminous core and surrounding outer flow to couple most favorably and the luminous core pinches off to form a series of flamelets with a single overall wavelength. Further discussion of these observations may be found in the paper by Strawa and Cantwell (1985) listed below. The topology of the unsteady velocity field in these flames will be determined by means of conditionally sampled two velocity component Laser Doppler Anemometry. Single velocity component measurements at several different test section pressures currently are in progress. Flow visualization of the type depicted here has been carried out at test section pressures up to 65 psia (cold gas Reynolds numbers of approximately 2600) and although the flame is quite three–dimensional the periodicity of the flow is good even to the extent that much of the 3–D structure is quite repeatable from cycle to cycle.

The topology of the reaction field will be determined by a two–dimensional time–resolved visualization of the regions of intense chemical activity in the flame. These measurements will be performed utilizing a laser induced fluorescence technique to detect hydrocarbon radical species (CH and C_2) which are present only in the reaction zone. A schematic diagram of the optical system is shown in figure 2. Work is currently under way to develop an improved high speed Schlieren system based on a recently acquired Spin Physics video system and to evaluate laser sources and detection methods for intermediate species visualization.

Publications

1) Strawa, Anthony W., and Cantwell, Brian J., 1985, Visualization of the Structure of a Pulsed Methane–Air Diffusion Flame, Physics of Fluids Letters (in press).

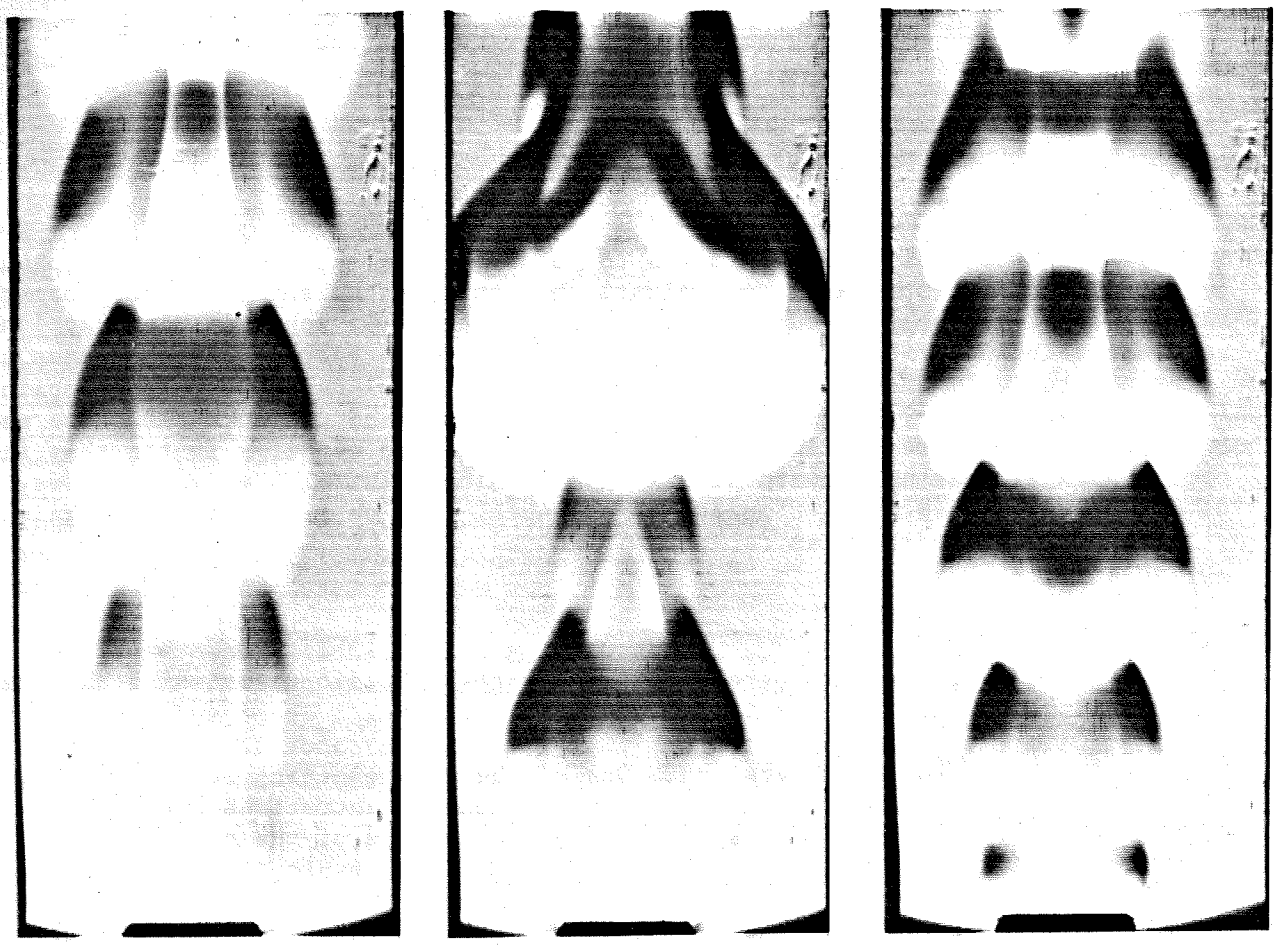

Figure 1 Schlieren photographs of a driven co–flowing methane–air diffusion flame. Jet velocity 49 cm/sec, outer flow velocity 46 cm/sec, jet diameter 2.2 cm. Excitation frequency from left to right: unexcited, 10 Hz, 22 Hz.

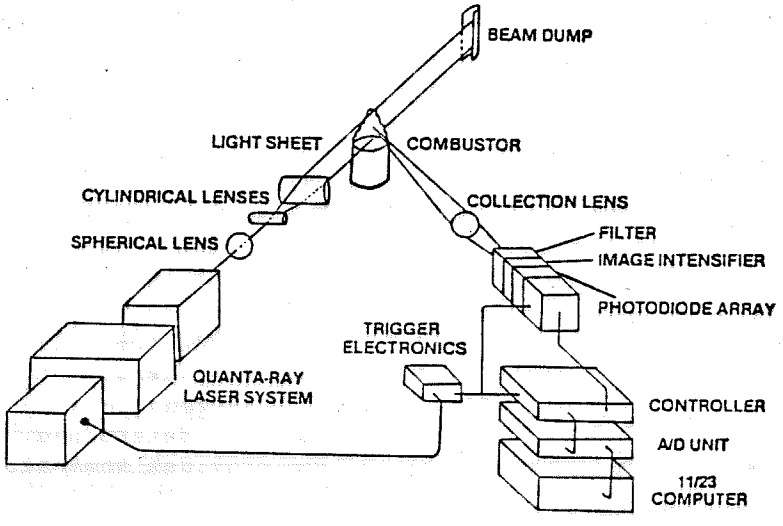

Figure 2 Sketch of the LIF measurement technique.

IONIC MECHANISMS OF SOOT FORMATION

AFOSR Contract No. F49620-83-C-0150

Principal Investigator: H.F. Calcote

AeroChem Research Laboratories, Inc.
P.O. Box 12
Princeton, NJ 08542

SUMMARY/OVERVIEW

The object of this program is to determine the mechanism of soot formation in flames, and especially to evaluate the ionic mechanism, i.e., the formation of a chemi-ion soot precursor followed by a series of ion-molecule reactions to produce incipient soot particles. Low pressure hydrocarbon-oxygen flames are being studied. The major experimental tool is a molecular beam ion sampling mass spectrometer, supplemented by Langmuir probe and thermocouple probe measurements. We are currently obtaining detailed ion profiles in the same flames in which Bittner and Howard at MIT have obtained neutral species profiles. Our objective is to provide complete experimental data on several flames against which to compare theories.

TECHNICAL DISCUSSION

We summarize here progress on some of the specific tasks which have been pursued since the last meeting.

1. Total Ion Concentration. One of the more exciting results during this period was the determination of total ion concentrations in well-studied acetylene/oxygen flames, thus providing a comparison of the concentration of ions relative to the concentration of soot.[1] This result is presented in Fig. 1. The ion number density was determined using a Langmuir probe. From about 1.5 cm to 3.5 cm from the burner, the ion concentration agrees very closely with a measurement by Homann and Stroefer[2] who used a molecular beam ion sampling-Faraday cup arrangement. The neutral and charged soot measurements are from the work of Howard and associates.[3] We have arbitrarily adjusted their data to match the ion number density measured at 3.5 cm, since both techniques measure the same quantity, "total ions or charged particles". The small "bump" early in the ion profile is real although its significance is not understood; similar bumps have also been observed in neutral species profiles.[4] It is difficult to sample with a cooled mass spectrometer probe within 1 cm of the burner, so we are building a small, metal-coated quartz probe to explore this region of the flame in more detail.

2. Individual Ion Profiles. Detailed ion spectra, such as shown in Fig. 2, have been obtained for several flames and are currently being interpreted. There are two calibration difficulties: (1) determining the actual ion masses and (2) converting the measured ion currents into ion concentrations. The mass spectrometer is calibrated up to 208 amu by adding metals to a flame (K, Rb, Cs, and Pb). To further extend the calibration range, deuterated acetylene was substituted for normal acetylene. The observed shift in hydrocarbon ion mass gave the number of hydrogens in each molecule and, since the remainder is carbon, the specific mass is determined. This calibration is nearly completed up to about 600 amu and provides some structural information based on the ion C/H ratios.

Calibration of ion currents to individual ion concentrations is more difficult and this task lies mostly ahead of us. Since we now have a reliable Langmuir probe theory and protocol for obtaining total ion concentrations, and we have accurate flame temperature measurements[5] we will calibrate the mass spectrometer ion currents against the Langmuir probe total ion concentrations by using a series of simultaneous equations involving the mass-dependent throughput parameters and a series of flames with different ion spectra (see Fig. 2). To the extent that equilibria have been demonstrated for metal ions in flames, these will also be used at lower masses. We plan to extend the mass range of our instrument from its current 600 amu to about 2000 amu in the near future.

3. Temperature Observations. Soot thresholds, soot yields, and flame temperatures (two-wavelength emission pyrometry) were measured in laminar premixed atmospheric pressure flames of toluene and decalin with varying O_2/N_2 ratios.[6] The results were surprising, Fig. 3, in that the measured flame temperature at the soot threshold was independent of the O_2/N_2 ratio although as expected the soot threshold equivalence ratio varied with the O_2/N_2 ratio. These data indicate that for mixtures with soot thresholds at higher equivalence ratios (i.e., with larger O_2/N_2 ratios), the heat releasing reactions do not go to completion. This would account for the increasing difference (with increasing ϕ_c) between calculated and measured temperature. Additionally, in these flames the plateau soot volume fractions for each fuel were found, at any given value of the measured temperature, to be independent of the fuel/O_2 or O_2/N_2 ratios.

These observations relate to a thesis we are currently pursuing, namely that soot formation exceeds equilibrium near threshold but falls below equilibrium for very sooty flames. This thesis would be very interesting in terms of the mechanism of soot formation and would explain some paradoxes in the ionic mechanism of soot formation.

ACKNOWLEDGMENT

The significant contributions of Drs. D.G. Keil and D.B. Olson are gratefully acknowledged.

References

1. Keil, D.G., Gill, R.J., Olson, D.B., and Calcote, H.F., Twentieth Symposium (International) on Combustion (The Combustion Institute, Pittsburgh, in press).

2. Homann, K.H. and Stroefer, E., in Soot in Combustion Systems and Its Toxic Properties, J. Lahaye and G. Prado, Eds. (Plenum Press, New York, 1983) p. 217.

3. Howard, J.B., Wersborg, B.L., and Williams, G.C., Faraday Symp. Chem. Soc. 7, 109 (1973).

4. Bittner, J.D. and Howard, J.B., in Particulate Carbon: Formation During Combustion, D.C. Siegla and G.W. Smith, Eds. (Plenum Press, New York, 1981) p. 109.

5. Keil, D.G., Gill, R.J., Olson, D.B., and Calcote, H.F., in The Chemistry of Combustion Processes, T.M. Sloane, Ed., ACS Symposium Series 249 (American Chemical Society, Washington, DC 1984) p. 33.

6. Olson, D.B. and Madronich, S., Combust. Flame 60, 203 (1985).

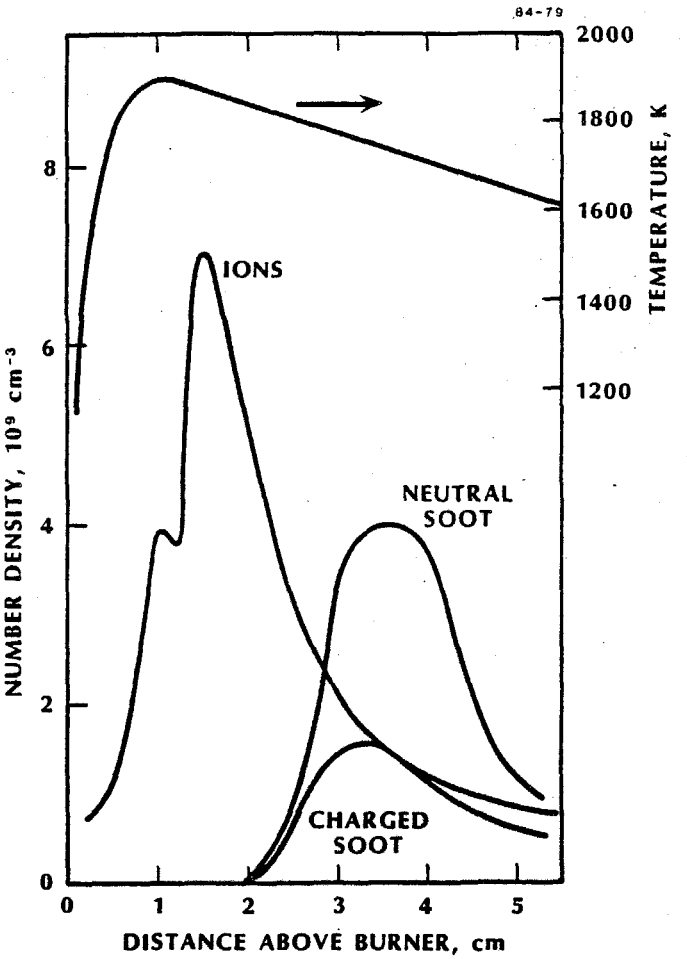

FIGURE 1 ION AND SOOT PROFILES IN AN ACETYLENE-OXYGEN FLAME AT 2.7 kPa

Equivalence Ratio = 3.0; NEUTRAL SOOT and CHARGED SOOT from Ref. 3.

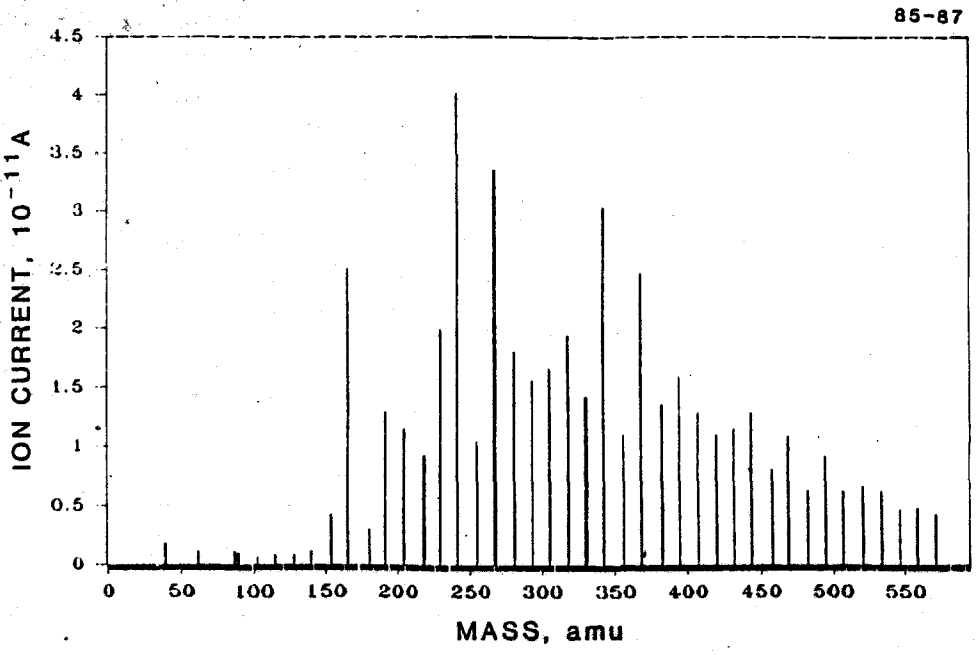

FIGURE 2 MASS SPECTRA OF AN ACETYLENE-OXYGEN FLAME AT 2.7 kPa

Equivalence Ratio = 3.0; Distance Above Burner = 2.4 cm.

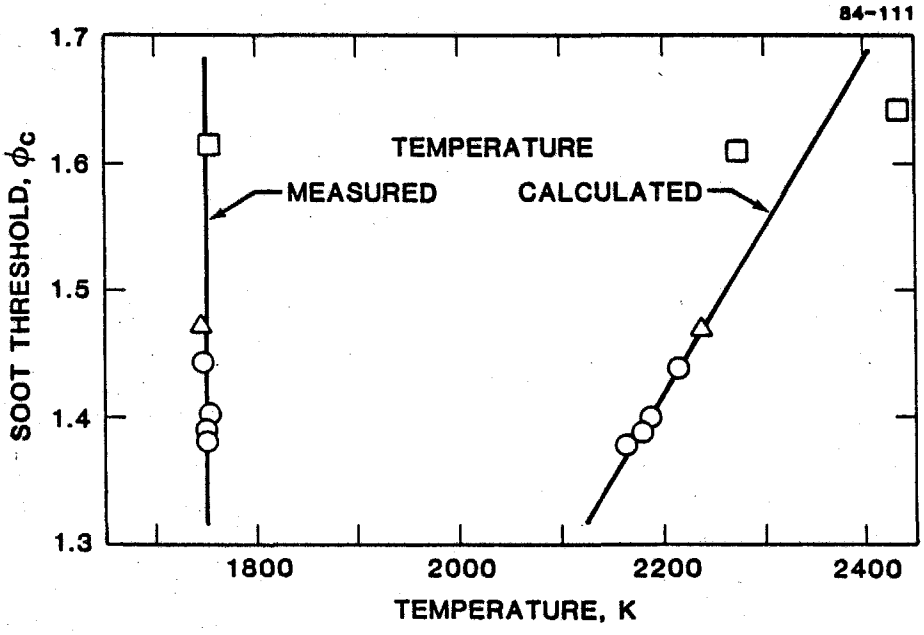

FIGURE 3 COMPARISON OF CALCULATED AND MEASURED TEMPERATURES FOR SOOT THRESHOLDS

Toluene - O_2-N_2 Premixed Flame at 1 atm.

$\frac{O_2}{O_2 + N_2}$ indicated by points: △ = 0.21,

○ < 0.21, □ > 0.21.

EXAMINATION OF MECHANISMS AND FUEL-MOLECULAR EFFECTS ON SOOT FORMATION

(AFOSR Grant/Contract No. F49620-85-C-0012)
Principal Investigator: Meredith B. Colket, III

United Technologies Research Center
East Hartford, CT 06108

SUMMARY/OVERVIEW:

A variety of hydrocarbons are being pyrolyzed and/or oxidized in a single-pulse shock tube. Intermediate and final products (including C_1-C_{10} hydrocarbons and hydrogen) are being quantitatively analyzed using capillary gas chromatography. Experimental data is being used to guide detailed chemical kinetic modeling of hydrocarbon pyrolysis and the data will be used to build or test comprehensive models of soot production.

TECHNICAL DISCUSSION:

Various concentrations of vinylacetylene and benzene in argon have been pyrolyzed in a single-pulse shock tube (SPST) over the ranges of 1100 to 2500 K, five to eight atmospheres, and dwell times of 550 to 800 microseconds. In addition, hydrocarbon mixtures have been pyrolyzed including mixtures of benzene/acetylene and toluene/acetylene in argon. Total carbon atom densities have ranged from about 2×10^{16} to 2×10^{18} carbon atoms/cc. Final concentrations of hydrocarbons were quantitatively determined using a CP Sil 5 CB (1 micron film thickness) fused silica capillary column and flame ionization detection. Hydrogen was analyzed using a silica gel packed column and a thermal conductivity detector. Typical results are shown in Figs. 1 and 2 for the pyrolysis of 1.17% benzene in argon. Presented in these figures are the final product distribution after the test gas has been shock heated for approximately 700 microseconds and then quenched by the rarefaction wave. These figures represent collected results from a series of eighteen separate shocks covering a range of post-shock temperatures. The general features, i.e., production of aromatics over the 1500 to 1900 K temperature range, and the dominance of hydrogen and 'equilibrium' concentrations of the acetylenes above 2200 K is apparent in virtually all fuels. For the non-aromatic fuels, equilibrium concentrations are generally achieved above 1900 to 2000 K. At temperatures below 1500 to 1600 K, the kinetics and product distribution are controlled by the decomposition of the parent hydrocarbon.

Figure 1 exhibits a relatively large amount of hydrogen produced at low temperatures. Modeling demonstrates that this 'low temperature' hydrogen is principally formed via the sequence:

$$C_6H_6 \text{-----} > C_6H_5 + H$$
$$C_6H_5 + C_6H_6 \text{-----} > C_{12}H_{10} + H$$
$$H + C_6H_6 \text{-----} > C_6H_5 + H_2$$

Near 1400 K biphenyl should be produced in amounts comparable to that of hydrogen yet is apparently lost during the sampling process or in the inlet system to the gas chromatograph. The amount of mass converted to biphenyl at 1400 K would be approximately a few percent of the total mass and is consistent with the measured mass balance and calculated H/C ratios of the missing material. Above 1800 K, the calculated H/C ratio is 0.1 suggesting the formation of very large polynuclear aromatics or even soot. The low ratio of 0.1 observed in these benzene experiments is atypical, since for most other hydrocarbons the H/C ratio of the missing material ranges from 0.2 to 0.3 above 1700 K. This difference between benzene and other hydrocarbons may not be significant in light of the potential errors in calculating the H/C ratios of the missing material.

Detailed chemical kinetic modeling of the experimental data is in progress using a modified version of the Chemkin Shock Tube Code developed at Sandia National Laboratories. In the case of benzene and acetylene very good agreement has been obtained with overall pyrolysis rates and with product formation using existing (or slightly modified) chemical kinetic models. Some limited modeling work has been performed on the production and growth of aromatics during pyrolysis of aliphatics. Preliminary results suggest that acetylene is undoubtedly a key species to the production and growth of aromatics, just as acetylene has been found to be important to the growth of solid soot particles. The principle explanation of this phenomena is primarily related to the dominance of acetylene under pyrolytic conditions. Modeling of acetylene pyrolysis has been guided by the experimental work at UTRC as well as ongoing research at MIT, USC, and LSU. Results suggest that below 1400 K,

$$C_2H_2 + H \text{-----} > C_2H_3$$
$$C_2H_2 + C_2H_2 \text{-----} > C_4H_5$$
$$C_4H_5 + C_2H_2 \text{-----} > C_6H_7 \text{-----} > c\text{-}C_6H_7$$
$$c\text{-}C_6H_7 \text{-----} > C_6H_6 + H$$

As temperature increases, aromatics are produced via the sequence:

$$C_2H_2 + C_2H_2 \text{-----} > C_4H_3 + H$$
$$C_4H_3 + C_2H_2 \text{-----} > C_6H_5 \text{-----} > \text{phenyl}$$
$$\text{phenyl} + C_2H_2 \text{-----} > \text{phenylacetylene}$$

Experimental profiles suggest that above 1600 K phenylacetylene will rapidly grow to higher molecular weight hydrocarbons.

Some of the most recent experimental and modeling results are summarized in the following article.

Colket, M.B. "Single-Pulse Shock Tube Examination of Hydrocarbon Pyrolysis and Soot Formation". To be presented at the 15th International Symposium on Shock Waves and Shock Tubes, July 29-August 1, 1985.

FIGURE 1 1.17% BENZENE PYROLYSIS
SPST data, 700 microseconds, aliphatics

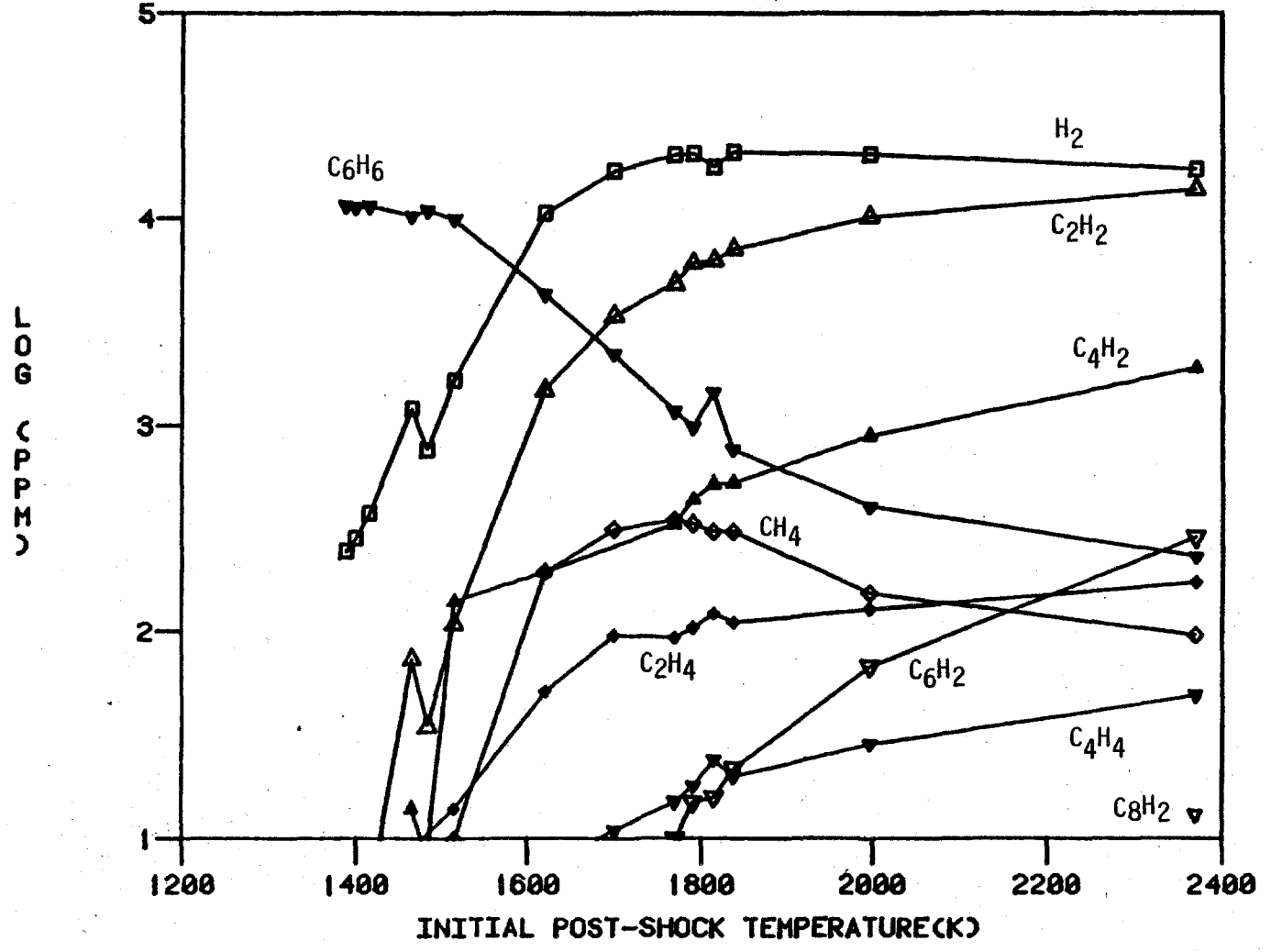

FIGURE 2 1.17% BENZENE PYROLYSIS
SPST data, 700 microseconds, aromatics

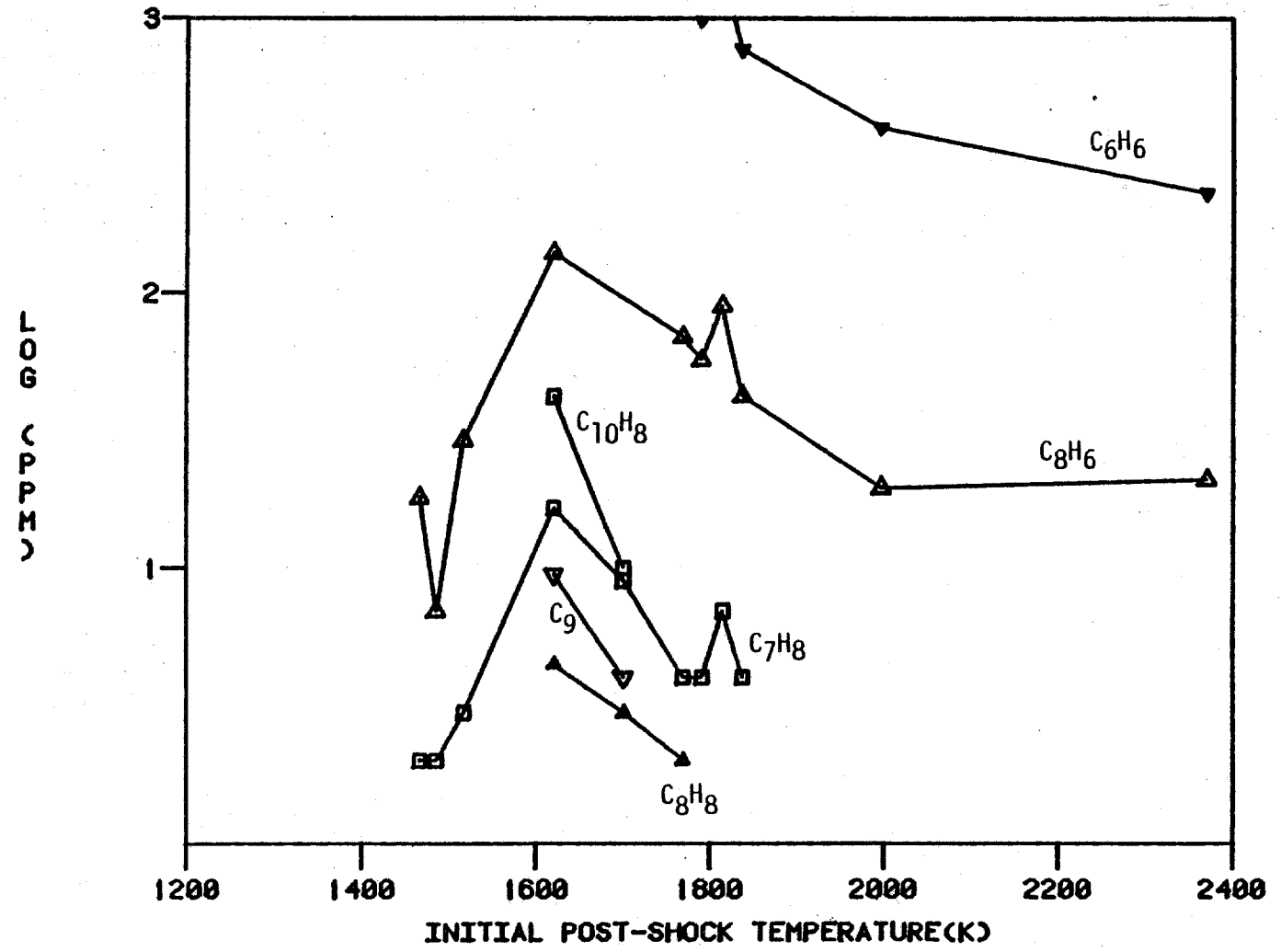

TITLE: RESEARCH ON MECHANISMS OF EXCITING PRESSURE OSCILLATIONS IN RAMJET ENGINES

(AFOSR Grant Number: AFOSR-84-0286)

Principal Investigators: F. E. C. Culick, Frank E. Marble, and E. E. Zukoski

California Institute of Technology
Pasadena, California 91125

SUMMARY/OVERVIEW

An analytical and experimental study is being made of the role of combustion in large vortical structures in the mechanism of unsteady and unstable burning in air-breathing engines. A large body of experimental evidence supports the contention that these periodic fluctuations are themselves generated by the nonsteady flow over the flame holders and other surfaces. The mechanism itself is relatively independent of the acoustic configuration of the powerplant and its installation and hence constitutes the fundamental element of the combustion instability process. Whether or not the mechanism is excited does, however, depend upon the detailed acoustic properties of the combustion chamber and its environment and in many circumstances it is apparent that non-linear acoustics plays an essential role. As a consequence, the program includes detailed analytical studies of linear and non-linear acoustics in combustion configurations as a means of coupling the instability mechanism to a particular environment. The effective separation of the instability process into i) its mechanism and ii) its environment is aimed at eventually providing means of rational scaling of laboratory size experiments.

TECHNICAL DISCUSSION

The program includes both analysis and experiments. The analytical work divides broadly into two parts: (1) Studies of the basic gasdynamic phenomena in non-steady two- and three-dimensional fields with strongly exothermic chemical reactions. The emphasis is on the combustion processes in vortex structures and the fluid-dynamic stability of the flow fields generated by the interaction of non-uniform fields with acoustic waves, and (2) development of the theoretical framework for studying pressure oscillations, constructed so as to accommodate the results of item (1). We intend that the analyses should provide not only general understanding of the possible mechanisms for pressure oscillations, but also scaling laws and guidelines for experimental work and for full-scale devices. We are carrying out both linear and non-linear analysis. The first provides information about the conditions under which

oscillations will occur; and the second is required to determine the amplitudes to which unstable oscillations will grow. The experimental work is concerned with unsteady combustion processes which occur in flows past steps and flameholders, and concentrates on processes which occur in the shear layers and recirculation zone regions. Tests are being carried out at Caltech in a small scale burner which has the geometry of a ramjet dump burner. In the report for this year, the experimental work will be discussed.

The process under study involves the coupling between acoustic modes of the system and unsteady heat addition which results from unsteady burning in large vortices. These vortices are formed periodically at the flame holder lip by the velocity fluctuations associated with the acoustic field. Two phenomena should be distinguished here. The first concerns the production and development of the small scale structures which have been observed in isothermal shear layers and which are not directly related to acoustic disturbances or gross fluctuations in heat release. The second concerns large structures which have been observed in flame holder as well as dump burner systems and which are related to the shedding of vortices from the recirculation zone under the influence of longitudinal pressure disturbances. We believe that these large structures play a key role in the combustion instability problem and that they are not simply connected with the small structures.

The experiments are being carried out in a small blowdown facility which supplies a metered fuel-air mixture to a combustion system which consists of a plenum chamber and a combustion chamber whose lengths can be varied so that the fundamental resonant frequencies of the system vary from 190 to 530 hz. The combustion chamber is a rectangular duct 2.55 cm high, 7.6 cm wide and can be as long as 1 m. The flame holder is a 1.92 cm high rearward facing step which extends across the 7.6 cm width of the duct. For the data discussed here the exit is not choked. The stability limits for this system allow operation at fuel-air ratios in the range between 0.7 and 1.2 of the stoichiometric value for velocities in the range between 20 and 100 meters/sec. Instrumentation includes 6 to 10 high-frequency response pressure transducers located along the combustion chamber and at various points in the supply system. Estimates of fluctuations in local values of the heat release rate are made from measurements of the intensity of light emitted from the burning gas over a volume which extends across the 7.6 cm width of the duct and has an axial extent of 3 mm. Movies of shadowgraph images taken at about 6000 frames/sec and microsecond exposure shadowgraph photographs are used to visualize the flow. The pressure and light intensity signals are digitized and then are analyzed with Fast Fourier Transforms to obtain the spectra for these signals. Cross correlations between the light and pressure signals are being analyzed to check the Rayleigh criteria for instability.

A linearized and one dimensional acoustic analysis developed earlier in this program has been used to study the acoustic modes of this system. This numerical model includes the various area changes in the duct cross section area, the contraction of the duct at the flame holder and the increased speed of sound in the combustion chamber. The model has been extended this year to allow us to study

the effects of an arbitrary forcing function which crudely models the effects of nonsteady heat addition at the flame holder. This addition also allows us to understand better the relative phases of the oscillations in various parts of the system. The model also allows us to predict the amplitudes of velocity fluctuations at the flame holder lip when the pressure fluctuations are measured in the experiments.

We have developed a physical model for one of the modes of combustion instability exhibited by this system which is based on the following observations. The most dramatic changes produced by the combustion instability in question is the change it produces in the shear layer which develops in the region just down of the flame holder lip and which separates the unburnt flow from the hot recirculation zone gases. When the instability is absent, the shear layer is relatively steady and exhibits the small vortices which we have come to associate with the shear layer. In contrast, when the instability is present, the shear layer is grossly distorted by the presence of large vortices which are periodically shed from the flame holder lip at the same frequency as an accompanying large amplitude oscillation in the pressure.

The frequency of the oscillation is always one of the duct modes and thus the frequency can be modified, by changing the length of the plenum chamber or combustion chamber, over the range from 180 to 530 hz. The oscillation can be eliminated by increasing the damping of the acoustic waves in the system, e.g. by placing steel wool in the plenum chamber.

The vortices grow rapidly as they move down stream and they impinge on the lower wall of the combustion chamber at a point between 3 and 6 ducts heights downstream of the holder. The velocity of the downstream motion of the vortex is only weakly dependent on the mean velocity at the flame holder and increases as the amplitude of the pressure oscillation increases. The vortices are shed when the magnitude of the pressure fluctuation at the flame holder begins to fall from its maximum value; the vortex moves downstream and impinges on the wall when the amplitude of the pressure fluctuation is positive and is increasing. Fluctuations in intensity of the light generated by the combustion process suggest that the heat release rate reaches its maximum acceleration when the vortex reaches the wall and when the fluctuation amplitude is close to zero and is rising.

Examination of the cross correlations of the pressure and light signals suggest that the fluctuations act to feed energy into the acoustic field in the region near the flame holder, but that farther downstream the fluctuations have a damping effect.

These results suggest the following model: The acoustic field produces a large amplitude velocity fluctuation at the flame holder lip which, in turn, causes a vortex to be shed from the lip. A marked acceleration in the heat release rate is produced shortly after the vortex reaches the wall. This process generates a pressure pulse which feeds energy into the acoustic field when the phase relationship between the pulse and acoustic pressure

oscillation have the proper phase. The delay between the time when the vortex reaches the the wall and the acceleration in heat release occurs is a function of the chemical properties of the fuel-air mixture and thus depends on the fuel-air ratio and a characteristic chemical time for the mixture.

During the present contract year, we have started to investigate the effects on this instability of the chemical parameters of the system mentioned in the last paragraph. We are doing this by exploring the dependence on the fuel-air ratio of the premixed gases and by changing the fuel from pure methane to mixtures of methane and hydrogen. When pure methane is used as fuel, the instability is observed to occur for fuel-air ratios between 0.78 and 1.2 of the stoichiometric mixture ratio. When a mixture of 15% hydrogen and 85% methane is used as fuel, the same instability is observed but the lower limit for instability shifts to a value of 0.57 of stoichiometric. We believe that this shift can be understood in terms of the differences in a chemical reaction time for the two mixtures. Estimates for the chemical time we are using here are based on values measured experimentally in earlier experimental work on bluff body flame stabilization.

We are continuing to investigate the influence of chemical parameters on the instability process and are also, the influence of flameholder geometry. Finally, the growth and motion of the vortices in this type of system is being examined in a separate experiments involving the motion of isolated vortices.

Several reports are available now which describe the experimental aspect of our work. For example, see the Thesis by Dr. Dune A. Smith and the condensed version which was presented at the AIAA Propulsion Conference earlier this month. A number of papers are also available concerning the theoretical aspects of our work.

Smith, Duane A., "An Experimental Study of Acoustically Excited, Vortex Driven, Combustion Instability within a Reaward Facing Step Combustor." PhD Thesis, California Institute of Technology, Pasadena California, 1985.

Smith, Duane A. and Zukoski, Edward E., "Combustion Instability Sustained by Unsteady Vortex Combustion", AIAA/SAE/ASME 21st Joint Propulsion Conference, Monterey, California, July 1985.

CARBON MONOXIDE AND TURBULENCE-CHEMISTRY INTERACTIONS: BLOW OFF AND EXTINCTION OF TURBULENT JET DIFFUSION FLAMES

Principal Investigators: M. C. Drake and S. M. Correa

General Electric
Corporate Research and Development Center
Schenectady, New York 12301

SUMMARY/OVERVIEW

Development of a fundamental understanding of turbulence-chemistry interactions remains one of the most important and challenging problems in turbulent reacting flows. This program couples laser-based measurements and computer modeling of well-characterized laboratory-scale $CO/H_2/N_2$ jet diffusion flames to study the effects of finite rate chemistry and localized extinction in turbulent combustion. The long-range goal is to use this fundamental understanding in advanced combustor design and for control of lean and high altitude blow out in practical aircraft engines.

TECHNICAL DISCUSSION

A fundamental understanding of turbulent diffusion flames requires detailed knowledge of turbulent fuel/air mixing, combustion chemistry, and turbulence-chemistry interactions. None of these processes can be reliably calculated from rigorous fundamental theories. However, turbulent fuel/air mixing in single nonreacting and reacting turbulent jet flows can be successfully accounted for using k-ε turbulence models with assumed shape probability density functions (pdf's) of a conserved scalar mixture fraction. This model/experiment agreement occurs even though the k-ε model does not specifically account for the large-scale structures which are known to dominate the jet mixing process. Combustion chemistry (detailed mechanisms and reaction rates) is well established for the oxidation of H_2 and CO but still somewhat speculative for hydrocarbons. Turbulence-chemistry interactions are only beginning to be explored.

The approach of this joint experimental/computational program is to study turbulence-chemistry interactions in pilot flame stabilized, turbulent jet diffusion flames of $CO/H_2/N_2$ fuel where the turbulent fuel/air mixing and combustion chemistry are reasonably well known. Experimentally our unique combustor facilities and laser measurement techniques developed at GE will be used to provide time- and space-resolved measurements of probability density functions of velocity, temperature, major species concentrations, density, mixture fraction and OH concentration of a point in the flow and two-dimensional images of OH concentration to provide qualitative extent of localized extinction. Computationally, various analytical methods (single-scalar

mixture fraction pdf model with equilibrium or laminar flamelet assumptions and two- or three-scalar approaches using mixture fraction and extent of reaction variables) will be developed for incorporating CO to CO_2 finite rate chemistry into turbulence models using assumed shape pdf/k-ε theory. Detailed experimental-model comparison will be used to assess model capabilities and to provide a more fundamental understanding of turbulence-chemistry interactions and extinction.

As an example, Fig. 1 summarizes previous results on a Re=8500 $CO/H_2/N_2$ turbulent jet diffusion flame (using no pilot-flame stabilization) with initial fuel and air velocities of 55 and 2.4 m/s respectively. Measurements (using laser velocimetry, pulsed Raman scattering, single-pulse saturated OH fluorescence and NO_x probe sampling) are compared to turbulent combustion models using a standard k-ε/turbulence model and two different chemistry submodels (an equilibrium chemistry-assumed shape pdf model or a two-scalar pdf approach which allows for nonequilibrium radial pool concentrations). The quantities on the left in Fig. 1 are the same for either chemistry submodel. However, as shown in the right of Fig. 1, the nonequilibrium model results are in much better agreement with experiment, demonstrating that nonequilibrium lowers average flame temperatures by as much as 250K, raises average OH concentrations by a factor of six, and raise thermal NO_x concentrations by a factor of three.

Future AFOSR work will extend these experimental measurements to higher Reynolds numbers using pilot-flame stabilized turbulent jet flames where localized extinction is expected to become increasing important. Other experimental work on laminar opposed-flow diffusion flames with the same $CO/H_2/N_2$ fuels provide the foundation for stretched laminar flamelet models in turbulent combustion. Computationally, a three-scalar pdf model which allows CO to be out of partial equilibrium with the nonequilibrium radical pool at low temperatures has been developed and a stretched laminar flamelet model is being constructed.

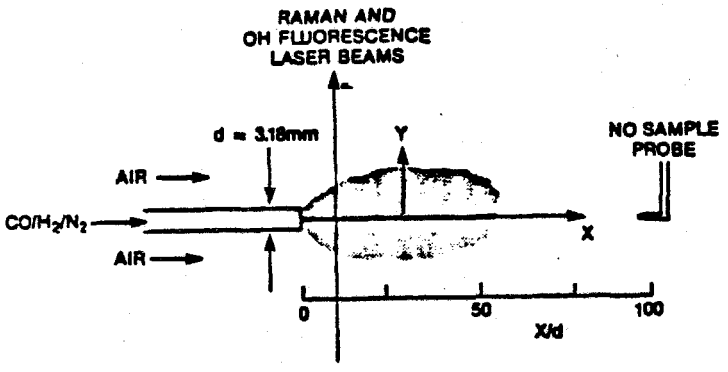

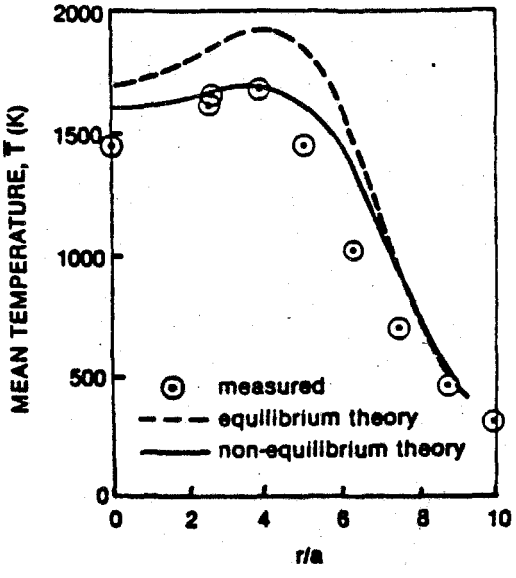

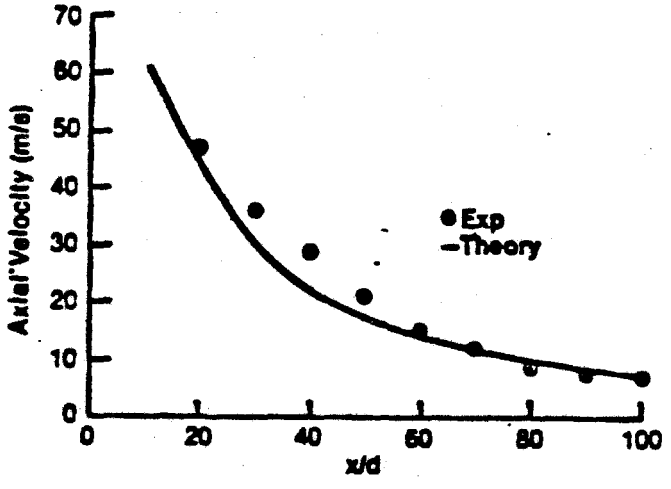

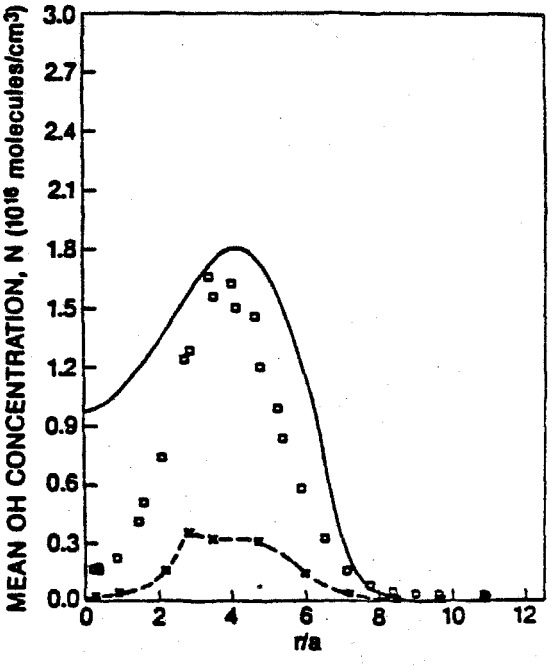

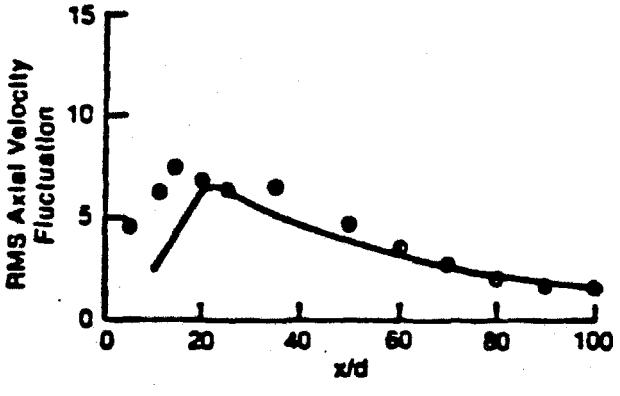

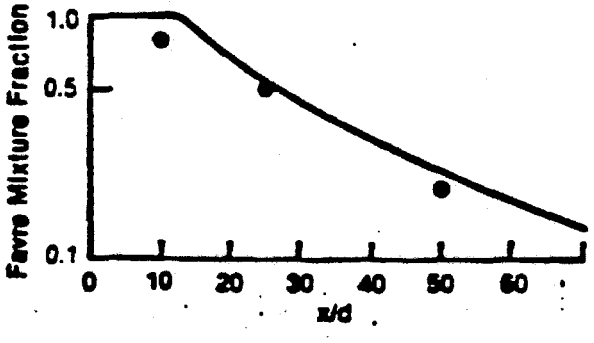

	NO_x YIELD $(10^{-6} kg/s)$
Measured	3.4
Equil.	1.1
Nonequil	2.6

NUMERICAL SIMULATION OF TURBULENT FLAMES USING VORTEX METHODS

AFOSR Grant No. CPE-8404811

Principal Investigator: Ahmed F. Ghoniem

Department of Mechanical Engineering
Massachusetts Institute of Technology
Cambridge, MA 02139

SUMMARY

The goal of this research program is to develop accurate and efficient computational algorithms for the direct numerical simulation of turbulence, in particular in multi-component, chemically reacting systems. Lagrangian and hybrid vortex schemes are employed to obtain time-dependent solutions of the unaveraged Navier-Stokes equations at high Reynolds numbers. Attention is focused on a set of test cases of premixed flames stabilized in confined shear flow environment. Solutions obtained are used to study the flow stability and the mechanisms of turbulence-combustion interactions that control the stabilization of turbulent flames.

TECHNICAL DISSCUSION

Direct numerical simulation of turbulence has been stimulated by: (1) the lack of semi-empirical models that can describe general constitutive relations of turbulence; (2) the recent development of highly accurate numerical approximations of the governing equations, untampered with artificial errors that mask the underlying physics; and (3) the rapid growth of computational power that allowed the application of these methods to more than just highly idealized flow fields. In that regard, vortex methods can prove to be of a particular value because they can be designed with high accuracy at large Reynolds numbers and because of their Lagrangian form that deals naturally with the convection non-linearity. The latter allows flexibility in treating turbulent shear flows, where zones of high concentration of vorticity, while continuously changing with time, occupy a small and highly convoluted portion of the total field.

Recent developments in the theory of vortex approximations, [1], including the formulation of high order schemes, the study of the effect of time integration error and the extension to three dimensions, are used in this program to study three generic forms of turbulent shear flows: a confined shear mixing layer, a recirculating flow established behind a sudden expansion, and a flow over a cavity in a channel.

The mixing of two streams initially flowing at two different velocities has been attributed, through extensive experimental and some numerical exploration, to the formation of a highly organized vorticity pattern. Our results in figures 1 and 2, describe the geometrical configuration and the dynamic interactions of vortex structures in this flow. The vortex sheet animated at the splitter plate rolls up into small vortex eddies, triggered by perturbations introduced in the numerical procedure. Small eddies interact by pairing, forming larger eddies. Numerical results indicate that

a pairing interaction is area-preserving, thus it occurs without extra irrotational fluid being mixed within the area occupied by vorticity. However, individual vortices grow by entraining surrounding fluid during their unencumbered flow. Figures 3 and 4 show that the two-dimensional numerical simulation can successfully predict average streamwise velocities and fluctuations. However, it overpredicts the cross stream fluctuations. The total sum of the two fluctuating components, computed in two dimensions, agrees with the total sum of the three fluctuating components measured experimentally. Thus, the disagreement is due to the lack of the three-dimensional effects, [2].

We have started a study on the effect of forcing, accomplished by superimposing small amplitude streamwise oscillations on the approaching stream, on enhancing or hampering the mixing process by intruding on the dynamics of the vorticity layer. Results of this simulation, shown in figures 5 and 6, indicate that forcing at the natural frequency of the layer, obtained by a spectral analysis of the velocity data of the unforced layer, causes an early roll-up of the vortex sheet into a set of eddies, accompanied by a delay in the pairing process. The response frequency--the frequency of formation of the eddies--is the same as the forcing frequency, i.e. a lock-in mechanism is established downstream of the splitter plate. On the other hand, forcing at a frequency around the first subharmonic promotes early pairing interactions, associated with a substantial increase in the thickness of the layer at the early stages of development. Frequently in the simulation, the pairing involves three eddies and is accomplished faster than two-eddy pairing in unforced layers. The effect of forcing decays quickly downstream and the layer resumes its growth as an unforced layer. Results are currently analyzed for a spectrum of forcing frequency and amplitudes, [3].

The lack of agreement between the two-dimensional computations and experimental data stimulated a study on three-dimensional vortex simulation that introduces systematically the processes of stretching and tilting in the vorticity dynamics. A vortex segment algorithm, based on discretizing the vorticity field among a number of worm-like filaments and treating each filament as a set of straight segments, has been formulated and is being coded for use with a temporally developing shear layer at high Reynolds number. Of particular interest is the formation of streamwise vortex patterns due to the spanwise fluctuations and their effect on the growth of the initial vorticity layer. Preliminary results indicate that streamwise perturbations constitute the most unstable mode, and that the formation and interactions of the spanwise vortex structures are insensitive to perturbations along their axes. The algorithm is computationally intensive, and is being revised for higher efficiency.

Recirculation zones are formed in most continuous flow combustion systems to stabilize turbulent flames by maintaining a constant supply of hot products. The dynamics of recirculating flows is complicated by the interaction between the separating shear layer and the recirculation bubble and is strongly dependent on the Reynolds number of the approaching stream, thus it represents a stronger challenge to numerical simulations. We applied the same vortex simulation to predict the changes in the flow structure with increasing the Reynolds number R. Four distinct regimes can be identified: a steady viscous flow at R=50, a laminar flow at R=125, a transition around R=500 and an early turbulent flow at R=5000, [4]. Figures 7 and 8 show instantaneous realizations of the streamline plots for R=125 and 5000. Currently, we are analyzing the time-dependent data to determine the most unstable frequency of this flow. This frequency will then be related to the dominant frequency of oscillation of the combustion process.

References

1. Ghoniem, A.F., "Numerical simulation of turbulent reacting flow," for presentation at the 1985 AMS-SIAM Summer Seminar on Reacting Flows: Combustion and Chemical Reactors, Cornell University, Ithaca, N.Y. July 1985.

2. Ng, K.K.,and Ghoniem, A.F., "Numerical Simulation of a Confined Shear Layer," for presentation at The 10th International Colloquium on Dynamics of Explosions and Reactive Systems, August 4-9, 1985, Berkeley, CA.

3. Ng, K.K., and Ghoniem, A.F., "Frequency-modulation of a developing shear layer," to be submitted to Phys. Fluids.

4. Ghoniem, A.F. and Sethian, J.A., "Dynamics of Turbulent Structures in a Recirculating Flow; a Computational Study," AIAA-85-0146.

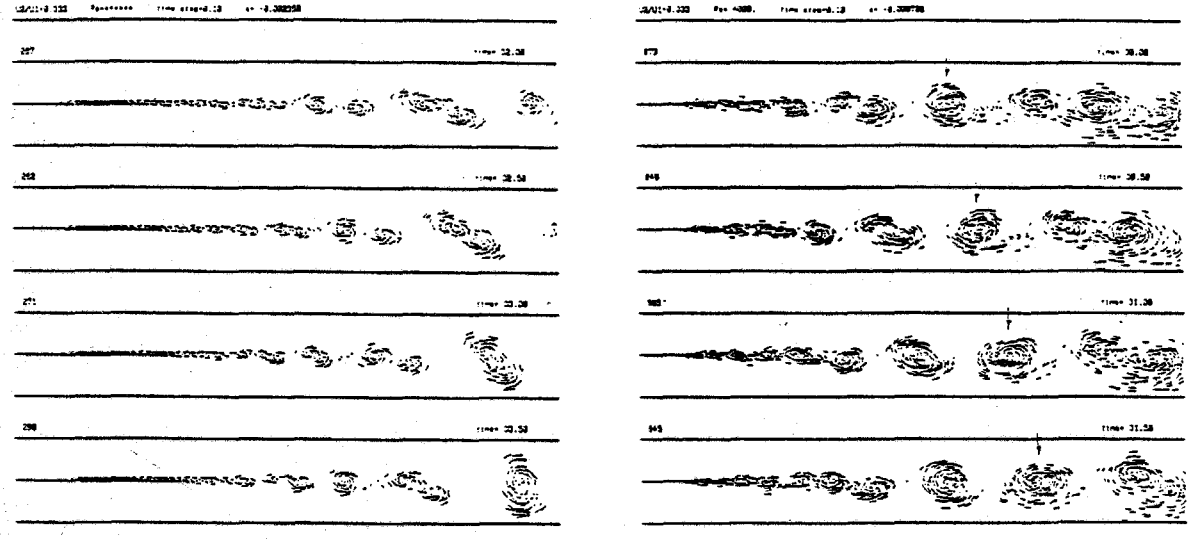

Figures 1 and 2 depicting the formation and dynamic interactions in an inviscid and a viscous (R=4000) shear layer.

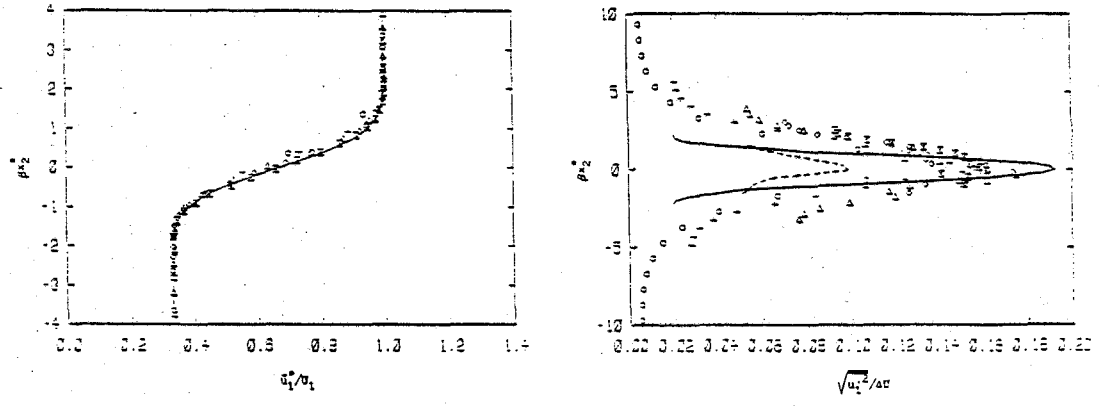

Figures 3 and 4 show the average streamwise velocity and fluctuations compared to experimental data.

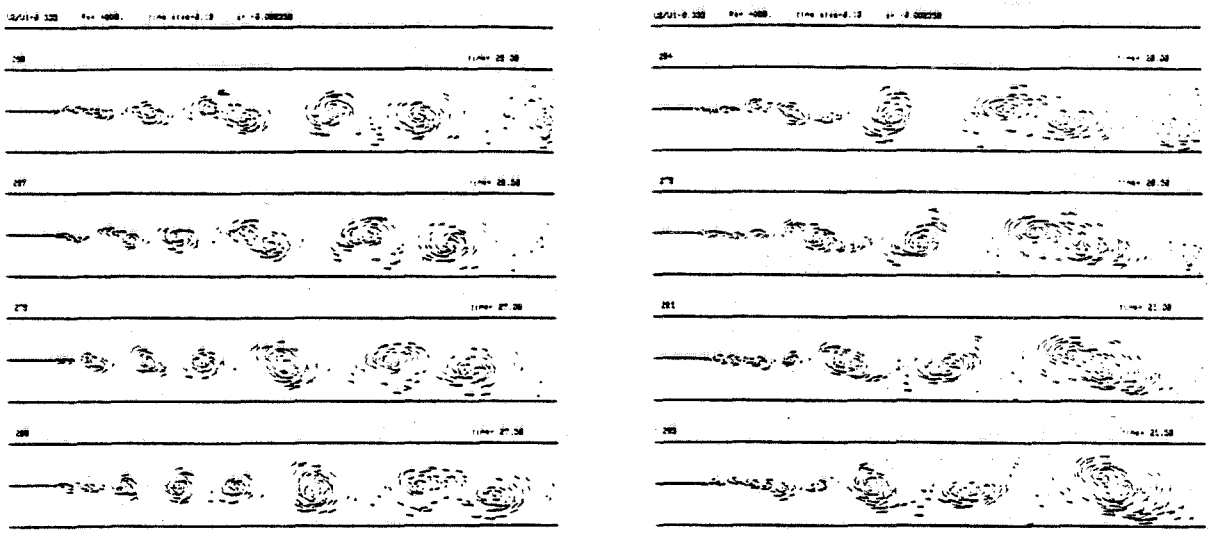

Figures 5 and 6 present the effect of forcing at the natural frequency and the first subharmonic, respectively, on the dynamics of the large eddies.

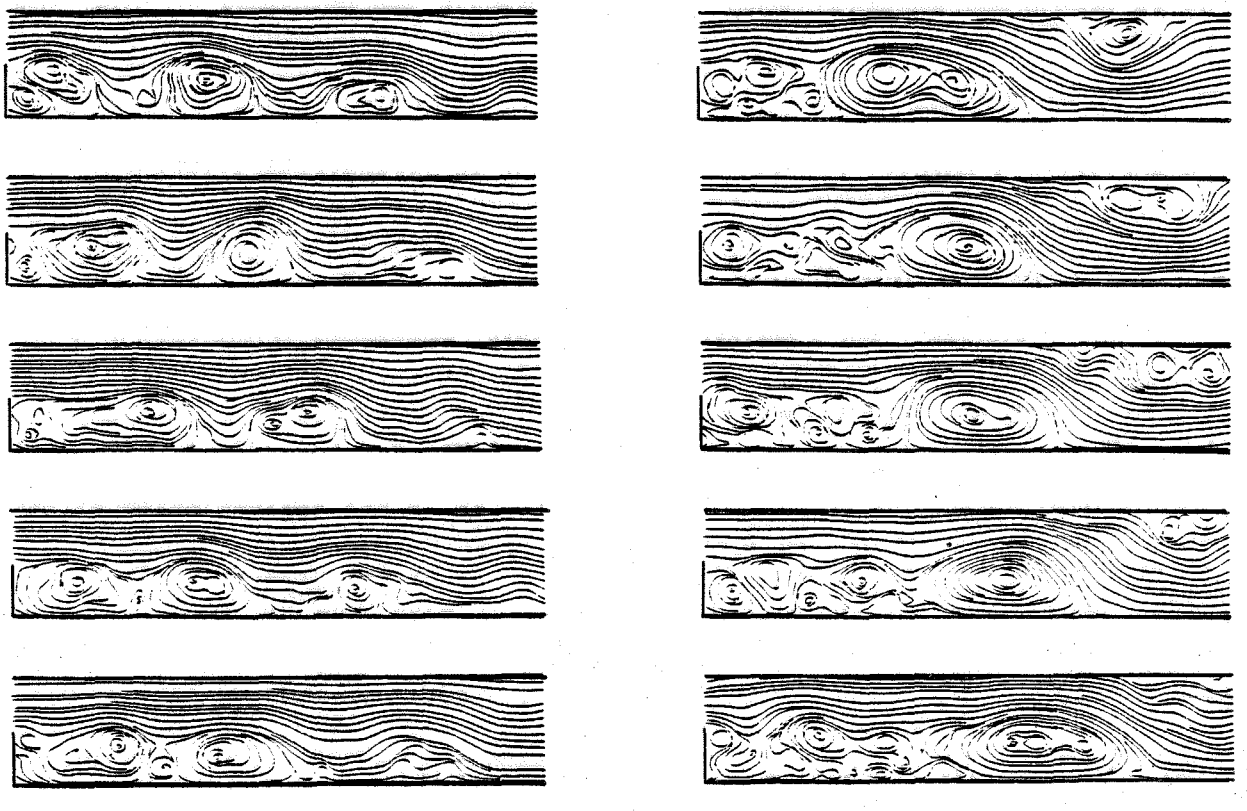

Figures 7 and 8 show the instantaneous streamline plots for R=125 and 5000, respectively, for a recirculating flow behind a step.

FUELS COMBUSTION RESEARCH

(A) Soot Formation and Aromatic Oxidation
(B) High Energy Density (Boron) Slurry Combustion

(AFOSR Contract No. F49620-82-K-0011)

Principal Investigators: Irvin Glassman, Frederick L. Dryer, Forman A. Williams

Department of Mechanical and Aerospace Engineering
Princeton University
Princeton, New Jersey 08544

SUMMARY/OVERVIEW

Recognizing the uncertainties as to future available fuel sources and characteristics, a research program that concentrates on chemically related combustion problems has been established at Princeton University. Current research encompasses the pyrolysis and oxidation of aliphatic hydrocarbons; the pyrolysis and oxidation of aromatic hydrocarbons; the mechanisms of soot formation and destruction; the vaporization/combustion properties of high energy density slurry fuels, particularly those containing boron. Attention is focused on problem areas associated with both current and future fuel properties with particular attention on the role of aromatic hydrocarbons and slurry fuels, particularly of boron.

Little is known about the processes which control the formation of soot in combustion systems and the effect of fuel type, particularly aromatics. By use of pre-mixed and diffusion flame systems in which flame temperatures are controlled, it is possible to determine the relative effects of flame temperature, equivalence ratio, C/H ratio and fuel structure in a particular system. Corresponding studies of the high temperature oxidation and pyrolysis mechanisms of aromatic, naphthenic and paraffinic fuels using the Princeton turbulent flow reactor are not only providing important kinetic data, but also the fundamental information necessary to understand the controlling processes in soot formation.

Thermochemical calculations demonstrate appreciable advantages associated with the addition of boron to fuels, particularly for air-breathing propulsion concepts. Isolated free droplet combustion and particle (cloud) suspension combustion techniques, together with theoretical studies, are used to elucidate and develop models for the combustion of high energy density slurry fuels, particularly those containing boron.

TECHNICAL DISCUSSION

Soot Formation and Aromatics Oxidation

During this period further measurements were made under pre-mixed flame conditions of the critical sooting equivalence ratio (Ψ_c) of fuel. To date, practically all possible types of hydrocarbon fuel structures have been evaluated.

More importantly, it has been shown that when compared at the same temperature an excellent correlation could be obtained by plotting Ψ_c (based on a stoichiometry to CO and H_2O) as a function of the total number of carbon to carbon bonds. A simple model of the processes occurring in a pre-mixed flame predicts that the size of the fuel molecule and the C/H ratio are the fundamental parameters which govern the rate of soot formation. Recall, it is the competitive reactions of fuel pyrolysis and hydroxyl attack on the percursors formed that govern soot formation under pre-mixed conditions (1). The size of the molecule determines the rate of pyrolysis of the fuel since size controls the radical pool. The C/H ratio essentially establishes the hydroxyl radical concentration. Since a double bond in the structure would be counted as two bonds and signifies less H, one can readily perceive why the parameter of number of C-C bond works so well. The model and all data have been reported in recent publications (2,3) and the data are shown in Figure 1. The importance of this correlation is that it implies that for pre-mixed conditions the original fuel structure plays no role in the soot formation process. To verify this implication mixtures of fuels were evaluated. As reported last time, mixture A tested is 33% and 66% ethene, and has the same C/H ratio as butene and the same average number of C-C bonds. Mixture B tested is 66% octene and 33% ethene and has the same C/H ratio and average number of C-C bonds as hexene. New data on acetylene/benzene mixtures have been obtained and as one will note (Figure 2), all mixture data fall on the correlating curve, thus confirming the concept.

Much new data have been obtained, as well, on sooting tendencies of fuel under diffusion flame conditions. All these data are shown in Figure 3, in which the log of one over the mass flow rate of the fuel (FFM) is plotted as a function of (1/T). The fact that straight line correlations were obtained for all fuels indicates that fuel pyrolysis is a controlling step on soot formation under diffusion flame conditions and fuel structure is important. In order to show the fuel trends clearly, all the data points have been omitted from Figure 3. The significance of these data is that if a fuel pyrolysis mechanism is known, its relative tendency to soot can be predicted. For example, it is known that cyclopropane immediately pyrolyzes to propene; thus, it is not surprising that the Princeton smoke height test results show that cylopropane and propene have the same tendency to soot. All the data and its analysis from our study of pyrolysis kinetics have been reported in other recent publications (4,5). Perhaps more importantly, Frenklach and co-workers (6,7) by shock tube measurements have found the same order of sooting tendencies of acetylene, butene, butadiene, allene and the aromatics. This agreement is most significant in that it gives further validation to the well controlled, simple Princeton smoke height experiment. Application of all our soot results to power plants is discussed in a recent AFOSR Report (3). New data have been obtained on benzene/hexene mixtures to determine the possibility of fuel mixture synergism. Figure 4 shows these results and would indicate no synergistic effect. This trend could be due to diffusion flame configuration in that the hexene could pyrolyze early in the flame and form soot before there is substantial indication of benzene pyrolysis.

During the past year, the experimental effort in the area of the oxidation of aromatics has been concentrated mainly on the flow reactor studies of normal and

isopropyl benzene. The experiments were aimed at testing the analogy between the reactions of the alkylated aromatics and those of the corresponding alkanes.

Experimental results from the oxidation of normal propyl benzene are presented in Figure 5. If selectivity for the abstraction of a benzylic hydrogen (the hydrogen attached to the carbon atoms next to the benzene ring) were very large, the only product from a radical attack on the propyl side chain would be styrene. The styrene would be produced by abstraction of a benzylic hydrogen followed by the loss of a methyl group. Indeed, the results show that styrene is an important product for this fuel; however, it is not the only major one. Therefore, benzylic hydrogen abstraction does not dominate the abstraction from the propyl group. In fact, the presence of toluene and benzaldehyde, early in the reaction strongly suggests that benzyl radicals are present. The most likely route to the benzyl radicals is the abstraction of a primary hydrogen from the end of the propyl group followed by loss of ethylene. The important conclusion to be drawn from these observations with respect to the analogy with the oxidation of propane is that the abstraction of all hydrogen from any site on the propyl side chain must be occurring, not simply from benzylic locations.

Based on the experience with n - propylbenzene, the analogy to the early reactions of propane was used to predict the major stable products that would be found in the oxidation of isopropyl benzene. Because the side chain of isopropyl benzene contains only benzylic and primary hydrogens, only two products are expected to result from radical attack on the side chain. The loss of a primary hydrogen should produce styrene and the abstraction of a benzylic hydrogen will yield methylstyrene. In fact, the experimental results of Figure 6 confirm these predictions. Thus, the analogy to alkanes successfully predicts the products of fuel consumption, and the ability to make qualitative predictions based on the analogy is confirmed.

In view of the simplicity of the experimental results for isopropyl benzene, an attempt was made to obtain the branching ratio for the production of styrene and methylstyrene for the oxidation of iso-propyl benzene. The ratio also represents the selectivity for benzylic hydrogen abstraction compared to primary hydrogen abstraction, and such kinetic information is critical to the eventual modelling of the oxidation of these aromatic fuels. Because the conditions chosen for these experiments ensure that consumption of intermediates is small compared to their production, the slopes of the two product concentrations are a good approximation to their rate of production. Thus, the ratio of the slopes of methyl styrene and styrene gives an overall selectivity for benzylic versus primary hydrogen abstraction. When the ratio is multiplied by six to eliminate the effect of the greater number of primary hydrogens, the selectivity for benzylic versus primary abstraction is 3.5 to 1 in favor of the benzylic (9,10). This selectivity represents the first result of its kind for aromatics undergoing oxidation.

The experimental studies of the oxidation of propyl benzene have been part of a series of examinations of the oxidation of alklated aromatics. Last year, the experimental results from a study of the oxidation of ethylbenzene were reported. Additional kinetic parameters have since been derived from the analysis of the ethylbenzene results. The path to this accomplishment began with

the closer scrutiny of the apparent first order disappearance of the fuel. Because radical attack is the primary path for fuel consumption, the rate equation for the fuel is simply

$$dF/dt = - k [X] [F]$$

where X is any radical or atom. Since the experiment was nearly isothermal, the constant value of k[X] implies that the concentration of the radicals is approximately constant. Given this apparent steady state concentration of radicals, the ethyl benzene mechanism was subjected to a steady state analysis, and the resulting differential equations were used in a linear regression analysis of the experimental data. This regression analysis produced values for the rates of production and consumption of styrene in the ethyl benzene oxidation. This technique has been applied to the other experimental results for ethyl benzene and has produced consistent results. The analysis of the ethyl benzene data is incorporated in a paper on ethyl benzene that has been submitted for publication.

High Energy Density (Boron) Slurry Combustion

Our work on boron and slurry combustion has progressed significantly in both theory and experiment. A paper of our experimental work on the combustion behavior of free boron slurry droplet was presented at the joint Central/Western States Section Meeting of the Combustion Institute (11).

First observations of the combustion properties of free boron/JP-10 slurry droplets were made in high temperature, atmospheric pressure oxidizing streams under low Reynolds number conditions. Isolated droplets of commercially available slurries with initial diameter between 400 and 500 micrometers and initial solid mass fraction of 0.3 were studied using single-lens reflex and high speed cine photography under both self-illuminated and backlighted conditions. During the experiments, the mole fraction of oxygen in the surrounding high temperature environment (ca. 1900K) was varied between 0.07 and 0.39. Boron slurry droplets burned for short periods of time with a liquid vapor supported envelope diffusion flame structure, but then experienced violent disruption for all cases studied. The intensity of the disruption process was found to be strongly influenced by the temperature of the envelope diffusion flame. The ignition of the boron particles emitted from the initial fuel droplet was also affected by this flame temperature. As the envelope diffusion flame temperature was increased by increasing the environmental oxygen content, the disruption occurred at earlier times in the vapor phase buring period. Ignition of the boron particles at high envelope flame temperatures (> 2500K) was accompanied by a "popping" sound and a bright greenish flash of luminosity. The secondary atomization of the primary slurry droplet yielded much smaller solid agglomerates (< 50 microns) which were consumed very rapidly. The spontaneous atomization phenomena may be related to the presence of solids in this slurry as well as to the liquid phase composition.

The observed disruption appears to result from entrapment of the liquid components inside the droplet with subsequent superheating prior to vaporization.

Since a large rotating droplet usually emerges from the region of disruption, it appears that the site of the disruption is near the surface of the primary slurry droplet rather than deep in the interior. A number of different effects may contribute to this behavior. One possibility is that the presence of boron does not play an essential role. Less volatile additives with high Lewis numbers inside the liquid fuel may form a thin shell with an elevated surface temperature during vaporization, leading to homogeneous nucleation of the fuel inside; the nucleation site will be near the surface if the shell is thin and if the liquid temperature is appreciably nonuniform. The boron seems likely to modify this well-known mechanism of binary liquid mixtures by providing internal heterogeneous nucleation sites on slurry particles, thereby inducing earlier and less intense disruption. An alternative role of less volatile additives is that they may be heated to an extent at the droplet surface such that chemical interactions cause physical binding and agglomeration of boron particles at the surface. A relatively nonporous boron shell may thus develop, inhibiting vaporization, bringing the flame closer to the surface, and conducting heat into the interior, thereby promoting pressure buildup through internal vaporization that results in disruption. It is possible that this resistive boron shell would develop even for the burning of a sufficiently highly loaded slurry of a neat fuel without additives. Further study is needed to ascertain the relative importance of these various possibilities. Additional tests including work on the effects of various experimental parameters, such as solid loading, are in progress.

Theoretical and experimental studies have been completed concerning the transient processes that occur in two slurry droplet models during the period of liquid vaporization and combustion. For the first model (12), the solid loading is large and the overall droplet diameter, d, remains constant as the liquid vaporizes. In the second model, the solid loading is small and the droplet diameter decreases during part of the liquid vaporization period. The analysis employed theoretical techniques of singular perturbations with the expansion parameter, considered to be large or small, being the ratio of the energy required to raise the sphere to the liquid vaporization temperature, to that required for liquid vaporization. Theoretical results for both models include explicit expressions for the internal droplet temperature profiles (needed to predict disruptive burning), liquid vaporization time and flame radius. The various results and implications of the first model are discussed in a publication (12). The second model shows a classical d^2-law as the liquid vaporizes.

To test these theoretical analyses, experiments are in progress on the combustion of JP-10/boron slurry droplets suspended on fibers in air at room temperature and atmospheric pressure. Burning times for the hydrocarbon component and the time dependence of the droplet shape are recorded by high-speed, high-magnification cinematography for droplets of initial diameters between 0.8 and 3 mm and boron loadings between 0 and 70% by weight. The experimental results support the theoretical model in various qualitative respects. For example, at low boron loadings the flame diameter decreases during burning, but at high boron loadings, it remains nearly constant until burnout, in accord with theory. The d^2-law was observed experimentally for pure JP-10 droplets and at low boron loadings (<30%), until vaporization caused appreciable agglomeration, but at

high boron loadings (>50%) the droplet diameter remained approximately consta The experimental results are being used to refine estimates of properties for calculating burning rates. There are preliminary indications that in the hig loaded slurries the solid causes inhanced gas-phase fuel pyrolysis to lighter species that result in an increased thermal conductivty which thereby decrease the burning time by a much as 30%. Studies are continuing to check these conclusions.

REFERENCES

1. Glassman, I., "Phenomenological Models of Soot Processes in Combustion," AFOSR-TR-79-1147.

2. Takahashi, F. and Glassman, I., "Interpretation of Sooting Correlations Under Pre-Mixed Conditions," Eastern States Section/The Combustion Institute Paper No. 56 (1983).

3. Takahashi, F. and Glassman, I., "Sooting Correlations for Pre-Mixed Flames," Comb. Sci. and Tech. 37, 1 (1984).

4. Sidebotham, G. and Glassman, I., "Sooting Behavior of Cyclic Hydrocarbons in Laminar Diffusion," Eastern States Section/The Combustion Institute Paper No. 61 (1983).

5. Gomez, A., Sidebotham, G. and Glassman, I., "Sooting Behavior in Temperature Controlled Laminar Diffusion Flames," Comb. and Flame, 58, 45 (1984).

6. Frenklach, M., Taki, S., Durgaprasad, M.B. and Matula, R.A., "Soot Formation in Shock-Tube Pyrolysis of Acetylene, Allene and 1,3-Butadiene," Comb. and Flame 54, 81 (1983).

7. Frenklach, M., private communication (1984).

8. Glassman, I., "Soot Reduction in Power Plants," Princeton University MAE Dept. Report No. 1632, AFOSR-TR, 1983.

9. Litzinger, T.A., Brezinsky, K., and Glassman, I., "A Comparison of Results from the Oxidation of Normal and Isopropyl Benzene," Eastern States Section/The Combustion Institute Meeting, Paper No. 90, November 1984.

10. Litzinger, T.A., Brezinsky, K. and Glassman, I., "The Role of Selectivity for Radical Abstraction of Hydrogen Atoms in the Oxidation of Normal and Isopropyl Benzene" to be presented at the International Conference on Chemical Kinetics, National Bureau of Standards, June 1985.

11. Takahashi, F., Dryer, F.L., and Williams, F.A., "Combustion Behavior of Free Boron Slurry Droplets," Central/Western States section/The Combustion Institute Meeting, Paper No. 2-2B, April 1985; Princeton University MAE Department, Report No. 1702, 1985; AFOSR-TR (applied for), 1985.

12. Antaki, P., "Transient Processes in a Rigid Slurry Droplet Driving Liquid Vaporization and Combustion," Comb. Sci. and Tech., (to appear).

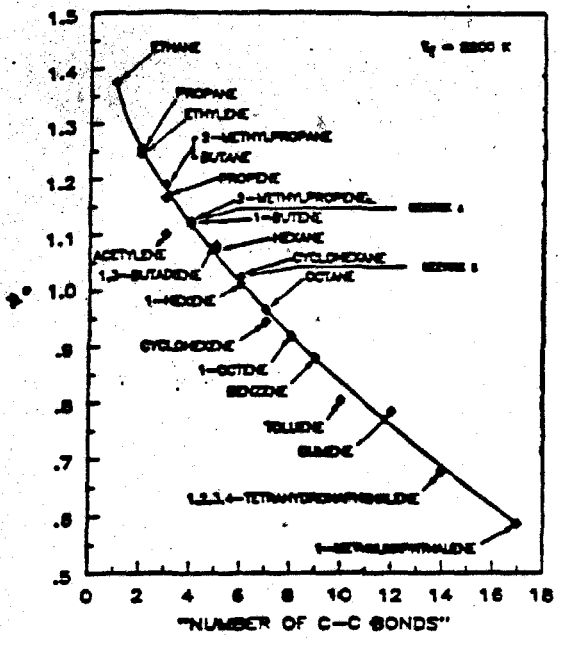

FIGURE 1 The pre-mixed flame correlation between the effective equivalence ratio to soot (ψ_c) at 2200 K and the number of C-C bonds in various fuels and fuel mixtures.

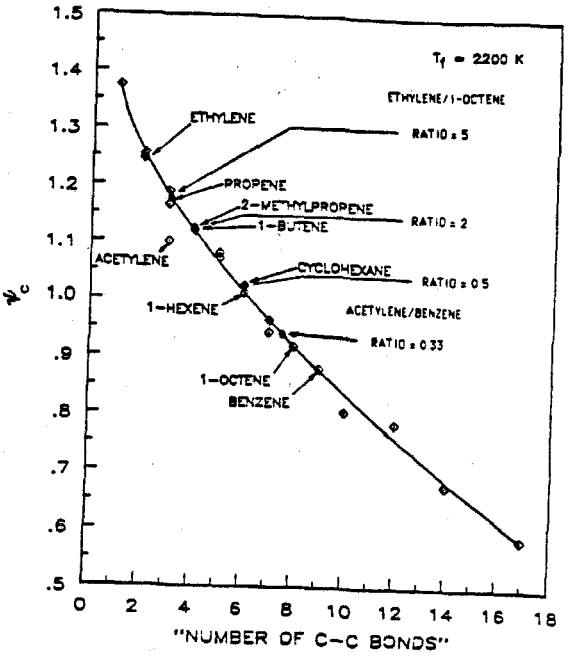

FIGURE 2 The correlation between the critical effective equivalence ratio at soot onset at 2200K and the number of c-c bonds.

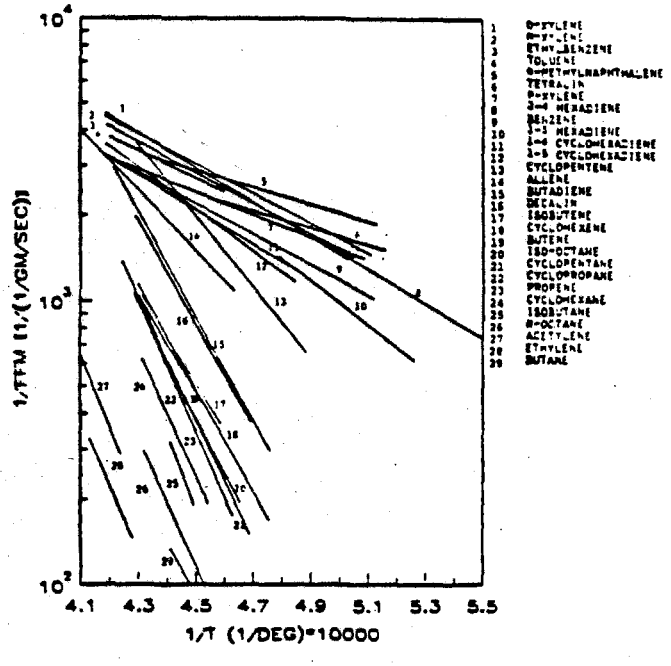

FIGURE 3 Fuel sooting tendencies under diffusion flame conditions. The log of the inverse of the fuel mass flow rate at the sooting height is plotted as a function of the inverse calculated stoichiometric flame temperature. The temperature variation is by nitrogen dilution.

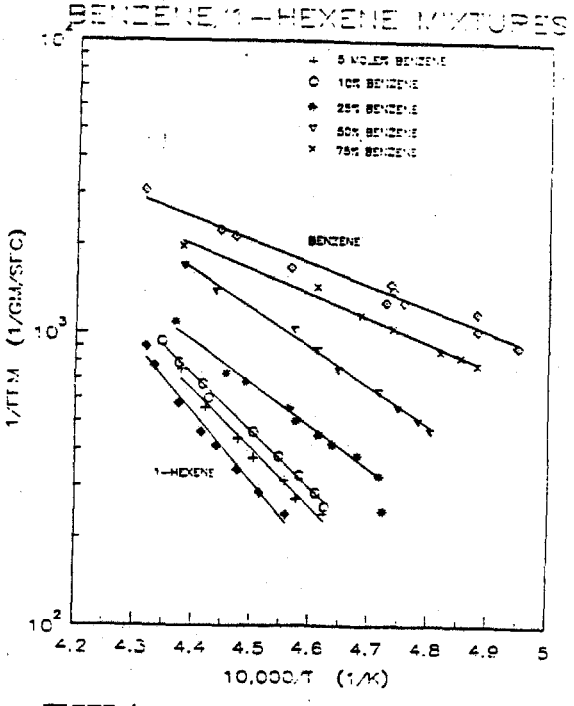

FIGURE 4 Sooting tendency as a function of adiabatic flame temperature.

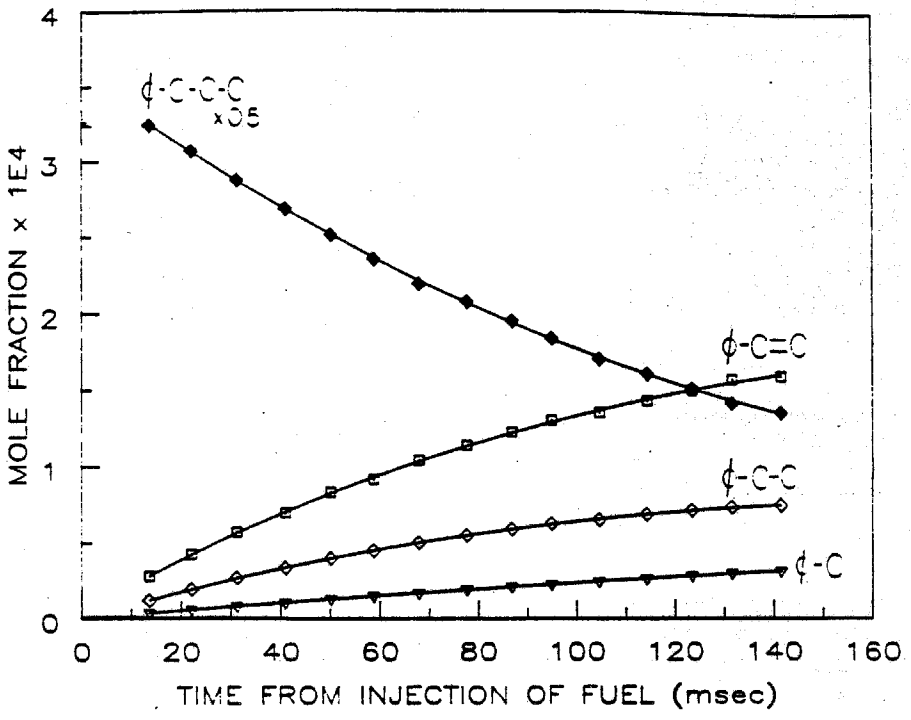

FIGURE 5

Species profiles from the oxidation of n-propyl benzene

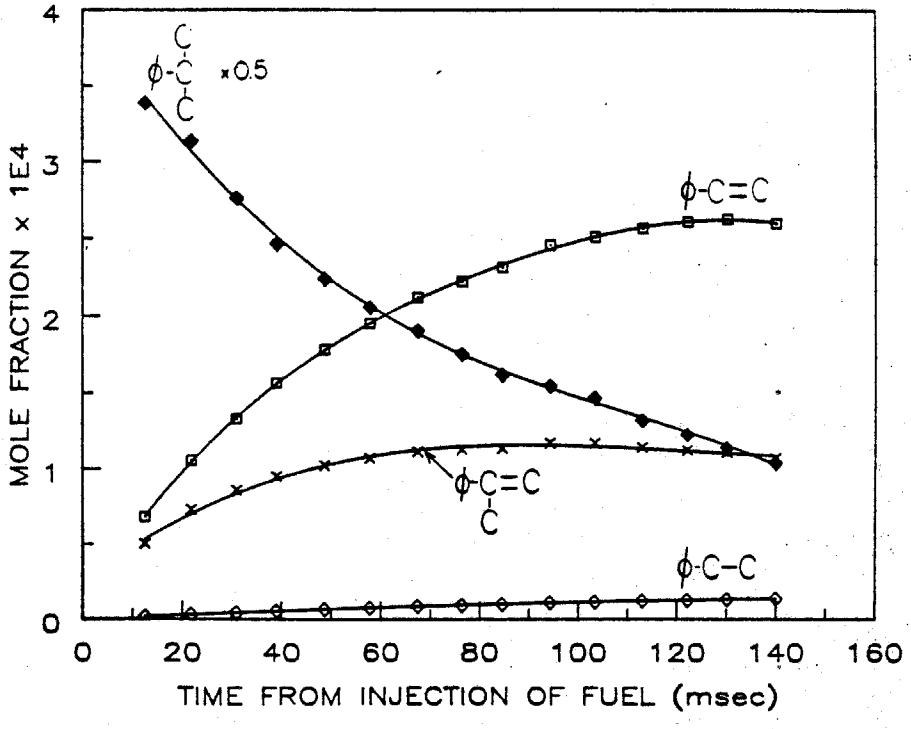

FIGURE 6

Species profiles from the oxidation of iso-propyl benzene

ABSTRACT

AFOSR/ONR Contractors Meeting in Combustion
24July 1984

TURBULENT COMBUSTION RESEARCH AT SANDIA NATIONAL LABORATORIES

Sheridan C. Johnston
Sandia National Laboratories
Livermore, CA 94550

A broad overview is given of current turbulent reacting flow research at the Sandia Combustion Research Facility, which is supported by the Department of Energy. The technical theme of the talk is the competitive role played by fluid mixing and chemical kinetics in turbulent combustion. These competitive effects are investigated using advanced laser diagnostics (e.g., two-dimensional imaging) and computer modeling approaches (e.g., vortex dynamics). Premixed flames are described in which laser-induced fluorescence is used to obtain quantitative images of the OH concentration behind a flame front. Results of transient flames generated by a combustion torch suggest a transition between flame quenching and subsequent reignition as the Damkohler number is increased. Axisymmetric vortex dynamics calculations are compared to these measurements. Nonpremixed flames are discussed and include turbulent jet flames (parabolic flow) and recirculating jet flames (elliptic flow). Raman scattering measurements obtained at single-point locations in these flames indicate that high strain rates cause local extinction; fluorescence imaging of C_2 in the same flames indicates that there are, indeed, holes in the flame sheet. Simultaneous imaging obtained using fluorescence and Rayleigh scattering reveal the complex flame structure involved. A sooting laminar flame (having the simplest fluid mechanics but the most complex chemistry) is examined using linear and nonlinear light scattering techniques, which provide information about soot generation rates, soot particle size, and temperature.

NUMERICAL SIMULATIONS OF SHEAR LAYER/ACOUSTIC WAVE INTERACTIONS IN A RAMJET COMBUSTOR

(ONR Contract No. N00014-84-C-0359)

Principal Investigators: Wen-Huei Jou and Suresh Menon

Flow Research Company
21414 68th Avenue South
Kent, Washington 98032

SUMMARY/OVERVIEW:

Numerical simulations are employed to understand the intricate physics of acoustic/vorticity interactions in a ramjet combustion chamber. The compressible Navier-Stokes equations are solved for cold flows using MacCormack's method. Both unforced flows and acoustically forced flows are simulated. The computed velocity field can be decomposed at any instance into potential (acoustic) and solenoidal (vortical) components to illuminate the physics. At present, a code is constructed and preliminary simulations are being performed. Results show that the shear layer behind the backward-facing step rolls up at the frequency of the most unstable mode, and the resulting vortices go through two pairings before re-attachment. Possible resonance mechanisms will be studied by matching the frequency of the acoustic oscillations and various frequencies of the vortical motions.

TECHNICAL DISCUSSION

Recent experiments by Schadow and his co-workers (1984, 1985) suggest that the vortex dynamics is strongly coupled with the acoustic oscillations inside a dump combustor. This coupling may affect the mixing of the gas and, hence, the combustion processes in a ramjet. The acoustic wave generated by the heat release due to combustion can then in turn affect the dynamics of the vortex and close the loop of a possible resonance.

The interaction is extremely complex. Only a simple analysis can be performed. For example, a simple linear acoustic analysis of a dump geometry with a long inlet and combustion chamber using matched asymptotic expansion shows that the lowest order eigen frequency can be predicted by the one-dimensional approximation. However, the detailed two-dimensional mode shape near the dump contains a singularity at the convex corner. This singularity implies that the acoustically induced disturbance there can be large locally, although the overall amplitude is small. One would expect the same conclusion for a diffraction problem in a propagation case. The resulting effect of this locally significant disturbance at the vicinity of the corner on the dynamics of the shear layer behind the step can be important. Through the convection of vorticity by an acoustically induced velocity field, it provides a large initial disturbance for the instability of the shear layer. On the other hand, the shear layer rollup and pairing provides a source of acoustic radiation. This type of simple analysis can only provide some initial understanding of the physics. Numerical simulations of the process can give a

great deal of insight into the physics involved. The present paper describes the initial effort of cold flow simulations. These simulations can reveal the nature of the first part of the resonance loop, i.e. the acoustic wave/shear layer interaction.

Axisymmetric compressible Navier-Stokes equation is solved by MacCormack's finite volume scheme. A body-fitted computational grid is generated. Near the wall of the inlet duct, grid lines are clustered to resolve the boundary layer. Computations are initiated by opening a valve at the downstream boundary. The expansion wave propagating upstream starts the flow through the device. The flow settles to a quasi-stationary oscillation after 10 longitudinal acoustic oscillations. Numerical boundary conditions are carefully studied to eliminate the possibility of generating nonphysical acoustic waves by incorrect boundary conditions.

Initial computations for laminar flow show the following features. The shear layer rolls up at a frequency that corresponds to the most unstable mode based on the momentum thickness at the step, i.e.,

$$f = \frac{0.018\ U}{\theta}$$

These vortices go through two pairings before re-attachment. The second pairing occurs alternatively. The vortices are convected into the boundary layer on the combustor wall, where the vorticity is of opposite sign, creating a row of counter-rotating vortices there. Part of the time sequence of vorticity contour plots is given in Figure 1.

Vorticity and pressure are recorded at different locations in the computational domain. These time histories are Fourier analyzed to obtain the spectrum. A typical example for vorticity is shown in Figure 2. A peak at the vortex rollup frequency is obvious. The pressure spectrum shows a dominant longitudinal frequency as well as a peak near the transverse mode. However, the pressure contains both the contribution from the acoustic motion and the vortical motion, and it is difficult to interpret the results. Also, it is known (Yates, 1979) that a row of vortices in a shear flow can produce a broad-band acoustic spectrum under excitation of a pure tone. We have developed a data reduction technique to separate the acoustic component of the velocity field from the computed velocity field. Figure 3a shows the stream function contour for the solenoidal field computed based on the vorticity field at a given time. Figure 3b and 3c give the contour of solenoidal velocity field (u, v) respectively. The acoustic velocity field can be obtained by subtracting the solenoidal field from the numerically computed velocity field. This separation can give us better insight to the physics.

References

Schadow, K. C., Wilson, K. J., Crump, J. E., and Foster, J. B. (1984) "Interaction Between Acoustics and Subsonic Ducted Flow with Dump," AIAA-84-0530, January.

Schadow, K. C., and Wilson, K. J. (1985) "Characterization of Large-Scale Structures in a Forced Ducted Flow with Dump," AIAA-85-0080, January.

Yates, J. E. (1979) "A Study of Scattering, Production, and Stimulated Emission of Sound by Vortex Flows," NASA Contractor Report No. 3139, May.

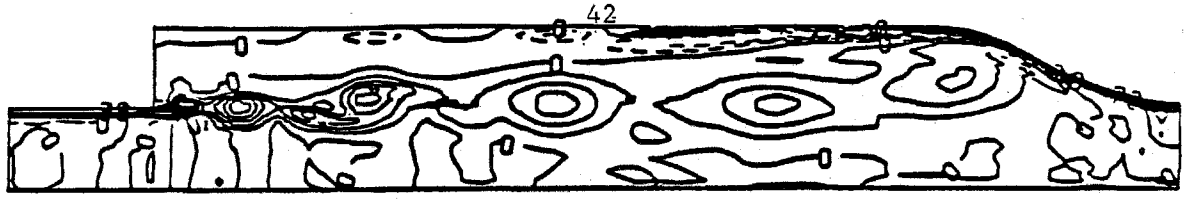

IST=9000. T=0.0280s
CØNTØUR FRØM -0.162E 06 TØ 0.720E 05
CØNTØUR INTERVAL IS 0.600E 04 SCALED BY 0.100E-02

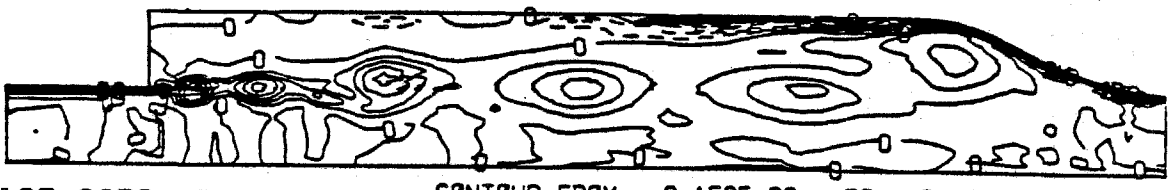

IST=9050. T=0.0282s
CØNTØUR FRØM -0.150E 06 TØ 0.192E 06
CØNTØUR INTERVAL IS 0.600E 04 SCALED BY 0.100E-02

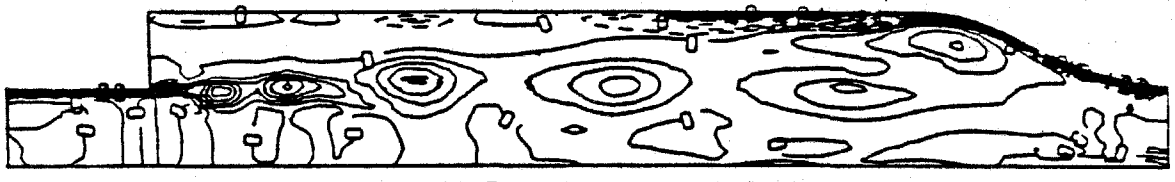

IST=9100. T=0.0283s
CØNTØUR FRØM -0.186E 06 TØ 0.186E 06
CØNTØUR INTERVAL IS 0.600E 04 SCALED BY 0.100E-02

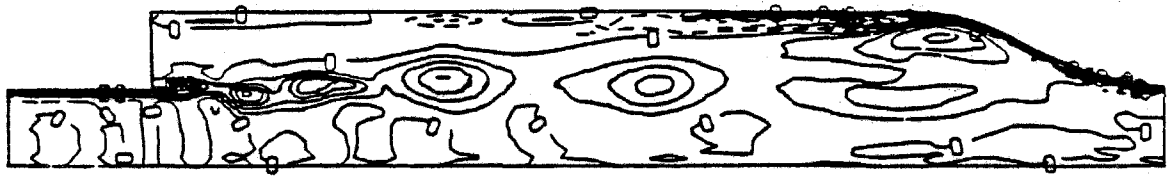

IST=9150. T=0.0285s
CØNTØUR FRØM -0.186E 06 TØ 0.174E 06
CØNTØUR INTERVAL IS 0.600E 04 SCALED BY 0.100E-02

IST=9200. T=0.0286s
CØNTØUR FRØM -0.210E 06 TØ 0.168E 06
CØNTØUR INTERVAL IS 0.600E 04 SCALED BY 0.100E-02

IST=9250. T=0.0287s
CØNTØUR FRØM -0.204E 06 TØ 0.156E 06
CØNTØUR INTERVAL IS 0.600E 04 SCALED BY 0.100E-02

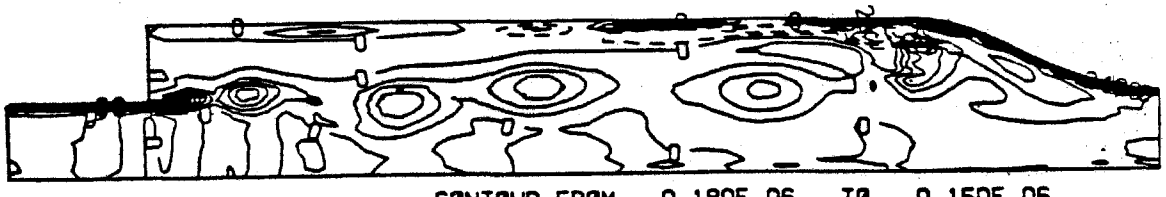

IST=9300. T=0.0290s
CØNTØUR FRØM -0.180E 06 TØ 0.150E 06
CØNTØUR INTERVAL IS 0.600E 04 SCALED BY 0.100E-02

Figure 1. Time sequence of vorticity contours for unforced flow.

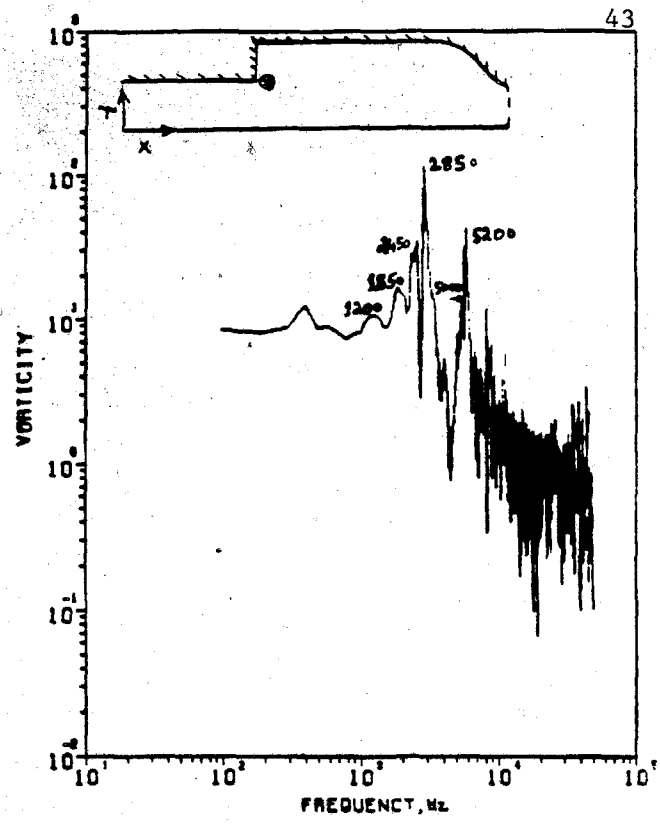

Figure 2. Vorticity Spectrum in the shear layer. Location is indicated by ⊗ in the inset figure.

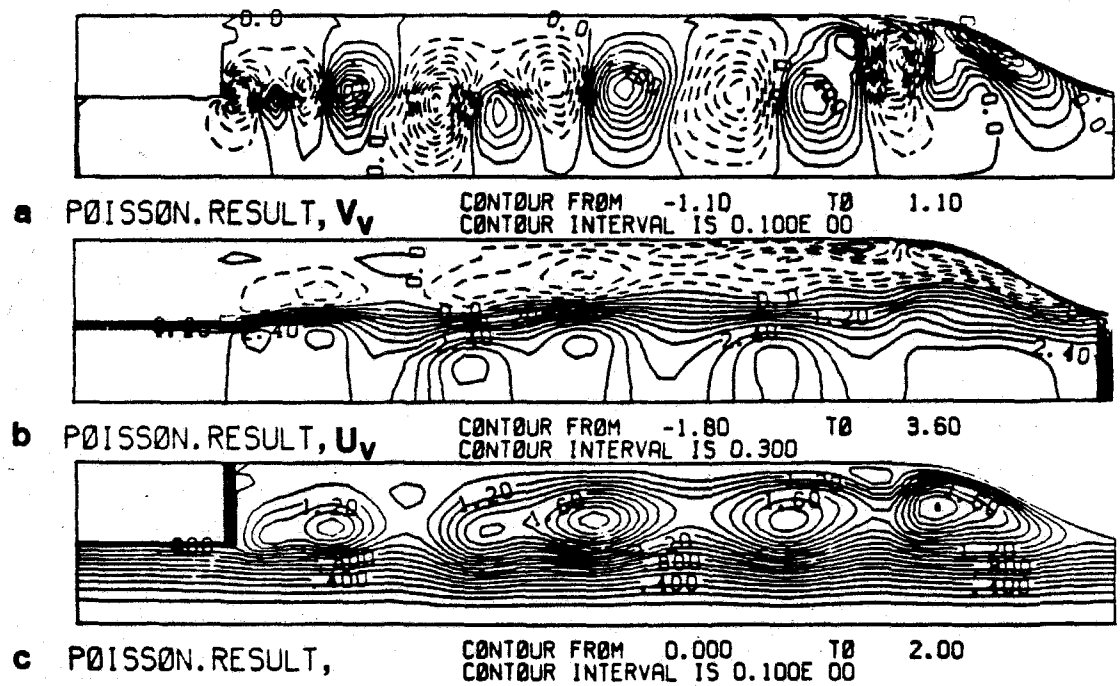

Figure 3. Solution for the Solenoid field at time, t = 0.0290 sec.

a The Transverse Velocity contours, V_V.

b The Streamwise Velocity contours, U_V.

c The Streamfunction contours,

DIRECT NUMERICAL SIMULATION OF AN UNPREMIXED TURBULENT JET FLAME

(AFOSR Contract No. F49620-85-C-00067DEF)

Principal Investigators: Wen-Huei Jou, Ralph W. Metcalfe and Peyman Givi

Flow Research Company
21414 68th Avenue South
Kent, Washington 98032

SUMMARY/OVERVIEW:

The purpose of this research is to use direct numerical simulation techniques to study combustion in turbulent diffusion flames and, in particular, to study flame extinction and liftoff phenomena. This method consists of accurately solving the time development of the relevant evolution equations (e.g., the time-dependent, nonlinear Navier-Stokes and reaction-convection-diffusion equations). A spatially developing plane jet is being studied. The first problem, dealing with the development of the proper computational tools and a method of implementing inflow/outflow boundary conditions for such flows, has been the major goal of the initial phase of this work. Application of the model to the reacting flow problem is the goal of upcoming research: First, we plan to modify the code to solve for the evolution of species quantities with temperature dependent reaction rates. Next, simulation of ignition and the study of flame propagation/stabilization will be considered, and finally the question of flame extinction, caused by the rollup of the vortices, will be addressed.

TECHNICAL DISCUSSION

Numerical predictions of turbulent diffusion flames have been the subject of numerous studies in recent years (1,2). In most of these studies, some kind of turbulence model, in one way or another, has been employed for the statistical prediction of hydro-chemical quantities of the turbulent field. The results have been very useful in answering some of the questions regarding turbulence-chemistry interactions in unpremixed systems. However, since some of the "physics" of the problem are modeled a priori, the results are of limited value in increasing our knowledge of the basic physics of such flows.

The ongoing work is an attempt to numerically simulate such flows directly without modeling. In particular, our attention is focused on the flame extinction and liftoff phenomena that occur in such flames (3). The calculations being performed employ a pseudospectral and a finite difference algorithm for solving the conservation equations for mass, momentum, species and energy for a turbulent reacting plane jet. Due to numerical limitations on the resolution, only moderate Reynolds and Damkohler numbers can be simulated. In order that the local Damkohler number be small enough for flame extinction to occur, a slow reaction (high activation energy) must be employed. In fact, this number can be varied to study its effect on the flame extinction problem. Based on the theory of Peters and Williams (3), a flame will extinguish itself if the strain rate, based on the dissipation of a

conserved scalar, is sufficiently high that the local reduced Damkohler number is lower than a critical value (4). This theory will be examined by correlating the flame extinction with the local dissipation rate using direct numerical simulations.

Recently, the direct numerical simulation technique has been successfully utilized in the study of temporally growing, chemically reacting turbulent mixing layers (5,6). In these calculations, the flow is assumed to be periodic in both the streamwise and the cross-stream directions. Pseudospectral methods have been employed for the calculations, and there have been encouraging comparisons between the simulation results and experimental data. Despite this success, however, there are basic deficiencies in employing such procedures for systems that are spatial in nature. For example, in order to treat spatially growing mixing layers numerically, inflow/outflow boundary conditions are needed, and numerical procedures have to be developed to be applicable for a nonperiodic computational domain.

The first step in this research, therefore, is to develop and implement numerical techniques that will enable us to perform simulations of spatially developing phenomena, such as the liftoff of diffusion jet flames. To enhance numerical resolution, only half of a plane jet is considered: as a model problem, we have selected a two-dimensional, nonreacting planar mixing layer, where two parallel flowing streams with different velocities begin to mix downstream of the trailing edge of a splitter plate partition.

For the laminar spatially developing mixing layer, a velocity profile containing a thin shear layer between the two streams is specified at the inflow. A zero-gradient condition at the downstream boundary is imposed to solve the equations with minimal upstream influence. Vortex rollup can be simulated by imposing a small periodic disturbance at the inflow in the form of the most unstable mode and its subharmonic.

Sample Results

For this two-dimensional configuration, a pseudospectral Fourier method (see Refs. 5 and 6) has been used in the cross-flow direction. In the streamwise direction a second-order-accurate finite difference method with equally spaced grid points has been employed. A hyperbolic tangent velocity profile is specified at the upstream boundary. The perturbations corresponding to the most unstable mode for a spatially growing mixing layer and its first subharmonic are determined from linear stability theory (7,8).

Our first simulations with a coarse mesh have focused on the effects of the most unstable perturbation and its first subharmonic. The effects of higher subharmonics will be reported later. The flow is conveniently characterized by two nondimensional parameters: First, the Reynolds number, $Re = (U_1 + U_2)\,\lambda/2\nu$, based on the initial shear layer thickness and kinematic viscosity, and second, the velocity ratio, $R = (U_1 - U_2)/(U_1 + U_2)$. For the coarse mesh calculations reported below, we have only considered very small Reynolds numbers ($Re \simeq 20$), and the value of R is set equal to 0.5.

In Figure 1, we present vorticity contour plots in the region between $0 < x/\lambda < 96$ and $0 < y/\lambda < 32$, where x and y are streamwise and transverse coordinates. There are 128 finite difference grid points in the x-direction and 32 Fourier modes in the y direction. A perturbation in the form of the most unstable mode is applied at $x = 0$. The rollup of this fundamental mode is shown clearly on this figure by the formation of vortices that are created at equal wavelengths.

The effects of adding the first subharmonic are shown in Figure 2. In this figure we present vorticity contour plots in the region between $0 < x/\lambda < 64$ with 128 grid points and $0 < y/\lambda < 32$ with 64 Fourier modes. The results of the vortex dynamics predicted here are in agreement with that of Davis and Moore (9), in the sense that the additional subharmonic would induce one merging. Figure 3 is a magnification of the vortex pairing occurring in Figure 2.

The fast decay of vorticity, shown in Figures 1-2 is due to the very low Reynolds number employed in the computations. More calculations with much higher Reynolds numbers are presently under way.

Work is continuing on the development of more accurate numerical schemes in the streamwise direction as well as for chemical reaction equations. To date, however, the results of the few simple numerical experiments that have been conducted have been encouraging.

References

(1) Bilger, R. W. (1980) "Turbulent Reacting Flows," edited by P. A. Libby and F. A. Williams, Springer-Verlag, New York, pp. 65-113.

(2) Givi, P. (1984) "Turbulent Reacting Flows," Ph.D. Thesis, Department of Mechanical Engineering, Carnegie-Mellon University, Pittsburgh, PA.

(3) Peters, N., and Williams, F. A. (1983) AIAA Journal, Vol. 21, No. 3, pp. 423-429.

(4) Linan, A. (1974) Acta Astronautica, Vol. 1, pp. 1007-1039.

(5) Riley, J. J., and Metcalfe, R. W. (1985) AIAA Paper 85-0321.

(6) McMurtry, P. A., Jou, W.-H., Riley, J. J., and Metcalfe, R. W. (1983) AIAA Paper 85-0143.

(7) Michalke, A. (1965) Journal of Fluid Mechanics, Vol. 23, Part 3, pp. 521-544.

(8) Monkewitz, P. A., and Huerre, P. (1982) Physics of Fluids, Vol. 25, No. 7, pp. 1137-1143.

(9) Davis, R. W., and Moore, E. F. (1985) Physics of Fluids, to appear.

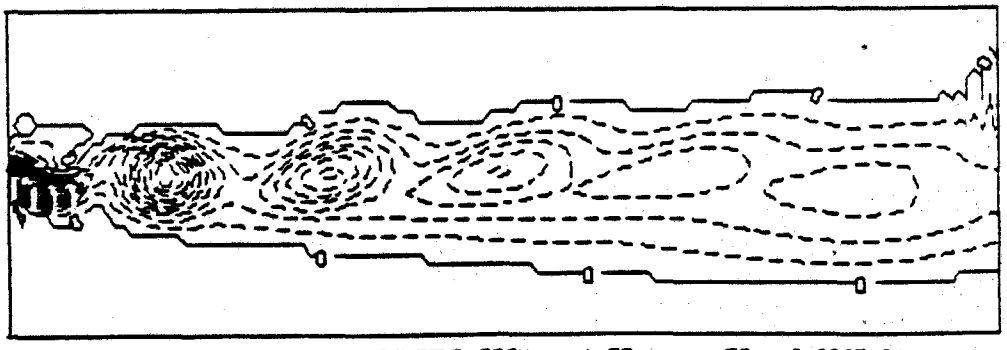

3367R

FIGURE 1

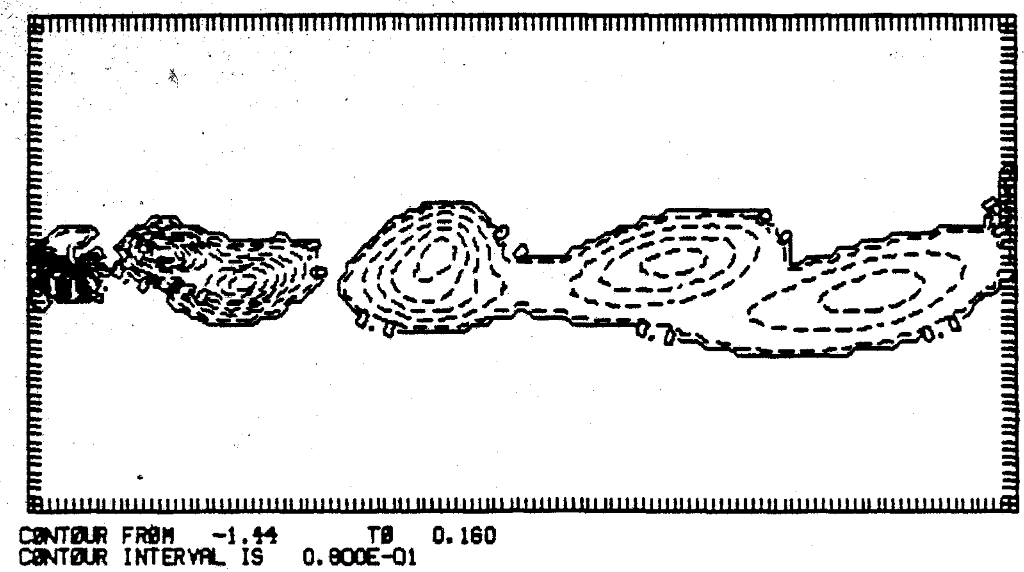

FIGURE 2

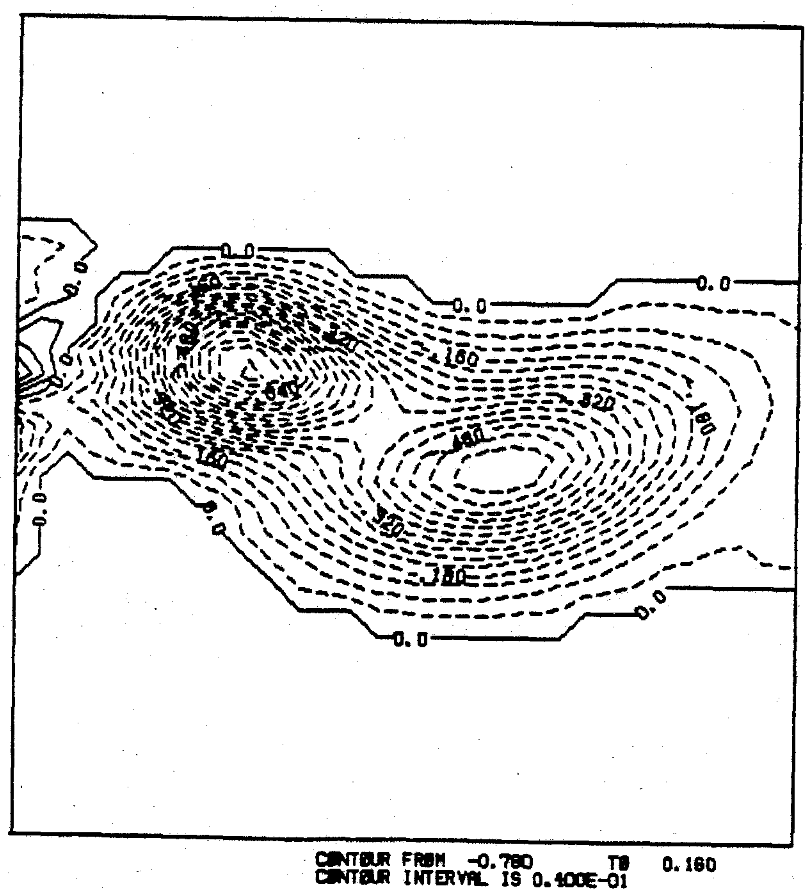

FIGURE 3

ASYNCHRONOUS OPTICAL SAMPLING FOR LASER-BASED COMBUSTION DIAGNOSTICS IN HIGH PRESSURE FLAMES

AFOSR Grant No. AFOSR-84-0323

Galen B. King
Normand M. Laurendeau
Fred E. Lytle

Flame Diagnostics Laboratory
School of Mechanical Engineering
Purdue University
West Lafayette, IN 47907

SUMMARY/OVERVIEW:

This grant is concerned with the development and subsequent testing of a new laser-based combustion diagnostic for the quantitative measurement of both major and minor species concentrations in high pressure flames. The technique, called Asynchronous Optical Sampling (AOS), is a state-of-the-art improvement in picosecond laser spectroscopy. AOS is a pump/probe method which will allow determination of both the electronic quenching rates and the state-to-state relaxation rates which are necessary for quantitative application of both laser-induced and laser-saturated fluorescence at high pressures. The specific goal of the project is to develop and prove the viability of the AOS technique as a practical combustion diagnostic. This will be achieved through measurements of the hydroxal radical in simple flames. Useful emission-based measurements require "real time" corrections for the effects of quenching; the AOS method can provide this capability.

TECHNICAL DISCUSSION

Pump/probe methods have become a standard technique for the measurement of time-resolved spectra. The AOS technique is a novel way of applying the pump/probe method. It overcomes many of the temporal problems inherent to the method; moreover, quenching rates can be obtained on a time scale necessary for practical combustion measurements.

In the AOS method, rather than using a single Nd:YAG laser to drive both the pump and probe dye lasers and an optical delay line to control the relative time difference between the two pulses, two Nd:YAG lasers are used to separately drive the pump and the probe lasers. Central to the AOS method is the fact that the two Nd:YAG lasers are mode-locked at slightly different frequencies. The mode-locking frequencies of these two lasers are carefully controlled to maintain a constant beat frequency. In other words, a periodic relative phase walk-out exists between the the pump and the probe lasers. This has the same effect as varying the length of the optical delay line in the more normal pump/probe method; however, the period of time needed to map the population of an exicted energy level is reduced from several minutes to a few milliseconds.

The basic AOS instrument is shown in Figure 1. A master synthesizer will be used to generate the mode-locking frequency for the pump laser system. This frequency will then be fed to a slave synthesizer which in turn will drive the mode-locker for the probe laser system. The frequency output of the slave will differ from the frequency of the master by a constant known amount; furthermore, since the slave synthesizer is tied to the master synthesizer, the walkout time of the pump/probe arrangement will remain internally consistent.

In actual operation, each successive probe pulse is delayed in time (relative to the pump pulse train) by a constantly increasing duration which is determined by the choice of the beat frequency (1, 10, or 100 kHz). For example, at a mode-locking frequency for the pump laser of 82 MHz and a beat frequency of 100 kHz, the population measurement from a given probe pulse will be obtained 14.9 psec later than that from its predecessor. The process will repeat itself when the cumulative delay equals the corresponding mode-locking period, i.e., 12.2 nsec. Thus, for a beat frequency of 100 kHz, we see that 820 probe pulses will be available in a single sweep of 12.2 nsec. Since pertinent fluorescence decay times are $\tilde{}$ 1 nsec, most of the digitized data will represent the probe laser intensity and will therefore look like a DC signal. Thus, the AOS technique has the net effect of impressing onto the probe laser intensity an AC waveform which is directly related to the fluorescence decay of the species under study. This AC waveform will repeat itself at the beat frequency of the system.

The AOS technique is thus an optical analogue of the sampling oscilloscope, which is normally used to measure fast repetitive electrical waveforms. In essence, a time transformation of the excited state decay is performed with the time scaled by the factor $(f_{pump}/(f_{pump}-f_{probe}))$ where f represents the mode-locking frequency of the two lasers. In the example discussed previously, f_{pump} = 82 MHz and $(f_{pump}-f_{probe})$ = 100 kHz; therefore, the actual 14.9 picoseconds occurring between each sample is converted to 12.2 nanoseconds for analysis by a boxcar averager. Hence, the total sampling time for 820 probe pulses is 10 μsec, which is still very rapid compared to most turbulent processes.

The trigger arrangement for the boxcar averager and signal processing system is also shown in Figure 1. Beam splitters are inserted into both the pump and the probe laser beams to direct a small portion of each beam onto a photodiode. When the pump and the probe pulses are coincident in time the boxcar is triggered. This trigger system will assure temporal consistency of the AOS arrangement and allow for easier wavelength changes of either the pump or the probe laser compared to the existing pump/probe methods. The emissive signal from the probe laser is measured with a second photodiode. The subsequent electral signal is processed with an AC preamplifier to remove the large DC component and then directed into the boxcar averager. A computer is used to control (1) the time delay between the trigger pulse and the gate-enabling signal for the fast sampler in the boxcar; and (2) for data management and analysis.

Since the frequency and/or wavelength of both the pump and the probe lasers can be independently controlled, specific electronic quenching rates between the excited and the ground states can also be determined. This assertion is valid because the stimulated emission (absorption) appears as a gain (loss) in the probe laser intensity; therefore, only the states which are directly connected by the probe laser frequency are sampled. The loss/gain in the probe laser beam provides information on the rate at which the depopulated lower level gains population from neighboring levels within the ground electronic state or the rate at which the populated upper

level transfers population to its neighboring levels within the excited electronic state. In other words, the AOS technique can yield information about state-to-state relaxation rates within the upper and the lower rotational manifolds.

Progress on the project so far has been directed towards the acquisition of the necessary scientific equipment from which the AOS instrument is being constructed. A separate DoD-URIP grant (AFOSR-84-0222) was used for this purpose. This acquisition period, which is now almost finished, has taken approximately nine months. At this time, enough of the key elements have been assembled to allow initial construction of the instrument.

The construction will proceed through three phases: (1) building of the basic AOS system using mode-locked synchronously-pumped dye lasers; (2) addition of cavity-dumpers to the AOS arrangement; and (3) addition of Q-switches to the new laser system. Three chemical systems will be tested to determine the status of the AOS method at each stage of its development. Two of the tests are liquid phase measurements while the remaining test is a flame measurement.

The first test of the AOS technique will be to measure the fluorescence lifetime of a standard erythrosin/methanol mixture. This mixture has a fluorescence lifetime of 160 ps [1]. In this test, the erythrosin will be pumped at 530 nm and probed at 590 nm. This system will provide tests of (1) the general operation of the AOS equipment and (2) its time resolution.

The second test will be to measure the ultra-fast absorption recovery time of the tri-phenylmethane dye, malachite green. The exponential time constant for this dye in methanol has been determined to be as fast as 2.1 ps [2]. The dye also has a two component relaxation which is a function of the solvent viscosity. Therefore, by varying the solvent viscosity from 1 to 1000 centipoise, the lifetime of the system can be varied from approximately 2 to 50 ps.

Finally, the AOS method will be tested in each stage of its development by measuring OH concentrations in low pressure laminar flames. This procedure will allow us to draw upon our experience with this free radical [3] and will also provide a conclusive test of the AOS technique in combustion systems.

After the AOS system has been built and tested, the final stage of development will demonstrate the viability of this new technique as a combustion diagnostic. Measurements of OH concentration will be made in laminar flames of increasing pressure to ensure utility in real systems.

References

[1] L. A. Hallidy and M. R. Topp, Chem. Phys. Letts. 46, 8 (1976)

[2] E. P. Ippen, C. V. Shank and A. Bergman, Chem. Phys. Letts. 38, 611 (1976)

[3] R. P. Lucht, D. W. Sweeney and N. M. Laurendeau, Combust. Flame, 50, 189 (1983).

Basic AOS Instrument

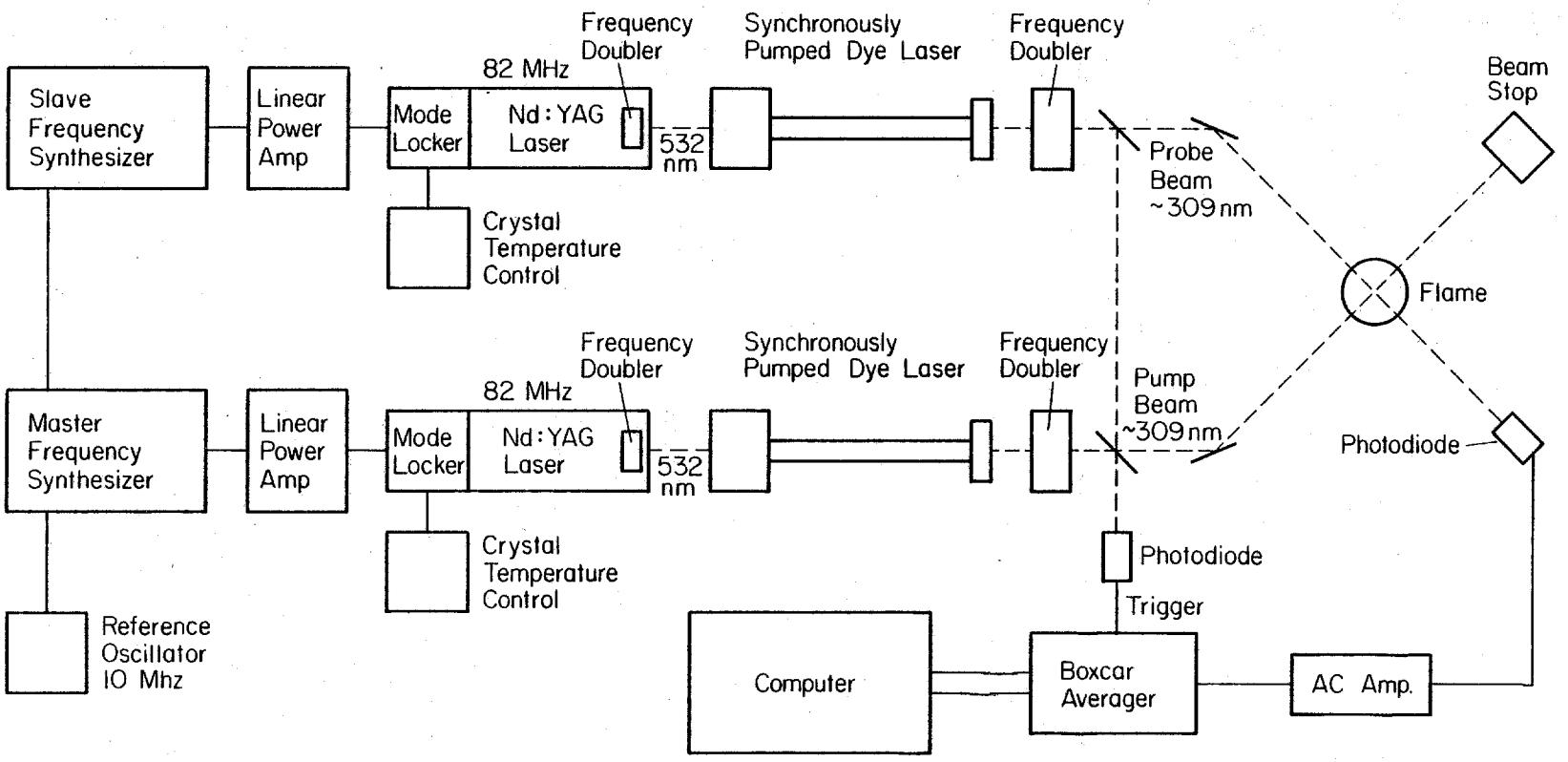

RADIATIVE AUGMENTED COMBUSTION

(AFOSR Contract No. F49620-83-C-0133)

Principal Investigator: Moshe Lavid

ML ENERGIA, Inc.
P.O. Box 1468
Princeton, NJ 08542

SUMMARY/OVERVIEW:

Radiative augmented combustion has been identified as a potential technique for extending current aircraft operating limits associated with combustion processes. Advanced vacuum ultraviolet (VUV) and ultraviolet (UV) light sources are used to selectively photodissociate reactants, intermediates and other inhibiting species into reactive radicals. Subsequent increases in concentration of these radicals can modify the overall kinetics and produce radiative ignition and combustion enhancement. The potential of this technique was previously demonstrated under static fluid conditions. Recently, it has been also demonstrated under flow conditions. The most significant accomplishment was obtaining successful ignitions with velocities up to 200 m/s.

TECHNICAL DISCUSSION

Many combustion applications are presently limited by constraints imposed by the combusion process itself, such as flammability, flame propagation, ignition and stability. Consequently much attention is being given to techniques which can augment combustion by extending these limits. One such promising technique is radiative augmented combustion. It is based on the fact that short wavelength radiation (VUV/UV) is capable of photodissociating stable molecules, combustion intermediates and other inhibiting species into reactive radicals. Selective changes in radical concentrations can modify the overall kinetics by both providing chain-initiators and removing chain-terminators, resulting in radiative ignition and combustion enhancements.

This program emphasizes research on the interaction between VUV/UV radiation and combustion under flow conditions. It is expected that in addition to demonstrating proof of concept by radiatively igniting combustible mixtures at conditions where thermal ignition is unreliable, it will also provide non-intrusive (optical) flameholding and increase flame speed. Since the role of photodissociation reactions within the whole kinetic scheme is currently not completely understood, it is further expected that the research will identify the most effective photodissociation paths. Consequently, the program is divided into two main subjects: ignition and enhancement. Each subject consists of an experimental effort supplemented by an analytical effort.

EXPERIMENTAL EFFORT

The main object of the experimental work is to demonstrate both ignition and combustion enhancement under flow conditions. For this purpose two test apparatus were designed and constructed.

Ignition: This apparatus features a flowing combustible mixture that is passed

directly over a VUV/UV source, eliminating the need for an optical window and thus completely nullifying the transmittance losses through it.

Experiments to determine radiative minimum ignition energy were conducted with hydrogen-air mixtures over a range of Damkohler numbers (D1) from 0.38 to 4.5. The equivalence ratio was varied from 0.3 to 1.2, and the energy resolution was to 0.5 joule. The results, in terms of electrical energy input to the lamps, are shown in Figure 1. As predicted by our analytical model, minimum ignition energy is insensitive to D1 for $D1 \gg 1$, and it increases rapidly for smaller values of D1. Furthermore, for $D1 \gg 1$, the effect of equivalence ratio on minimum ignition energy is not strong. However, it is important to note that fuel-lean mixtures are more favorable for photochemcial ignition than other mixtures, with the optimal equivalence ratio at about 0.5. This finding is in good agreement with previous results obtained with excimer lasers under static condition (1).

Enhancement: The enhancement apparatus called the "pancake" burner is shown in Figure 2. The combustible mixture exits as a jet from a small orifice in the thin top plate of a plenum chamber producing a conical flame. The orifice diameter is of the order of two mm and the optical pathlength from the window to the flame front is very short, 2 - 4 mm. This "pancake" design was chosen because of the experimental simplifications it offers in achieving axisymmetric illumination with stort optical pathlenghts. It also has the window on the cold reactants side of the flame where it is not subjected to products high temperature.

Radiative combustion enhancement is measured in terms of increases in burning velocity by detecting flame deflection. The sensitivity of the flame cone half angle, θ, to relative changes in burning velocity U is given by:

$$d\theta = \tan\theta \times dU/U$$

In order to improve detection it is desireable to stablize shallow flames with cone half angles at about 10 degrees. Then, 10% change in burning velocity will correspond to a 1 degree in half angle. The diagnostic system for measuring such small deflections was designed, built and tested. Both shadow and Schlieren photography have been successfully used. The system was found exceedingly sensitive and capable of responding even to very small changes of density generated by hydrogen-air flames near the lean flammability limit. Direct photography was not used because of inadequate luminosity emitted by hydrogen flames in the visible spectrum.

ANALYTICAL EFFORT

The analytical effort has also proceeded on two fronts: ignition and enhancement.

Ignition: A new model capable of simulating radiative ignition under flow conditions was developed. The model is based upon the continuity equation, and it includes the unimolecular photochemical reaction $O2 \rightarrow O+O$, which is excited by 10^{-4} sec square pulse of the ILC radiation with spectral distribution in the region 140 to 250 nm (2).

The criterion for ignition is that it occurs when the photochemically induced atomic oxygen concentration achieves a value of 10^{+16} atoms/cc. This critical concentration was calculated previously (3) for static systems, and it should be the same for dynamic systems. The dependent variable is F, which is the ratio of

oxygen atom concentration to that of the critical concentration. Thus, when F is equal to or greater than unity ignition occurs. The distance along the flow direction measured from the leading edge of the window is X, and the window extends from X = 0 to X = 1. The Dankohler number, D1, is defined as the ratio between the convective time across the window and the photochemical reaction time (the duration of the radiative pulse). Figure 3 is a representative of the analytical results. It presents Log F vs X for different Dankohler numbers. It is shown that even for D1 = 0.01 (velocity of 7,500 m/s) dissociation achieves 100 times the required critical value for ignition at the window edge. As D1 increases (flow slows down) F obtains its maximum value over almost the entire window length and then falls precipitiously downstream. If Dankohler number were zero (velocity equal to infinity), F would everywhere be zero, whereas if it were infinity (velocity equal to zero - static case), F would be a square pulse extending from X = 0 to X = 1. The conclusion drawn from this modeling is that even for very small D1 (high velocities) the ILC light source is capable of achieving ignition. This finding was later collaborated by the above described experimental results.

Enhancement: We have continued to use the HCT model to investigate the nature and extent of photochemical reactions on combustion enhancement. Laminar flame speeds were calculated for base cases employing the usual kinetics for hydrogen-air mixtures, and for cases in which photodissociation of either molecular oxygen or the hydroperoxyl radical was simulated. The approach used was to include the unimolecular photodissociation reaction with specified rate constants. All runs were at equivalance ratio of 0.4 and atmospheric pressure. Recent results are:

* The previously reported enhancement of 28% strongly depends on the rate of HO2 photodissociation. Critical rate constant is being sought.
* A modest enhancement of 9% was observed by increasing the rate of O2 photodissociation. Additional runs are needed to investigate the effect of variation of the limits of temperature window to allow the modeled photodissociation of molecular oxygen to extend further into the flame front.
* The enhancement mechanisms based on O2 photodissociation appear to be different from those based on HO2.

Finally, the analytical results and the understanding gained will be employed to determine optimal conditions for the best practical delivery of radiation energy in our experimental effort.

SUMMARY

The recent achievement of successful photochemical ignitions under flow condition further support the concept of Radiative Augmented Combustion. These findings are also collaborated by analytical results predicted by the new ignition model developed to investigate the effects of flow upon photochemical ignition. These encouraging experimental results at high flow velocities give us confidence that Radiative Augmented Combustion can become a potentially viable technique for extending current aircraft operating limits associated with combustion phenomena. Applications to gas turbine engine systems can be envisioned both for improved combustion operation and flameholding. Some future areas are: high altitude relight following flame-out, zero-drag flameholder, and added flexibility with the use of alternate fuels.

REFERENCES

1. Lavid, M., and Stevens, J.G., "Photochemical Ignition of Premixed Hydrogen/Oxidizer Mixtures with Excimer Lasers", Combust. Flame, Vol. 60, 2 (1985).
2. Cerkanowicz, A.E., "Radiation Augmented Combustion", Interim Technical Report AFOSR-TR-79-1096, (1979).
3. Lavid, M., "Radiative Augmented Combustion", First Annual Technical Report AFOSR-TR-84- , (1984).

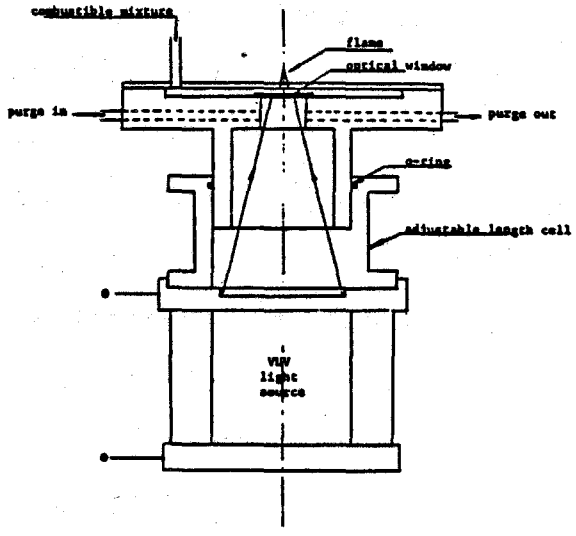

FIGURE 2
PANCAKE BURNER

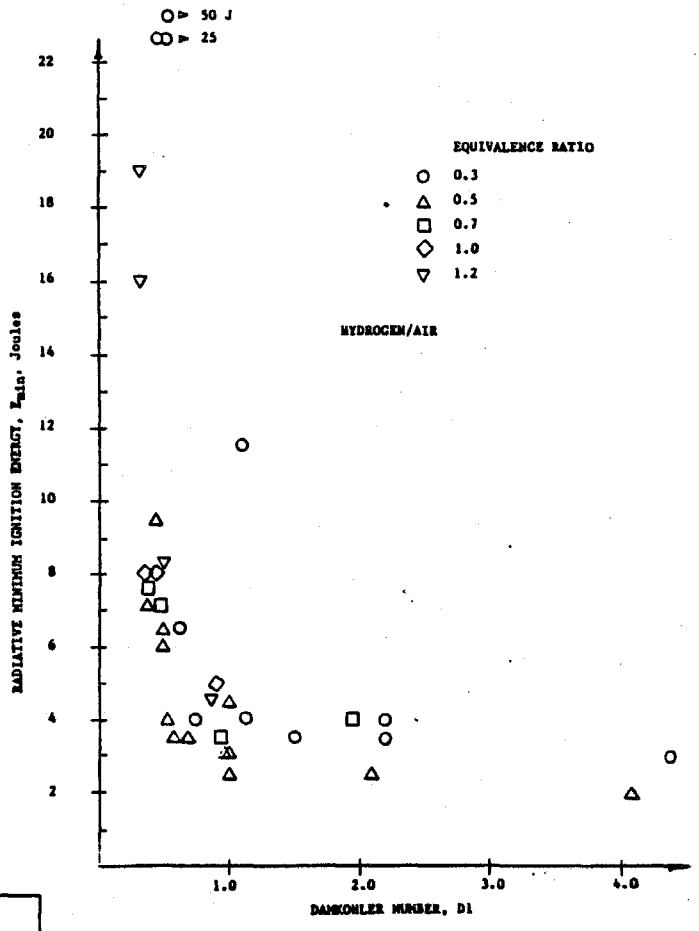

FIGURE 1. RADIATIVE MINIMUM IGNITION ENERGY VS. DAMKOHLER NUMBER FOR HYDROGEN-AIR MIXTURES AT VARIOUS EQUIVALENCE RATIOS.

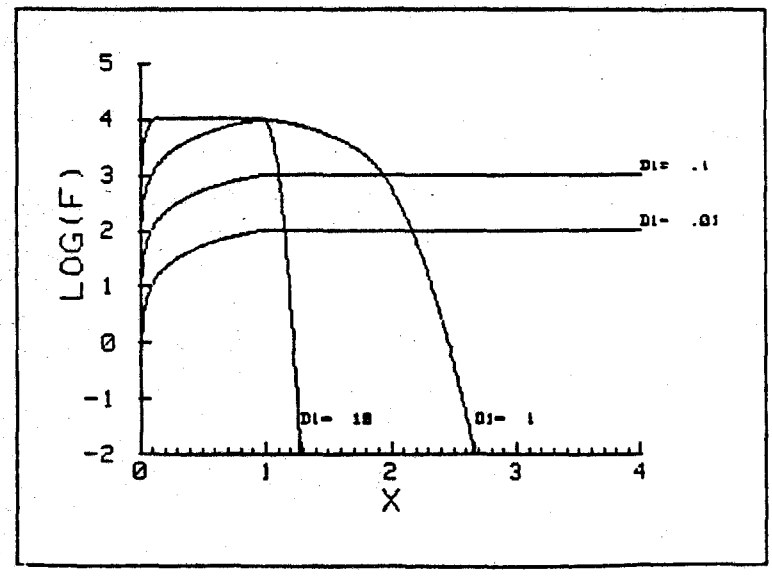

Figure 3
Log F vs X For y = 0 With Spectral Input From 145 to 245 nm For Damkohler numbers From 0.01 to 10. Total energy input 1 joule.

AERODYNAMIC AND KINETIC PROCESSES IN FLAMES

(AFOSR Grant No. 85-0147)

C.K. Law

Department of Mechanical Engineering
University of California
Davis, California 95616

SUMMARY

The flame response in realistic situations is governed by the detailed kinetics of chemical reactions, the diffusion of heat and mass, and the aerodynamic processes of stretching, turbulence, and large-scale flow nonuniformity. In this newly-initiated research program, the flame structure will be experimentally studied by using a variety of modular burners. Investigations will be conducted on laminar premixed and diffusion flames, turbulent premixed flames, and combustion under atmospheric and high-pressure environments. The results will be compared with predictions from asymptotic analyses and numerical simulation, and interpreted on the basis of aerodynamic stretching, preferential diffusion, and dominant reaction paths. It is anticipated that the study will yield fundamental understanding regarding the structure of laminar and turbulent flames, as well as such useful quantitative contributions as laminar and turbulent flame speeds, extinction and flammability limits, and kinetic codes validated through an extensive set of constraints. Recent data on effects of heat loss and stretch on the extinction/flammability limits of premixtures will be presented and discussed.

TECHNICAL DISCUSSIONS

Understanding of premixed combustion, both at the fundamental level as well as for combustor modeling, is usually based on the classical model involving the propagation of an adiabatic, one-dimensional, planar flame into

a quiescent combustible medium of given temperature and reactant concentrations. The model yields two combustion characteristics which are of fundamental significance, namely the flame temperature T_f, which is simply the adiabatic flame temperature T_{ad}, and the laminar flame speed S_L^o, which is a function of the thermal and chemical properties of the mixture, physically and parametrically representing its diffusivity, exothermicity, and reactivity. In realistic situations the flame response can be modified by three major factors, namely system nonadiabaticity, diffusional inequality, and aerodynamic stretching. Thus $T_f \neq T_{ad}$ and $S_L \neq S_L^o$.

The influence of nonadiabaticity on the flame behavior is conceptually obvious. The effects of aerodynamic stretching and preferential diffusion, however, are more subtle. By definition, stretch (κ) is the rate of change of the flame surface area, and can be manifested due to flow non-uniformity, flame curvature, and flame unsteadiness. As early as the fifties Karlovitz suggested that stretch is an important factor in extinguishing a flame. Recent theoretical and experimental studies have shown that stretch by itself has very little effect on the flame response because T_f remains at T_{ad}. However, when the diffusion rates of heat and the various species differ from each other, T_f can deviate from T_{ad} depending on the nature and intensity of stretch. Consequently the flame response can be significantly modified.

There are various practical implications based on the above discussions. For example, the determination of the laminar flame speed S_L^o is frequently conducted by using stretched flames (e.g., Bunsen flame) whose flame speed is not S_L^o. Thus the kinetic schemes and constants extracted by comparing the experimental S_L with the theoretical S_L^o will be incorrect.

Study of stretched flames is also of importance to the modeling of turbulent flames. That is, for situations under which the reaction zone thickness is much thinner than the characteristic turbulent eddy size, a

turbulent flame can be modeled as a wrinkled laminar flame. It is obvious that these wrinkled laminar flamelets are curved and situated in a highly nonuniform and fluctuating flow field. Thus they are strongly stretched flames and should be treated as such.

In the first phase of our experimental study a stagnation flow burner will be used to establish a flame with well-defined stretch rate κ, which is simply the velocity gradient, du/dx, upstream of the preheat zone. The flame speed S_L and the stretch rate κ can be determined by using LDV. Results will be obtained for S_L (ϕ,κ), where ϕ is the equivalence ratio for both atmospheric and high-pressure (<5atm) flames. The extinction limits will also be determined. The results will be of direct use for the modeling of turbulent flames. Furthermore, by extrapolating $S_L(\phi,\kappa)$ to κ=0 we should be able to accurately determine the laminar flame speed S_L^o, especially for high pressure flames. These results will be compared with the numerical predictions to identify the controlling kinetics.

Long-term research projects using the present approach will include high-pressure diffusion flames and turbulent premixed flames.

During the past few months since the initiation of the program, we have completed a project on measuring the extinction stretch rates of premixed flames of methane/air and propane/air mixtures. Of particular significance is the indication that the flammability limit of a mixture can be brought about without the need for heat loss or stretch.

TITLE: SOOT FORMATION AND FLAME RADIATION AT HIGH PRESSURES AND TEMPERATURES

AFOSR Grant No. 830374A

Principal Investigators: A. H. Lefebvre and P. E. Sojka

Thermal Sciences and Propulsion Center
School of Mechanical Engineering
Purdue University
West Lafayette, Indiana 47907

SUMMARY/OVERVIEW:

The effects of pressure and temperature on the sooting tendencies of four classes of hydrocarbon fuels will be determined. The radiant heat transfer from the soot to a simulated gas turbine combustor liner also will be measured. The concentration, size, temperature, and optical properties of the soot will then be related to the measured flame radiation through Mie-scattering calculations and the use of the radiative transfer equation. To accomplish this, the effects of the liquid spray field will be removed through use of gaseous fuels. The complications of flow field inhomogeneities will be minimized by using only one optical sight path through the combustor.

TECHNICAL DISCUSSION

The experimental test rig, shown in figure 1, features a sliding combustor that translates axially relative to a single pair of optical axis ports. This allows investigation of the flame variables as continuous functions of position. Because of this unique design, it is not possible to "lose" the peak soot concentration, flame temperature, or radiation intensity due to its occurrence between two adjacent sets of optical ports. In addition, the single set of optical ports minimizes disturbances keeping the flow field sensibly axisymmetric. The test rig fuel injector geometry can also be changed to transform the flame from essentially premixed to diffusion-controlled. This is accomplished through the use of two separate injectors, with varying numbers of orifices. The diffusion-controlled flame utilizes a single-orifice injector and the premixed flame utilizes an eight-orifice injector. The degree of mixing has been quantified and is presented in figure 2.

The gaseous fuels to be used comprise four classes of hydrocarbons: alkanes, alkenes, alkynes and cyclopropanes. The individual fuels, eight in all, include propane and butane, ethene, propene and 1-butene, ethyne (acetylene) and propyne, and cyclopropane. These fuels have been chosen for their variation in C/H mass ratio (from 4.47 to 11.92), their variation in number of carbon-carbon bonds (2 to 4) and their variation in number of rings (0 or 1). The fuels allow independent determination of the

effects of the number of fuel C-C bonds, fuel ring structure and fuel C/H ratio on soot formation and flame radiation. Table 1 summarizes the fuel data.

In order to determine the relationships between soot and radiation, it is necessary to measure the soot concentration and size distribution, the flame temperature and the flame radiation intensity. The optical properties of the soot must also be known. The latter will be calculated via Mie scattering theory.

Soot concentration will be measured with an isokinetic, water cooled probe, inserted into the combustor. The resultant stream of soot, combustion and dilution gases will be passed through a filter. The sample flow rate will be measured, and the mass deposition of soot on the filter paper will be determined by weighing, yielding the soot concentration. Samples of soot taken from the probe will be analyzed by a scanning electron microscope (SEM) to determine the size and structure of the individual soot particles. Preliminary SEM photographs are shown in figure 3. The size and shape of the soot paticles clearly shows the importance of agglomeration.

Flame temperatures will be determined first by the modified Schmidt technique [1], as shown in figure 4, and later using three-color pyrometry [2], shown in figure 5.

An analytical study of the wall radiation heat flux distribution was undertaken using the model of Menguc et al [3]. This model, for a finite, axisymmetric enclosure, uses the first or third spherical harmonics (P-1 or P-3) approximation to the radiation field. The model accounts for the inhomogeneity of both the medium and wall temperatures as well as variations in the medium radiative properties (such as extinction coefficient, single scattering albedo, etc.). A total of seven model parameters were investigated. The first, absorption coefficient, accounts for the sooting tendency of the fuel. The second, equivalence ratio, affects the radiative flux in two ways: (1) the type of gases and amount of soot formed and (2) the peak flame temperature. The third, radial temperature distribution, is representative of the physical type of flame involved: (1) a uniform radial temperature profile is characteristic of a premixed flame while (2) an exponentially decaying radial temperature profile is associated with a diffusion flame. The axial location of the flame front was also studied. The final three factors, associated with the wall fluxes, were wall emissivity, wall temperature distribution and liner diameter. The wall temperature distribution was modeled as either isothermal, as varying in temperature proportional to the combustor center-line temperature or as strongly cooled at the downstream end (simulating water cooling of the exit gases).

Conclusions drawn from the modeling study are (1) the combustor axial and radial temperature distributions strongly

influence wall heat fluxes, as shown in figure 6. Here, case I represents a medium with equivalence ratio of unity and a temperature which varies in the axial direction only (the premixed case). The effect of radial variation of the combustor temperature is shown by case II, (the diffusion case) presenting wall flux heat distribution for an equivalence ratio of one and a medium whose temperature distribution is varying radially, as well as axially. A comparison of cases I and II shows higher wall heat fluxes for a premixed flame than for a diffusion flame. This conclusion is based on an equal emissivity (equivalent soot formation) in both cases. Case III is identical to case I except that the equivalence ratio is one-half.

The wall temperature distribution has no significant effect on wall heat flux, as shown in figure 7. In cases I and II, there is no discernible difference in wall heat flux distribution when changing from an axially constant wall temperature distribution to one which varies proportional to the combustor centerline temperature. A comparison of case I (or II) and case III illustrates the effect of adding a water quench half way down the combustor: the wall heat flux rises, but only slightly, at the point of water injection.

REFERENCES

1. S. Silverman, "The Determination of Flame Temperature by Infrared Radiation," 3rd Symposium (International) on Combustion Flame and Explosion Phenomena, Williams and Wikins, Baltimore, 498-500 (1949).

2. N. Gat, L. M. Cohen, A. B. Witte and M. R. Denison, "Coal Pyrolysis under Rapid Heating with a CW Laser," CSS/CI paper 83-06, Lexington (March 1983).

3. P. M. Menguc and R. Viskanta, "Radiative Transfer in Finite Cylindrical Enclosures," presented at ASME Winter Annual Meeting, New Orleans (December 1984).

Table I. Gaseous fuels and their characteristics.

FUEL	C/H RATIO	C-C BONDS	
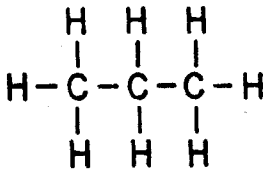	4.47	2	propane
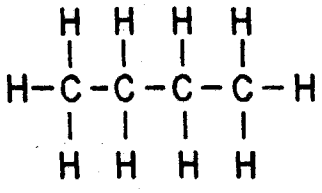	4.77	3	butane
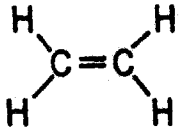	5.96	2	ethene
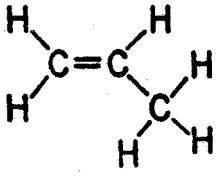	5.96	3	propene
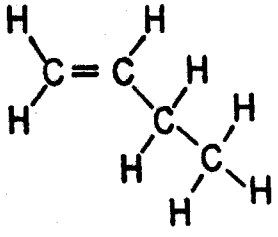	5.96	4	1-butene
	11.92	3	ethyne (acetylene)
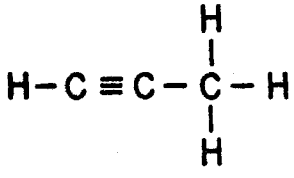	8.94	4	propyne
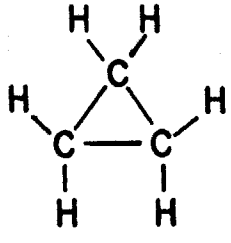	5.96	3	cyclopropane

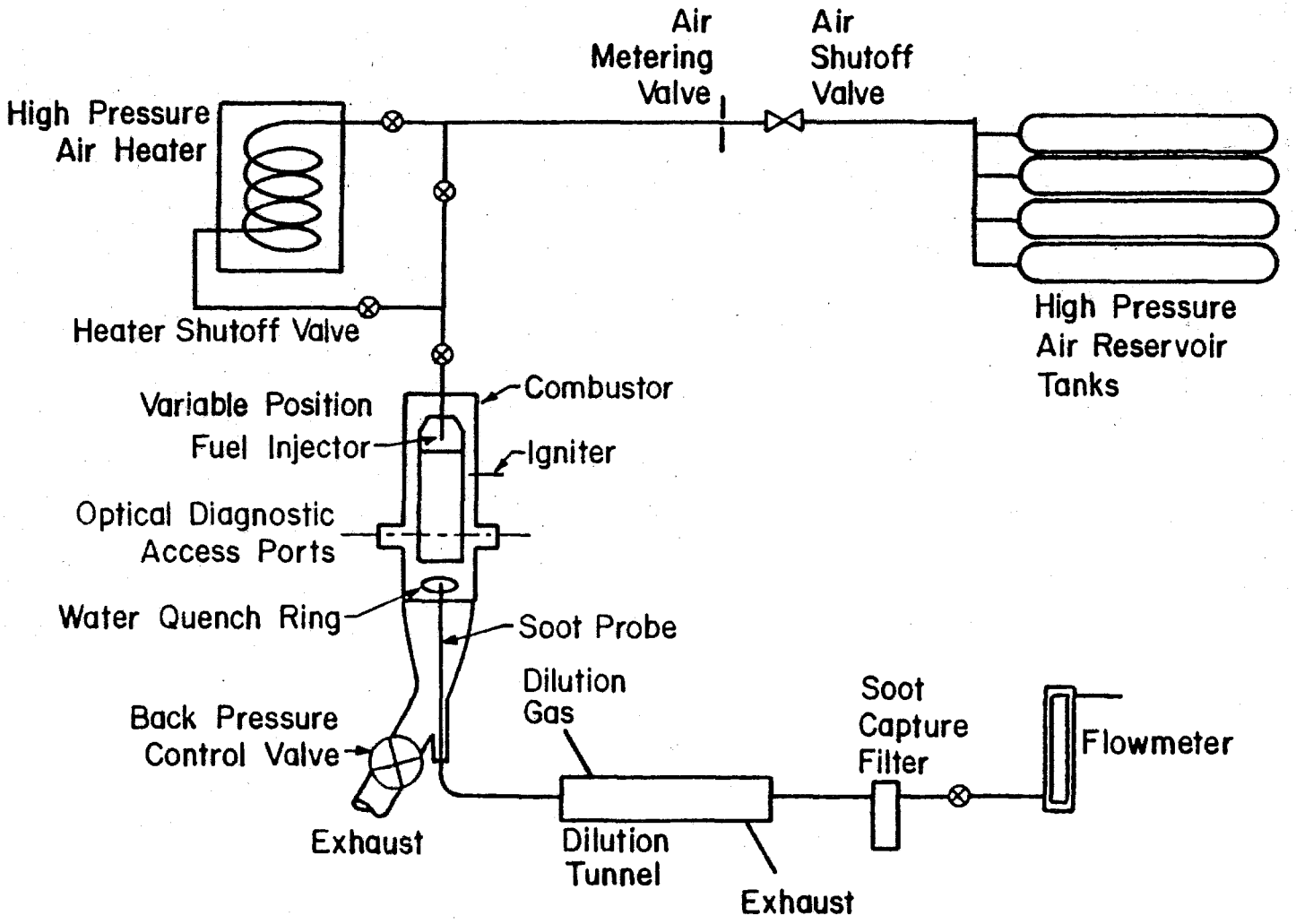

Figure 1. Test facility block diagram.

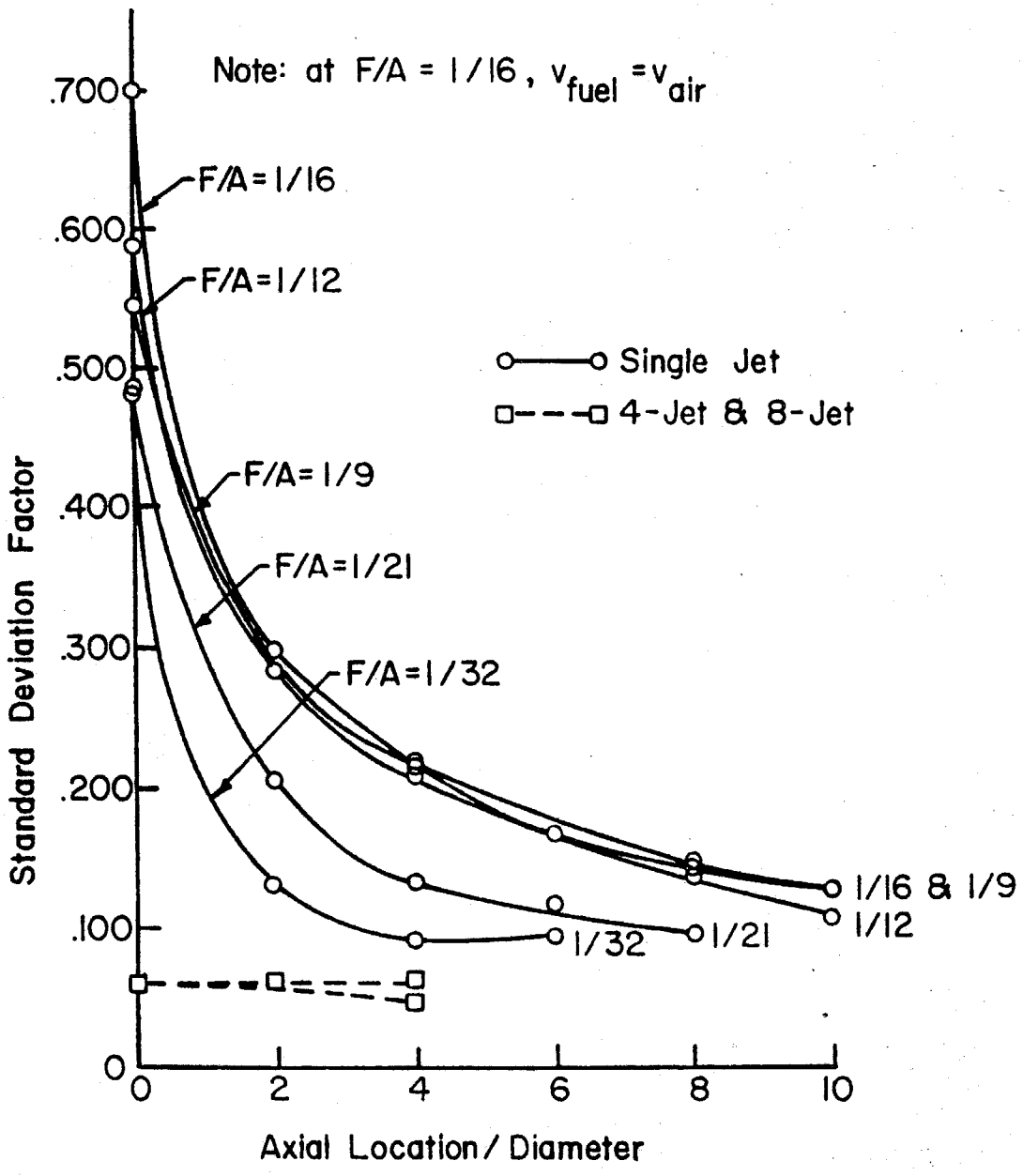

Figure 2. Mixing data for gaseous fuel injectors. Temperature standard deviation factor $\sqrt{\frac{\Sigma(T-Tm)^2}{(n-1)}}$ / $(T_f - Tm)$ is plotted vs. axial position (L/D) for both the single-orifice and eight-orifice nozzles.

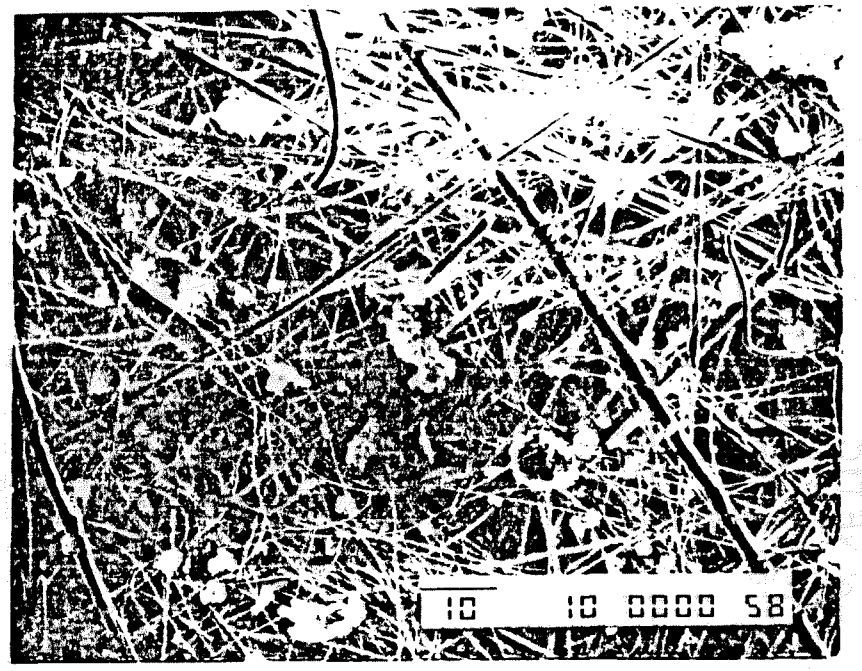

Figure 3a. Scanning electron microscope photograph of soot agglomerates. The horizontal bar above the "10" signifies 10 μm.

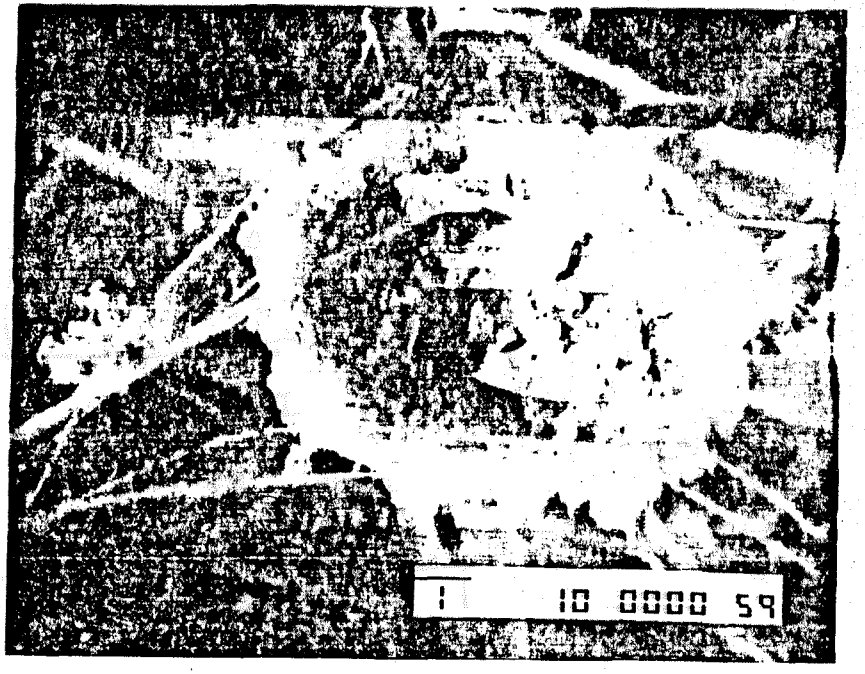

Figure 3b. Scanning electron microscope photograph of soot agglomerates. The horizontal bar above the "1" signifies 1 μm.

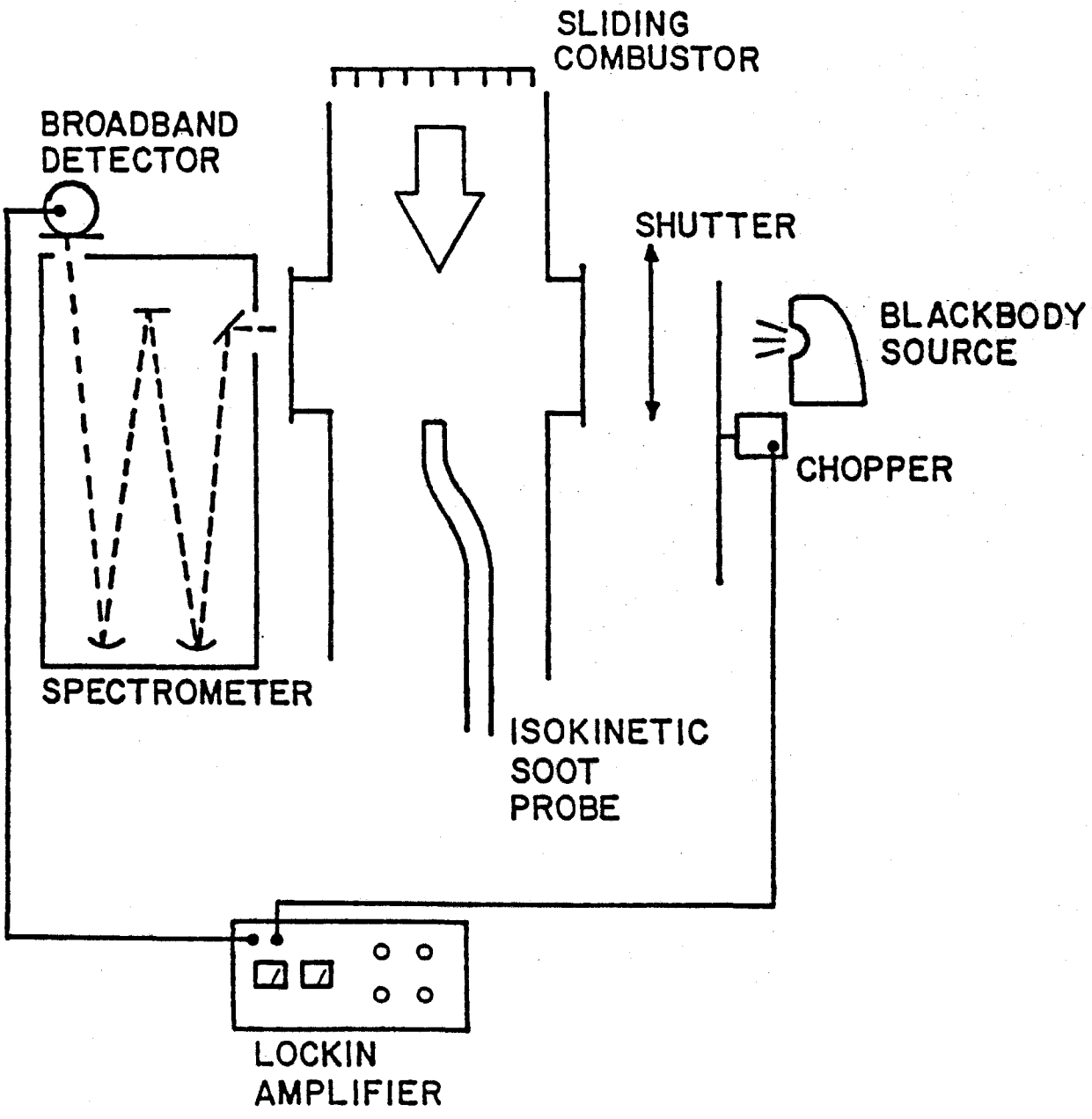

Figure 4. Schmidt technique schematic.

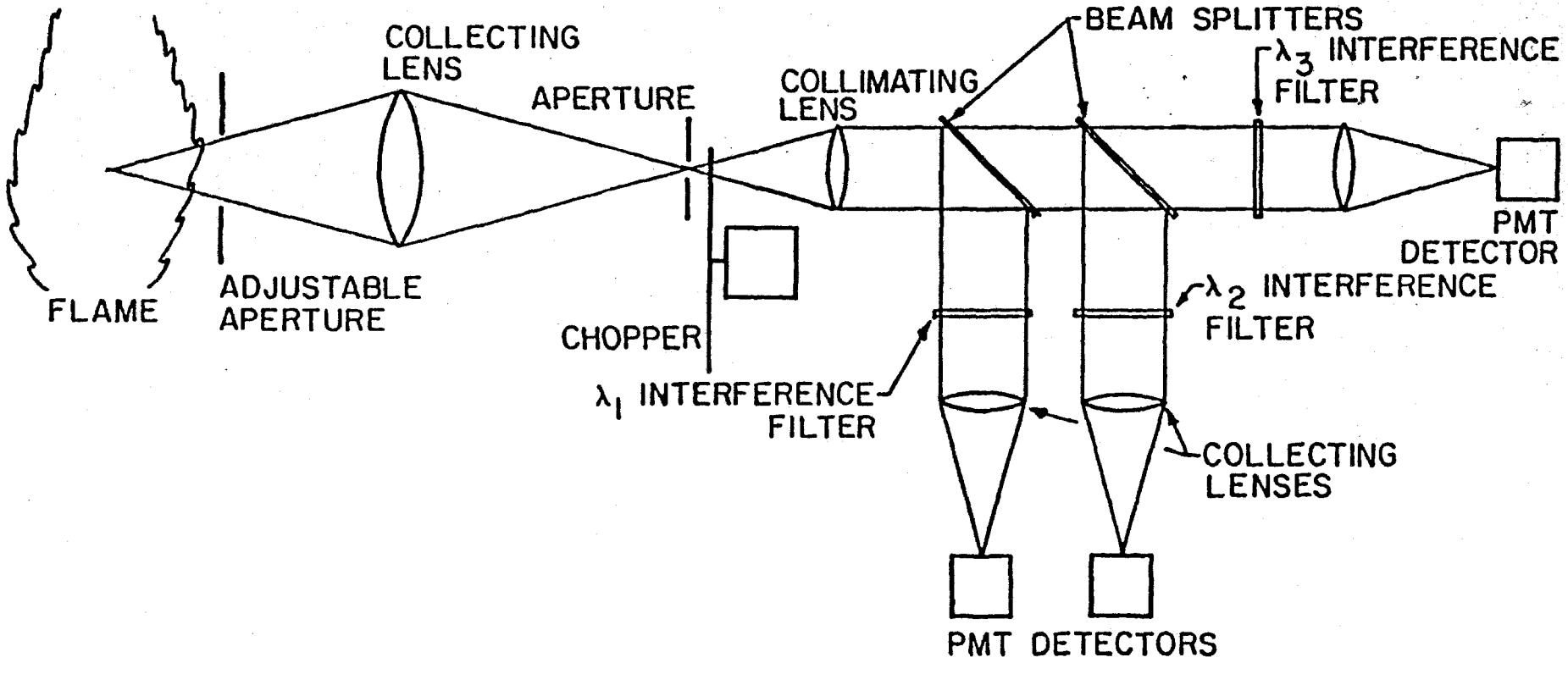

Figure 5. Three color pyrometry schematic.

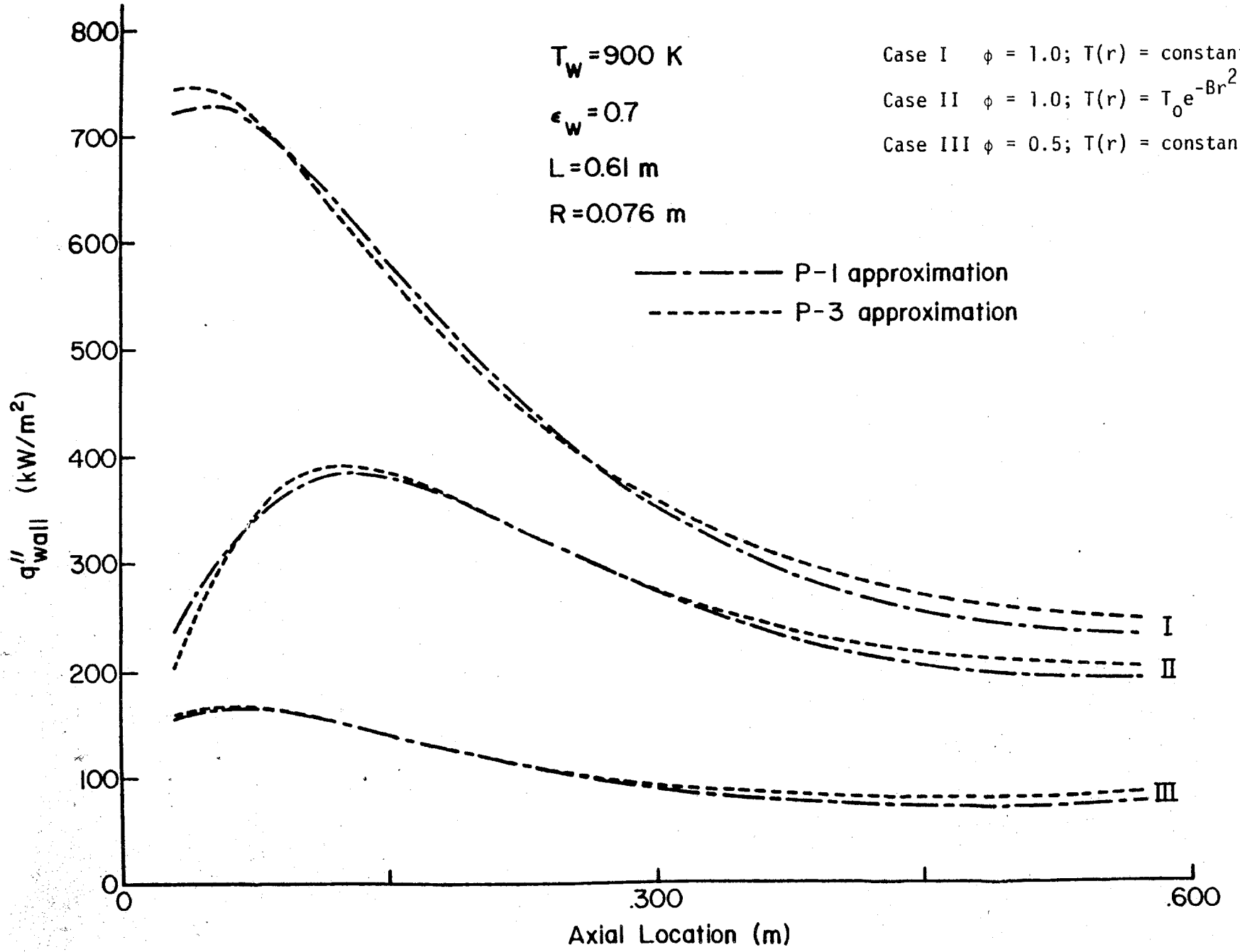

Figure 6. Wall heat flux vs. axial location: effects of combustor axial and radial temperature distributions.

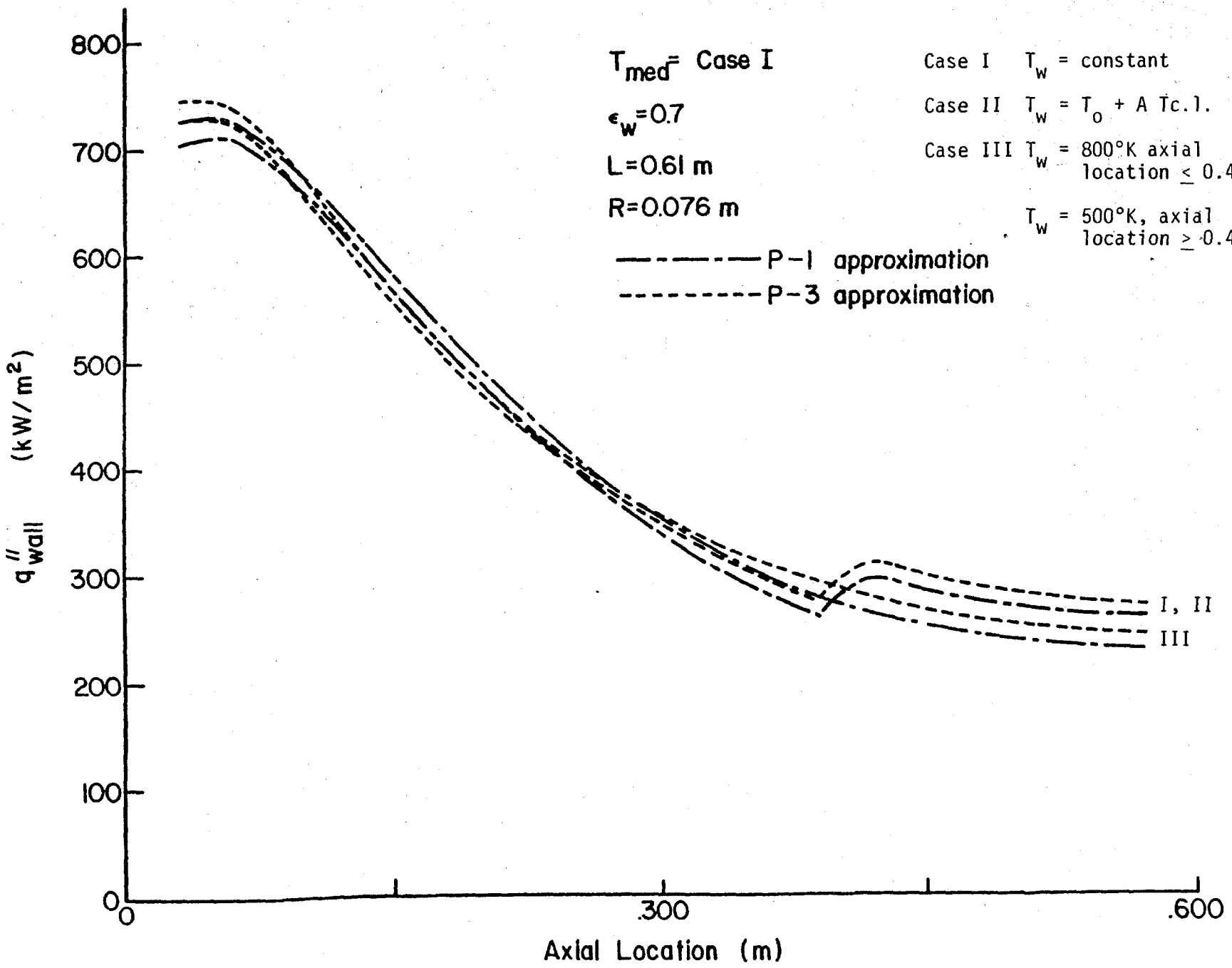

Figure 7. Wall heat flux vs. axial location: the effect of liner wall temperature.

CHEMICAL REACTIONS in TURBULENT MIXING FLOWS

AFOSR Grant 83-0213

H. W. Liepmann, J. E. Broadwell and P. E. Dimotakis

Graduate Aeronautical Laboratories
CALTECH, Pasadena, CA 91125

This is a continuing effort in both gas phase and liquid phase mixing, chemical reactions and combustion, in moderate to high Reynolds number turbulent free shear flows. This is primarily an experimental investi closely supported by theoretical and modeling efforts, as well as specific diagnostics developments, as dictated by specific needs of the experimental program.

1.0 Gas Phase Shear Layer Combustion

The work described below was conducted in the hydrogen-fluorine shear layer combustion facility.

Heat Release Effects in a Turbulent Reacting Shear Layer — By increasing the concentration of the hydrogen and fluorine reactants in equal density free streams, the amount of heat release was increased, corresponding to an adiabatic flame temperature rise of 900 K (1,200 K absolute). We were surprised to find that the thickness of the layer decreased with increasing heat release, corresponding to a 15% decrease in thickness for a 40% mean density reduction in the layer. This can be seen in figure 1, which depicts the normalized mean temperature (product) profile 1% thickness versus the relative mean density decrease as a result of the heat release. The normalized density-weighted product thickness is plotted in figure 2 and can be seen to depart from its low heat release values (see Mungal & Dimotakis 1984) as the mean density in the layer decreases as a result of the heat released. These results were obtained in a zero pressure gradient flow.

In a separate study, a favorable pressure gradient was applied to the flow, corresponding to a decrease of up to 1/3 of the total dynamic head of the low speed stream (accelerating flow), to study pressure gradient effects on the combusting layer. Except for the easily accounted for thinning of the layer, no other effects of the pressure gradient were observed. This part of the work was recently documented in the form of a Caltech Ph. D. thesis (Hermanson 1985). See also Hermanson, Mungal & Dimotakis (1985).

Work in this area is being extended to include free streams of unequal density, in both the low and high heat release limits.

Finite Rate Kinetic Effects — A brief discussion of the finite kinetic rate data was included in last year's abstract. Figure 3 shows a plot of the normalized product thickness versus the local Dahmkohler number (defined here as the local large eddy turn-over time divided by the chemical reaction time), as the overall chemical kinetic rate is varied. These data are obtained at our nominal flow conditions of U_1 = 22 m/s, x = 45.7 cm, U_1/U_2 = 0.4 under low heat release conditions. A theoretical analysis of the data, based on the Broadwell-Breidenthal model, for finite rate chemistry is presently underway.

Understanding the interaction of chemical kinetics with the turbulent mixing process in shear layer combustion is one of the most important issues in the general problem of supersonic combustion. This effort is pursued, in part, with this consideration in mind.

2.0 Mixing and Chemical Reactions in Turbulent Jets

These studies are undertaken to investigate turbulent jet mixing and chemical reactions in the limit of low heat release. Aspects of this part of the work are co-sponsored by the Gas Research Institute.

Entrainment, Mixing and Chemical Reactions in Turbulent Jets at High Schmidt Numbers — Experiments were conducted in liquid phase (high Schmidt number) turbulent jets. Laser induced fluorescence techniques were used, in both chemically reacting and non-reacting experiments, in combination with real time digital image analysis data acquisition methods. These experiments permitted direct measurements of the Probability Density Function (PDF) of the jet fluid mixture fraction. Several important results were established. The role of large scale structures in the entrainment and mixing processes was established in the far field of the jet. The resulting PDF (and the mixing process) reaches self-similarity in approximately 20 momentum diameters. A similarity form for the conserved scalar and the resulting PDF was discovered. Proper scaling of the flow in terms of the jet momentum diameter d^* (see Dahm & Dimotakis 1985) allows the "flame length" observed in liquid phase acid-base reactions to be correlated with gas phase combusting jets with high heat release and also two-phase jets (condensing vapor, halogen/liquid metal reactors etc.). The correlation of the normalized flame length L is shown in figure 4 plotted versus the stoichiometric mixture ratio ϕ for various reacting jets. A detailed

account of this work has been documented in the form of a Caltech Ph. D. thesis (Dahm 1985).

Gas phase turbulent jet mixing — A first phase, set of pilot experiments to verify performance calculations using laser Rayleigh scattering to measure binary gas phase mixture composition has been completed. We are now proceeding with the completion of the full scale facility in which a jet discharges from a 0.75" diameter nozzle into a 4'×4'×8' reservoir, with sufficient co-flow in the reservoir to satisfy the entrainment requirements of the jet to the measuring station. Single point measurements of the composition PDF are planned, which we expect to compare to our completed liquid phase data to investigate Schmidt number effects on turbulent mixing.

3.0 REFERENCES

DAHM, W. J. A. [1985] Experiments on Entrainment, Mixing and Chemical Reactions in Turbulent Jets at Large Schmidt Numbers, California Institute of Technology, Ph. D. thesis.

DAHM, W. J. A. and DIMOTAKIS, P. E. [1985] "Measurements of Entrainment and Mixing in Turbulent Jets", AIAA 23rd Aerospace Sciences Meeting 14-17 January 1985 (Reno, Nevada), AIAA Paper No. 85-0056.

HERMANSON, J. C. [1985] Heat Release Effects in a Turbulent, Reacting Shear Layer, California Institute of Technology, Ph. D. thesis.

HERMANSON, J. C., MUNGAL, M. G. and DIMOTAKIS, P. E. [1985] "Heat Release Effects on Shear Layer Growth and Entrainment", AIAA 23rd Aerospace Sciences Meeting 14-17 January 1985 (Reno, Nevada), AIAA Paper No. 85-0142.

MUNGAL, M. G. and DIMOTAKIS, P. E. [1984] "Mixing and combustion with low heat release in a turbulent mixing layer", J. Fluid Mech. 148, 349-382.

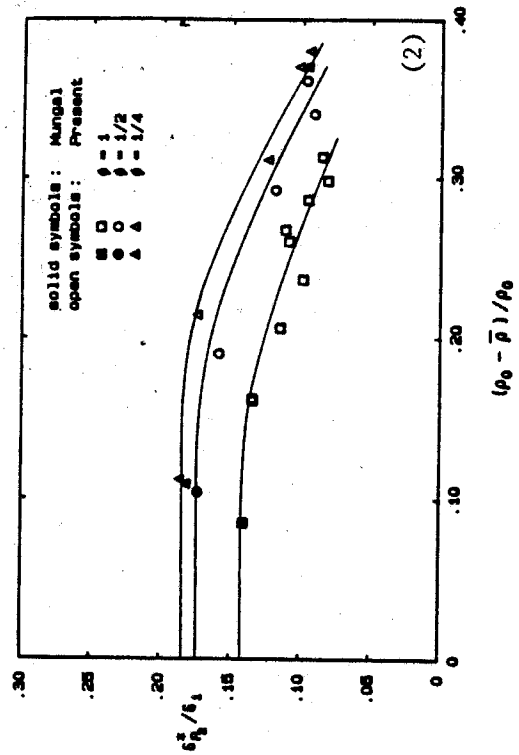
(2)
solid symbols : Mungal
open symbols : Present
ϕ = 1
ϕ = 1/2
ϕ = 1/4
δ_s^2/δ_1
$(\rho_0 - \bar{\rho})/\rho_0$

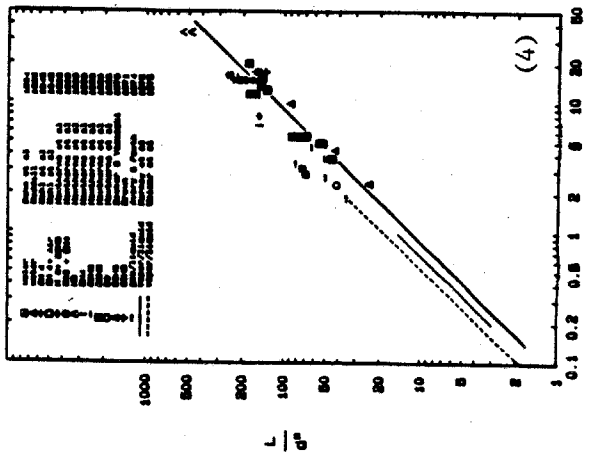
(4)
L / δ_s
ϕ

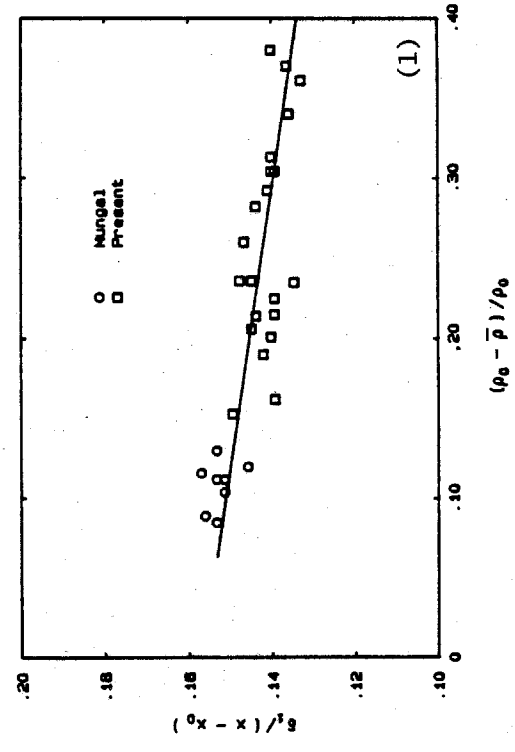
(1)
Mungal
Present
$\delta_s'/(x - x_0)$
$(\rho_0 - \bar{\rho})/\rho_0$

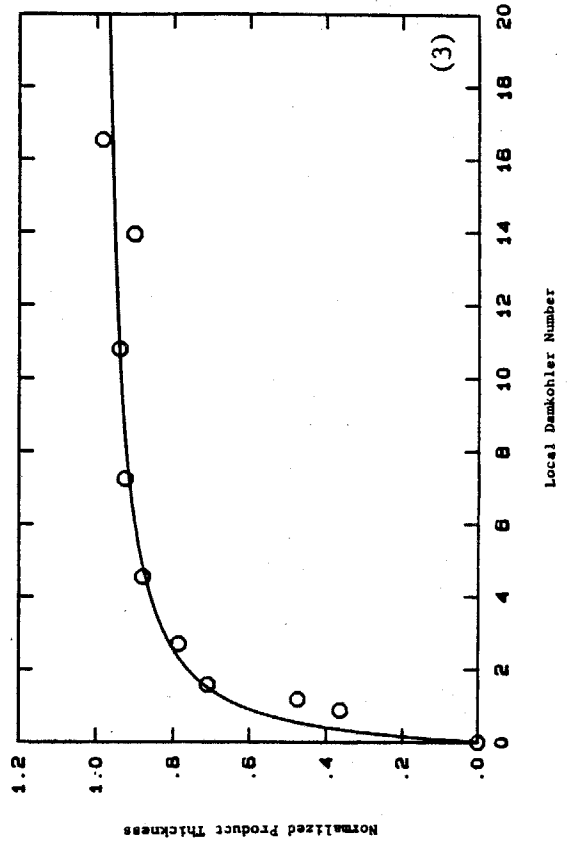
(3)
Normalized Product Thickness
Local Damkohler Number

RESEARCH IN TURBULENT AND UNSTEADY FLOWS

PROGRAM MANAGER: James M McMichael

AFOSR/NA
Bolling AFB DC 20332-65448

SUMMARY/OVERVIEW: The Air Force Office of Scientific Research program in Turbulent and Unsteady Flows is directed toward understanding the structure and dynamics of turbulence in shear flows and understanding the behavior of unsteady flows driven by time-dependent boundary conditions. Current program objectives and areas of interest are described, and future directions are discussed.

TECHNICAL DISCUSSION

Current AFOSR-sponsored research in turbulence seeks to identify, characterize and control basic physical mechanisms governing transition to turbulence, turbulence production and sustenance, aerodynamic drag, flow separation and reattachment, and turbulent mixing. Emphasis is on experiments oriented toward organized, deterministic structures and their interactions in free and bounded turbulent shear flows as well as experiments designed to explore new concepts for passive, active, and interactive control of turbulence characteristics.

Research in unsteady flows is motivated by the potential for exploiting unsteady effects to achieve enhanced agility and maneuverability in future generations of flight vehicles. This research focuses on the characteristics of dynamic stall on two and three dimensional lifting surfaces with emphasis on generic characteristics of attached and separated unsteady flows driven by time-dependent boundary conditions. Full exploitation of unsteady effects will require integrated research on nonlinear fluid-structure interactions coupled with advanced mathematical and physical concepts for both flow control and flight vehicle control.

Basic research issues addressed by the present program include:

1) The sensitivity of free shear flows to initial conditions and background disturbances, with emphasis on control of mixing and entrainment through active and interactive forcing.
2) The dynamics of multiscale and modal interactions in spatially developing free shear flows with emphasis on nonparallel and nonlinear mechanisms.
3) The receptivity of transitional boundary layers to initial and freestream disturbances.
4) Mechanisms for turbulence production and sustenance in bounded shear flows with emphasis on interaction between inner and outer flow structures.

5) Modification of turbulent boundary layer structure by curvature induced strain rates and compressibility.
6) Control of turbulent boundary layers through manipulation of inner and outer flow structures using passive, active and interactive techniques.
7) The development of mathematical and computational models of turbulence which adequately represent the physics of organized motions.
8) The mechanisms of dynamic stall and unsteady flow separation on two and three dimensional lifting surfaces.
9) The control of unsteady separation and reattachment by means of active forcing, with emphasis on motion history effects.

Research on the dynamics of unsteady flows will be increased by one million dollars in FY 86 through the AFOSR Maneuverability Initiative. The objective of this initiative is to develop the scientific and conceptual foundations for a new enabling technology which will exploit controlled unsteady separated flows for enhanced maneuverability in the post-stall environment. This objective will require fundamental research on the control of unsteady separated flows driven by time-dependent boundary conditions, investigation of highly coupled, nonlinear fluid-structure interactions, and devlopment of advanced actuator and flow control concepts. To this end, multi-investigator, interdisciplinary research efforts are encouraged. New research efforts will address the fundamental effects of three-dimensional geometries and three-dimensional motion on unsteady flow behavior, and examine the response to time-dependent boundary motions with multiple degrees of freedom. The influence of Reynolds and Mach number, as well as memory and motion history effects will be explored. Research will also attempt to develop concepts and techniques for passive, active and interactive control of unsteady separated flows. New predictive methods are also sought for complex nonlinear, time-dependent, highly coupled fluid-structure interactions.

Future research in turbulence will emphasize the potential for exploiting numerical simulations to examine the physics of turbulence. Increased emphasis will be placed on the interactive use of Laboratory minicomputers as an integral part of experimental configurations designed to explore new turbulence control techniques. New theoretical and computational approaches to turbulence incorporating deterministic structure concepts will also be explored. The potential applicability of concepts involving chaotic behavior in nonlinear dynamical systems to the description of turbulence in free and bounded shear flows will be investigated. Research will also address the need to develop advanced methods for processing and assimilating the enormous quantities of experimental and computational data which are becoming increasingly common in turbulence research. Such methods will rely on the development of new conceptual models for the structure of turbulent flows.

COMBUSTION RESEARCH FOR AEROPROPULSION SYSTEMS

Dr. Edward J. Mularz
Chief, Modeling and Verification Branch
Internal Fluid Mechanics Division

NASA Lewis Research Center
and Propulsion Laboratory, USARTL
21000 Brookpark Road, MS: 5-11
Cleveland, Ohio 44135

At NASA Lewis Research Center, combustion research is integrated into activity in internal fluid mechanics. The objectives of the research are to advance the understanding of flow physics, heat transfer and combustion processes which are fundamental to aeropropulsion, and to translate this knowledge into models and numerical codes of aerothermodynamic phenomena. The overall goal is to bring internal computational fluid mechanics to a state of practical application for propulsion systems. These models and numerical codes would then be available to the industry to incorporate into their own engine/component design systems.

The approach at Lewis is to establish an integrated computational-experimental research program. The activity consists of research on numerical methods, well-defined experiments for code and model verification, and the demonstration of computational codes for propulsion system components. In the area of combustion, research has been underway for some time in these three areas[1-4]. With a recent reorganization in the Aeronautics Program at Lewis, this research activity has been consolidated with similar research in other components such as compressors, turbines, and transition ducts and is continuing in the internal fluid mechanics research program. Although the amount of work currently being supported in combustion has been decreased in the new organization, the prime research needs in combustion are recognized.

This presentation will describe the current emphasis for research in internal fluid mechanics at Lewis and outline the activity in fundamental combustion research. Emerging opportunities for future research will also be presented.

References

1. "Combustion Fundamentals Research," NASA CP-2268, 1982.

2. Mularz, E. J., "New Trends in Combustion Research for Gas Turbine Engines," International Symposium on Air Breathing Engines, 6th, AIAA, Edited by F. S. Billig, 1983, pp. 37-44.

3. "Combustion Fundamentals Research," NASA CP-2309, 1984.

4. Mularz, E. J., and Claus, R. W., "Combustion Research for Gas Turbine Engines," NASA TM 86963, 1985.

CHARACTERIZATION OF DENSITY FLUCTUATIONS IN A PREMIXED TURBULENT V-SHAPED FLAME

(AFOSR Contract No. F44620-76-C-0083)

M. Namazian, I. G. Shepherd, L. Talbot

Department of Mechanical Engineering
University of California
Berkeley, CA 94720

SUMMARY/OVERVIEW:

This program has the broad aim of understanding some of the fundamental processes which occur during premixed gaseous combustion. The characteristic scales of scalar variables, such as temperature and density, in open premixed turbulent flames is the object of current experimental (1,2) and theoretical (3,4) interest. In these flames the "thin flame" approximation is well founded, and radical but realistic simplifications can be made to theoretical models which then provide directly testable predictions. Two-point Rayleigh data have been obtained from a turbulent V-shaped, premixed flame and compared with the predictions of two models: an extension of the Bray-Moss-Libby (BML) model (3) and a wrinkled laminar flame model (WLF) (4). The BML model describes turbulent premixed combustion by idealized probability density functions (pdfs) of a progress variable, c, where c=0 in the unburnt gas and c=1 in the burnt gas. A generalized description has been specialized to a one-point, two-time formulation from which may be derived (3) expressions for the autocorrelation, power spectrum and flame front passage times for the scalar variable, c. These results are compared with experimental values. A somewhat simpler description, the WLF model, considers the pdf of the position of a laminar flame within the turbulent flame brush. Cross-correlations and length scales have been derived and compared with empirical data.

TECHNICAL DISCUSSION:

Figure 1 shows a schematic diagram of the coaxial combustor used in this study. The premixed gases of fuel, ethylene or methane, and air flow through the center jet and are surrounded by an outer coaxial air jet at the same velocity. The inner and outer diameters are 5.1 cm and 10.2 cm, respectively. Grids or perforated plates generate a range of turbulence intensities (5%-10%) in the approach flow and the flame was stabilized on a 1 mm diameter rod 50 mm above the turbulence generation source. Using the method described in reference (2) gas density was measured at different locations downstream of the flame holder at equivalence ratios of 0.6 and 0.8 with approach flow mean velocities of 5 m/s and 7 m/s. Table 1 summarizes the experimental conditions of the eight flames studied.

TABLE I

Flame No.	Equivalence Ratio	U_∞ m/sec	Turbulence Source	u'/U_∞	Axial Measurement Location(mm)	Fuel
1	0.6	7.	grid	5%	20, 40 60 and 80	C_2H_4
2	0.6	7.	plate 1	8%	20, 60 and 80	C_2H_4
3	0.8	7.	grid	5%	20, 40	C_2H_4
4	0.6	5.	plate 1	8%	40	C_2H_4
5	0.8	5.	plate 1	8%	40	C_2H_4
6	0.6	7.	plate 2	10%	40	C_2H_4
7	0.6	7.	plate 1	8%	20 and 40	CH_4
8	0.8	7.	plate 1	8%	20 and 40	CH_4

The flames were characterized by the turbulent flame brush thickness which was obtained from the mean density profile by the maximum gradient method, figure 2. Increases in the equivalence ratio which will increase the laminar burning velocity and the burnt gas temperature generally have a more significant effect on the flame thickness than approach flow velocity or inlet turbulence.

The single-point experimental results from which may be derived the temporal characteristics of the scalar field compare very well with the predictions of the BML model. For example, in figure (3) the experimental and theoretical normalized power spectra are compared at points in the center of the flame brush. Good agreement was also obtained for the mean passage times and autocorrelation.

The WLF model provides predictions for spatial features of the flames. Non-dimensionalizing the flame density profile by the turbulent flame thickness, cf. figure (2), all the data may be collapsed onto a simple error function plot. This is compared with the equivalent modeled Gaussian distribution for the instantaneous flame position in figure (4). Further comparisons for the cross correlations and density length scales indicate that this representation models the measured values well.

REFERENCES

(1) Shepherd,I.G. and Moss,J.B.:Combustion Science and Technology, p.231, vol.33, 1983.

(2) Namazian, M., Talbot, L., Robben, F., and Cheng, R.K.: Nineteenth Symposium (Int'l) on Combustion, p.487, The Combustion Institute (1983).

(3) Bray, K.N.C., Libby, P.A., and Moss, J.B.: to appear in Combustion Science and Technology.

(4) Namazian, M., Talbot, L. and Robben, F.: Twentieth Symposium (Int'l) on Combustion, Ann Arbor, 1984.

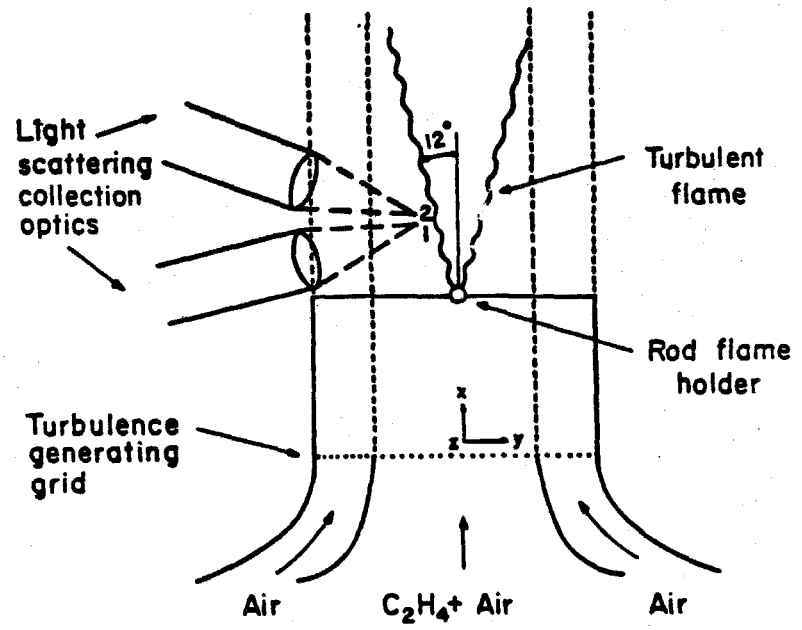

Figure 1. Schematic of the Experimental Apparatus for two-point Rayleigh Scattering Measurements.

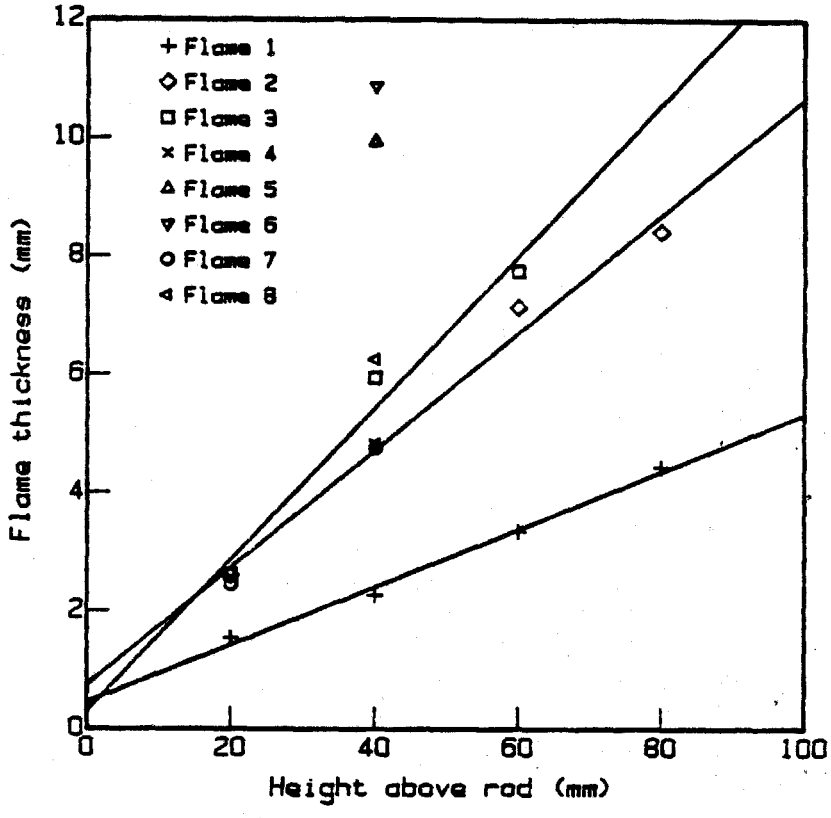

Figure 2. Variation of turbulent flame thickness with height above flameholder. Lines are least mean square fits for flames 1, 2 and 3.

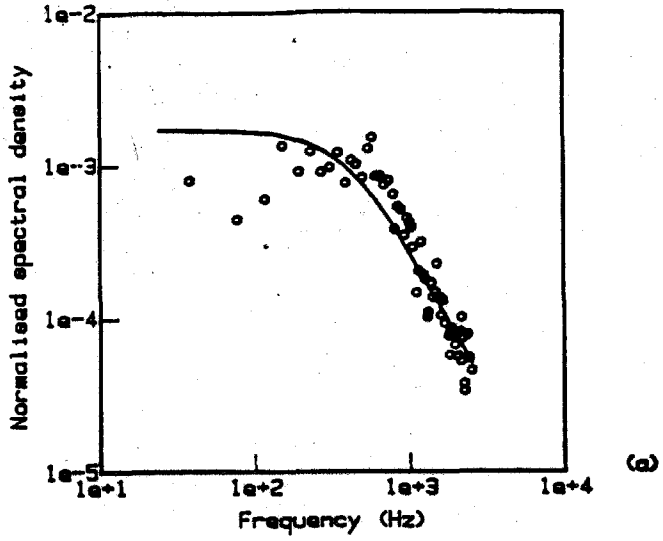

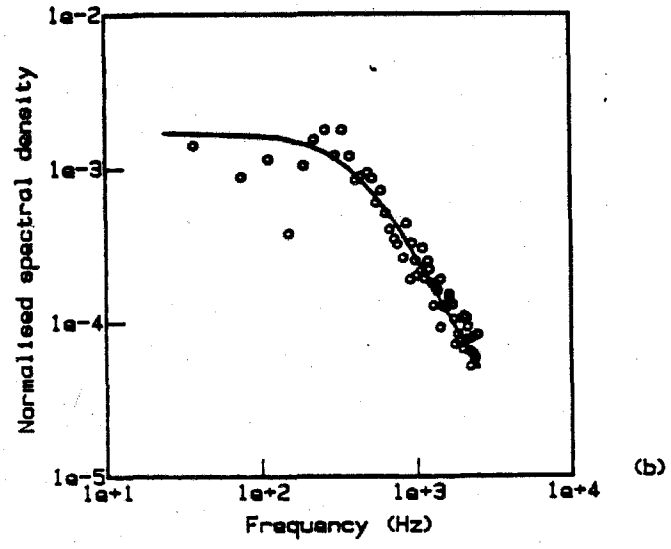

Figure 3. Normalized power spectra of density fluctuations. Height above rod: (a) 60 mm (b) 40 mm. Lines from BML model (3).

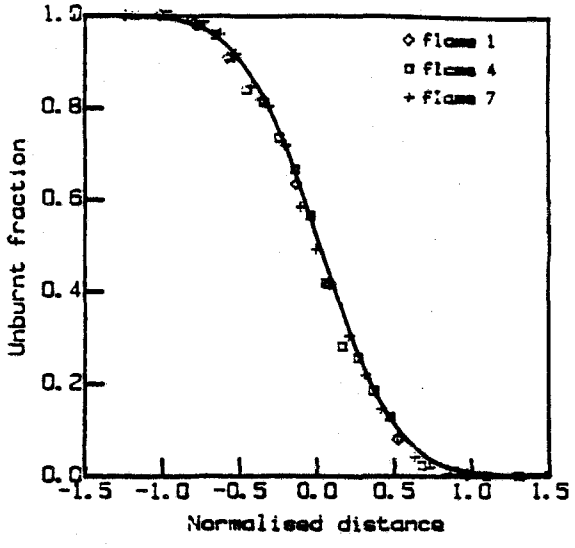

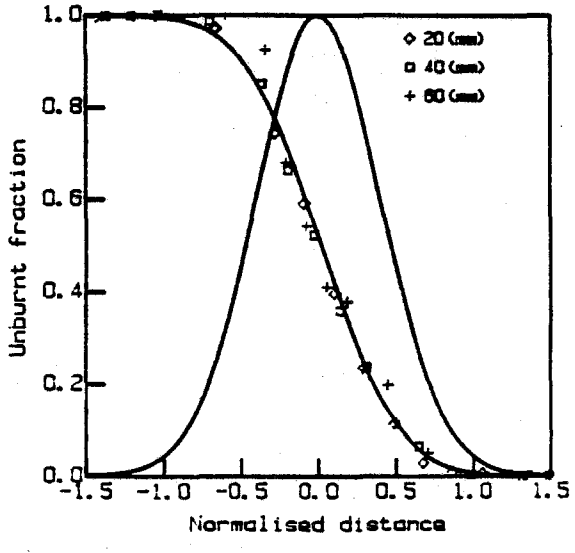

Figure 4. Normalized mean density profiles. (a) Height above flame-holder 40 mm., (b) Flame 3.

EXPERIMENTAL AND NUMERICAL CHARACTERIZATION OF RAMJET COMBUSTOR FLOWFIELDS

(AFOSR Grant/Contract No. 2308S1)

Principal Investigators: A.S. Nejad, R.R. Craig, P.L. Buckley, F.D. Stull, S.P. Vanka

Air Force Wright Aeronautical Laboratories
Aero Propulsion Laboratory
Ramjet Engine Division
Ramjet Technology Branch
Wright-Patterson AFB OH 45433-6563

SUMMARY/OVERVIEW:

The present program looks into the prediction and measurement of the mean velocity and fundamental turbulence quantities in flows relevant to ramjet combustors. This information will be used in the evaluation of existing turbulent transport models which are currently used in a variety of computational forms throughout the propulsion community. Both single component and two-color laser Doppler velocimetry have been employed to document the flow structure of a sudden expansion dump combustor, and the results are being compared to theoretical calculations by S.P. Vanka under our extramural research program, "Analytical Study of Three-Dimensional Combustion Processes." An elaborate test rig for cross-injection and atomization of various fuels (liquids and gases) into high velocity subsonic cross-streams has been designed and fabricated. Non-intrusive diagnostic techniques such as LDV, Fraunhofer diffraction for particle sizing, and various flow visualization schemes are planned and being developed for use in this study.

TECHNICAL DISCUSSION:

The available data in turbulent recirculating flows are limited. LDV is capable of making accurate measurements in these flows. Although shear stress measurements in a sudden expansion dump combustor have been attempted with a single component LDV by rotating the beam plane, the data appears to be unreliable. AFWAL/PORT has developed a unique LDV system capable of acquiring and storing 100,000 data samples/channel, which includes velocity component data and a 32 bit time value. A variable coincidence time window has been added to ensure simultaneous measurements of the velocity components. Since one of the major goals of this effort is to provide reliable experimental data for the evaluation of the existing codes, extensive effort has gone towards identifying and eliminating possible sources of measurement errors. The effects of seeding rate and coincidence time window on velocity measurements in highly turbulent flow regimes were throughly investigated. Generally, in two-component laser Doppler velocimetry, velocity correlation improves with decreasing coincidence time window. However, it was found that the coincidence time window acts as a discriminator against slower moving particles and accentuates the problem of velocity biasing, figure 1-3. Sets of 171,990 samples were recorded and analyzed via ensemble averaging, sample hold, hold sample integration, and two different time interval sampling

strategies to examine how effectively each technique could eliminate velocity biasing. The constant time interval sampling technique, which proves to eliminate velocity biasing from all reacting, non-reacting, and mixing flows, was chosen as the technique for velocity and turbulence measurements in a sudden expansion dump combustor, figures 4-5. The mass flux through the model based on integration of the axial velocity profiles at each measurement station downstream of the dump plane was within 2% of the mass flux measured with a turbine flowmeter. The tangential velocity patterns, however, were not anticipated, figures 6. The results show that there are two vortices imbedded in the flowfield between the dump plane and the end of the recirculation zone (reattachment point). This may be due to inaccuracies in model fabrication. A very precise model has been designed and will be fabricated in order to reduce the uncertainties associated with the measurements.

In Vanka's earlier work for the development of efficient numerical solution algorithms, a direct inversion technique was used. In his later work, a sparse matrix routine was employed. Although the technique provided significant reduction in CPU time over the SIMPLE algorithm (and its derivatives in the form of TEACH computer programs) its extension to three dimensions required large computer storage. An innovative numerical technique based on multigrids was, therefore, developed. Using this, both two and three dimensional calculations can be made very efficiently and with minimal storage. This algorithm is now being tested and developed for turbulent and reacting flows in ramjet combustors and ducted rocket configurations. This approach reduces CPU time by a factor of 5 to 10 over the original direct solution technique, providing in total, a factor up to 100 over the SIMPLE technique. For large problems, the speed-up can be as large as several hundred, see table 1.

The fuel injection and atomization test rig has been fabricated, instrumented, and checked. A comprehensive test matrix has been planned to study the effects of fuel/air interaction and injectant physical properties on atomization processes. New concepts of fuel atomization such as pre-atomization before injection (polyaphronated hydrocarbons) are also being developed.

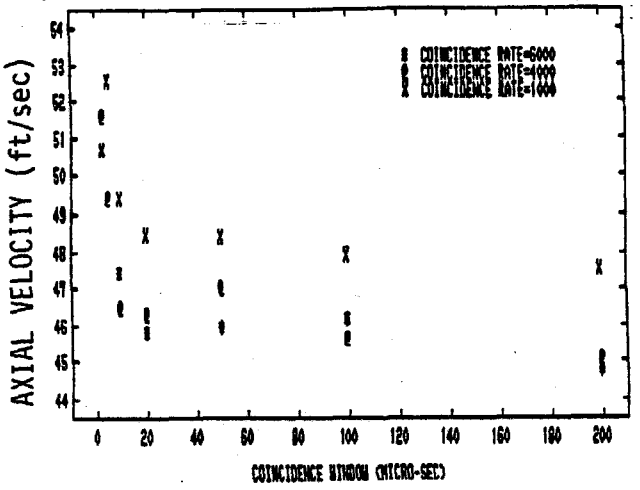

FIGURE 1: UNBIASED AXIAL VELOCITY AS A FUNCTION OF COINCIDENCE RATE & WINDOW.

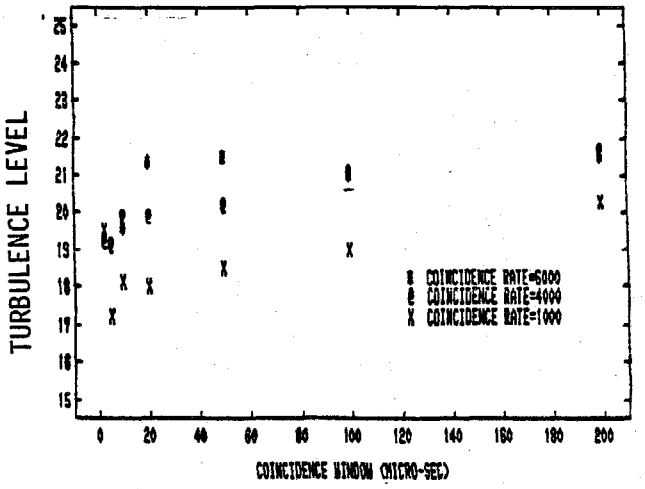

FIGURE 2: UNBIASED AXIAL TURBULENCE AS A FUNCTION OF COINCIDENCE RATE AND WINDOW.

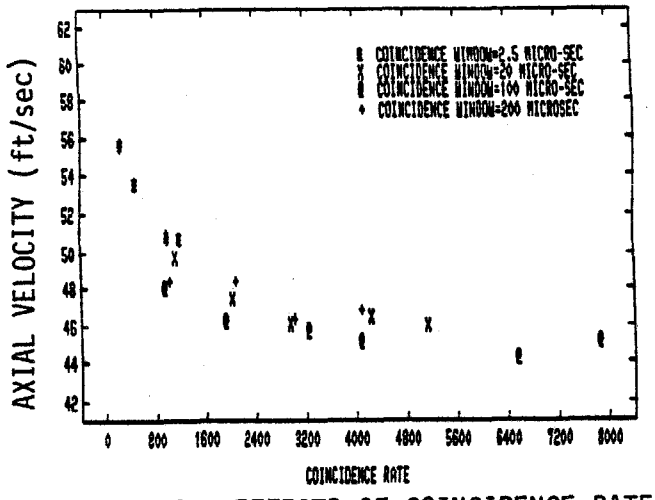

FIGURE 3: EFFECTS OF COINCIDENCE RATE AND WINDOW ON UNBIASED AXIAL VELOCITY

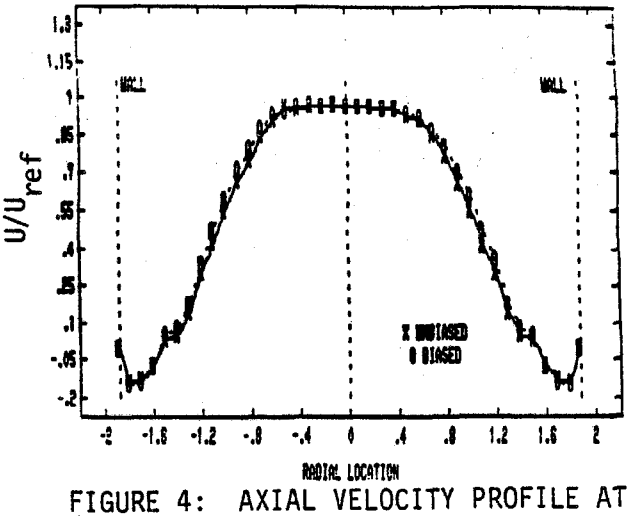

FIGURE 4: AXIAL VELOCITY PROFILE AT X/H = 5.0

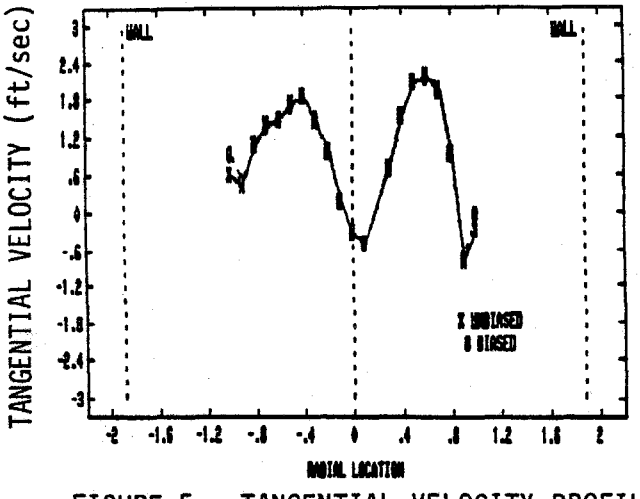

FIGURE 5: TANGENTIAL VELOCITY PROFILE AT X/H = 0.5

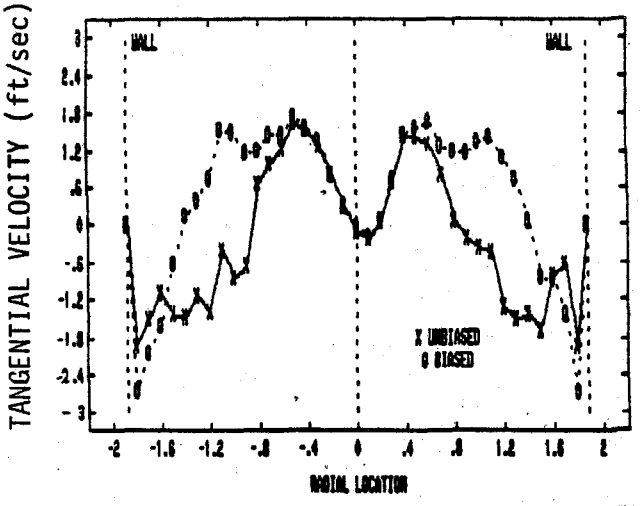

FIGURE 6: TANGENTIAL VELOCITY PROFILE AT X/H = 5.0

CPU TIMES (IBM3033)

CALCULATION	IMPROVED ALGORITHM (SEC)	SIMPLE (SEC)
LAMINAR SQUARE CAVITY:		
(RE = 1000)		
40X40	12.5	306.0
80X80	52.0	2,550.0
160X160	154.0	21,675.0 (P)
320X320	644.0	184,250.0 (P)
LAMINAR CUBE:		
(RE = 1000)		
16X16X16	34.0	
32X32X32	320.0	
64X64X64	2,268.0	
TURB. SUDDEN EXPANSION:		
82X82	45.0	
162X64	212.0	

GAS-PHASE OXIDATION OF BORON COMPOUNDS

(AFOSR Contract No. ISSA-85-000010)

Principal Investigators: Richard C. Oldenborg
Steven L. Baughcum

Los Alamos National Laboratory
Chemistry Division
Los Alamos, NM 87545

SUMMARY/OVERVIEW:

The emphasis in much of the previous boron rocket fuel research has been on particle ignition, yet roughly half of the potential energy content of boron rocket fuels is released in the gas-phase oxidation of BO(g) to B_2O_3(g). An efficient air-breathing combustion engine must incorporate the appropriate internal temperatures and residence times consistent with the completion of this gas-phase oxidation process. We are investigating the kinetics of the key gas-phase boron oxidation reactions so that a comprehensive reaction scheme can be assembled and evaluated. Our initial effort has concentrated on the BO + O_2 → BO_2 + O reaction, which is considered to be the key BO oxidation step in dry atmospheres. Volatile boron compounds such as BCl_3 are photolyzed with an excimer laser to provide an essentially instantaneous source of boron atoms. These quickly react with O_2 to yield BO. The time histories of the B, BO, and BO_2 are monitored using laser-induced fluorescence (LIF) and chemiluminescent techniques. Systematic variation of O_2 pressure and temperature (298-1300 K) should yield the desired rate parameters.

TECHNICAL DISCUSSION

Before attempting to study the reactions of BO radicals, we must know their formation rate in the B atom oxidation reaction

$$B + O_2 \rightarrow BO + O \; . \qquad [1]$$

Roughly 1% of the BO molecules from reaction [1] are produced in the electronically excited $A^2\Pi$ state.[1] Figure 1 shows a typical spectrum of the BO(A-X) chemiluminescence that is observed when 0.1 torr of BCl_3 is photolyzed at 193 nm in 0.4 torr O_2 and 24.5 in Ar at room temperature. The exothermicity of reaction [1] is 74.5 kcal/mole which limits the excitation of the BO molecules in the A state to $v' \leq 2$. In contrast, Fig. 1 shows a bimodal distribution of vibrational energy with excitation up to $v' = 8$. Emission from electronically-excited $B(3^2S)$ atoms is also observed (not shown) suggesting that the reaction of excited B atoms produced in the photolysis could account for the bimodal distribution and high level of vibrational excitation. The radiative lifetime of the $B(3^2S)$ is too short to permit significant reaction, but atomic B has a lower-lying metastable ^4P state at 28800 cm^{-1} which is a reasonable reactant. We have observed the production of excited ^4P atoms in the photolysis of other Group III

compounds such as $Ga(CH_3)_3$ and $GaCl_3$. The high vibrational levels ($v' \geq 4$) show a complicated time behavior that is consistent with a production mechanism involving excited B atoms. In contrast, Fig. 2 shows a typical time history of the $v' = 0$ level of the A state at 0.16 torr O_2 and 25 torr Ar. This waveform can readily be fit to a biexponential function using nonlinear least-square techniques. The rise time thus obtained is consistent with the radiative decay rate of the A state under these pressure conditions, while the fall time represents the depletion of B atoms by reaction [1]. By varying the O_2 pressure we deduce a rate constant for reaction [1] at 298 K of 3.8×10^{-11} cc/molecule-s. Comparison to the literature value[2] of $4.6 \pm 1.8 \times 10^{-11}$ shows good agreement and implies that this technique is a reasonable method for assessing this rate constant. Experiments are now in progress to follow the time history of the ground-state B atoms using LIF techniques to monitor their depletion directly and confirm this measurement.

The subsequent reactions of the ground-state BO radicals are studied by monitoring their time history using LIF techniques. The $v'' = 0$ level of the $BO(X^2\Sigma^+)$ state is probed by exciting the A-X transition on the (1,0) band near 403.5 nm and by observing the fluorescence of the (1,1) band near 436 nm. An LIF excitation spectrum of the (1,0) band is shown in Fig. 3. The spectrum consists of two clusters of rotational lines corresponding to excitation of the $A^2\Pi_{1/2}$ and $A^2\Pi_{3/2}$ states. A preliminary analysis of the spectrum indicates only BO is being probed with no features identifiable as resulting from BO_2. The time history of the BO product is measured by scanning the time delay between the probe and photolysis lasers, with each successive laser shot sampling a slightly different time delay. The LIF signal is integrated with a boxcar averager and then digitized to facilitate computer analysis. Figure 4 shows a typical BO time history for 0.16 torr O_2 and 25 torr Ar at room temperature. The rise time should correspond to the rate of reaction [1], but is obscured by the chemiluminescent emission. The fall time, however, does appear to be a clean single exponential decay and represents the rate of the depletion reaction

$$BO + O_2 \rightarrow BO_2 + O \quad . \qquad [2]$$

Analysis of the BO time profiles at different O_2 pressures yields a preliminary rate constant for reaction [2] at 298 K of 1.9×10^{-11} cc/molecules. This value is significantly larger than the previously measured value ($4.4 \pm 4 \times 10^{-12}$)[3] and the origin of this discrepancy is being investigated. If correct, this new rate constant implies that O_2 is a more important oxidizer of the BO than was previously supposed. LIF and chemiluminescence experiments are now in progress to assess the rate constant for reactions [1] and [2] at elevated temperatures.

References:

1. J. DeHaven, M. T. O'Conner, and P. Davidovits, J. Chem. Phys. 75, 1746 (1981).

2. I. P. Llewellyn, A. Fontijn, and M. A. A. Clyne, Chem. Phys. Letters 84, 504 (1981).

3. T. G. DiGiuseppe and P. Davidovits, J. Chem. Phys. 74, 3287 (1981).

$BO^*(A-X)$ CHEMILUMINESCENT SPECTRUM FROM $B+O_2$ REACTION

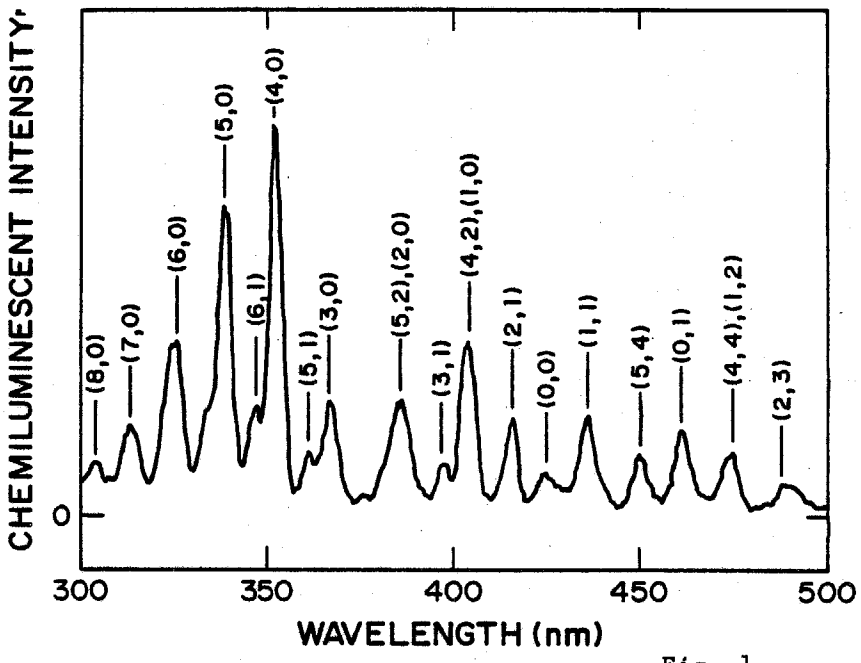

Fig. 1

TIME HISTORY OF BO(A-X) CHEMILUMINESCENCE

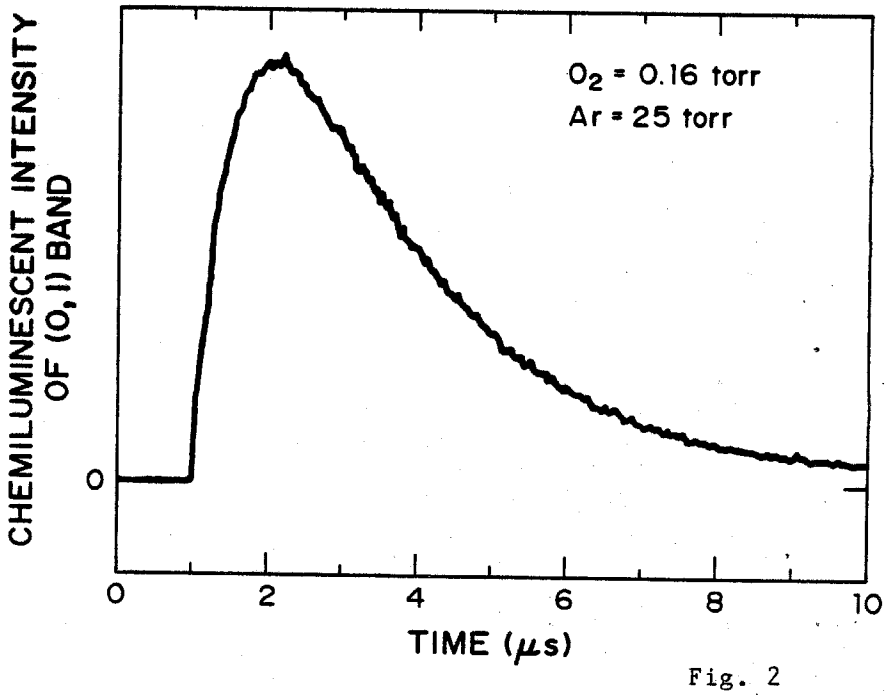

Fig. 2

CHM-VG-8104

FLUORESCENCE EXCITATION SPECTRUM OF BO(A-X)

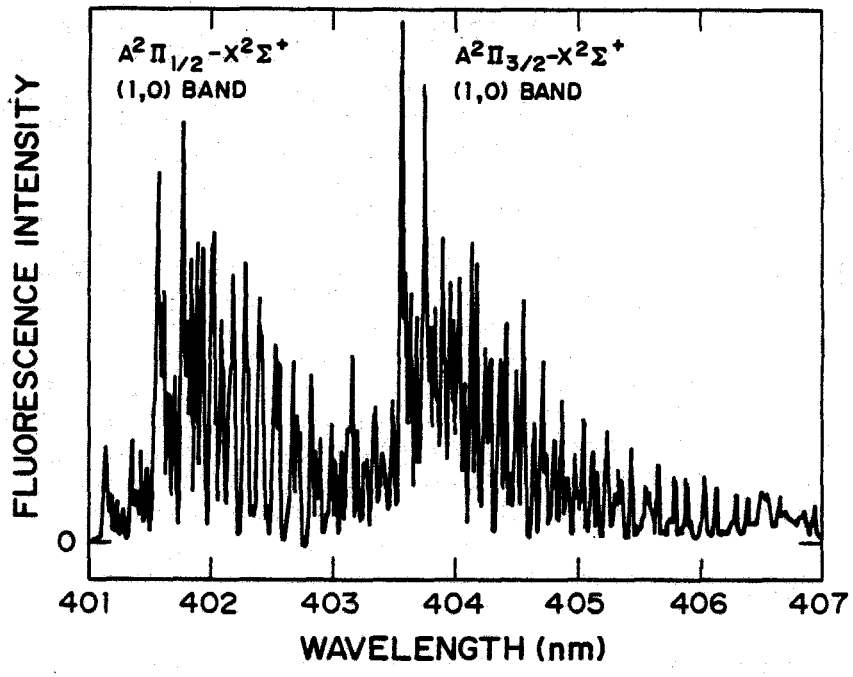

Fig. 3

TIME HISTORY OF BO (X, ν" = 0)

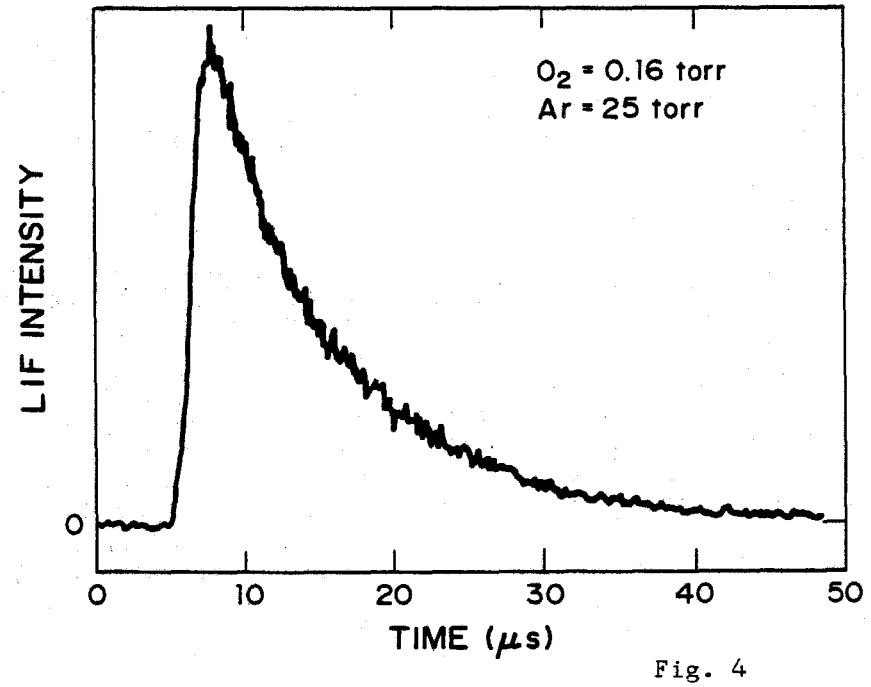

Fig. 4

CHM-VG-8106

NUMERICAL SIMULATIONS OF TRANSITION FROM LAMINAR TO TURBULENT FLOWS

(ONR Contract No. N0001485WR24036
ONR/NAVAIR Contract Nos. N0001485WR24033, N0001988WR51202)

Principal Investigators: Elaine S. Oran, Jay P. Boris,
John H. Gardner, K. Kailasanath

OVERVIEW:

The objective of the research in transitional and turbulent flows is to study the development and evolution of large scale structures initiated by the Kelvin-Helmholtz instability in shear flows. These studies are done numerically using time-dependent solutions of the compressible conservation equations. The three reactive and nonreactive currently studied model a planar splitter plate, an axisymmetric jet and an idealized central-dump ramjet combustor. From these studies we have gained some insights into the effects that control the mixing layer, the effects of acoustic waves on the instability in confined environments, and the basic reinitiation mechanism of the instability.

TECHNICAL DISCUSSION:

Here we summarize the results of time-dependent two-dimensional planar and axisymmetric numerical simulations of shear flows. These have been developed to isolate and investigate some of the mixing and feedback mechanisms involved in the development of reacting and nonreacting spatially evolving mixing layers. The studies of the physical mechanism has required numerical developments for inflow and outflow, and reflecting boundary conditions. Below we describe the numerical model, the results of the studies, and then point to the directions of future research.

Numerical Model:

The numerical model used to perform the simulations solves the time-dependent conservation equation for mass, momentum and energy in two dimensions using the Flux-Corrected Transport (FCT) algorithm. This is an explicit high-order, conservative, monotonic finite-difference algorithm incorporating variably spaced grids with no artificial viscosity for stabilization. A physical viscosity term may be added, but has no effect on the calculation unless it is either very large or computational cell sizes are small enough so that it is larger than the residual numerical diffusion.

We have developed and included a phenomenological model to introduce chemical ignition delays and subsequent energy release. A quantity called the induction parameter is convected with each fluid element to keep track of the time history of the temperature, pressure, and stoichiometry of the fluid. When the mixture is within the flammability limits and has been heated for a long enough time, the energy is released. This phenomenology has been well-calibrated for hydrogen-oxygen mixtures. The ignition delay, the energy release time, and the amount of energy released can be varied through input

parameters to model a variety of fuel-oxidizer systems.

Solving fluid problems with realistic outflow boundary conditions is difficult because information about the flow beyond the mesh is required to make the fluid near the boundaries behave properly. The simplest outflow model is to keep the momentum, energy, and density constant across the boundary, i.e., there is zero gradient. This causes secular errors in long calculations since it does not ensure that the assumed outer flow relaxes to background conditions. The outflow algorithm now used extrapolates the solution just off the edge of the computational mesh to relax toward the given background conditions. Extensive tests on the extrapolation used have shown that the results within the computational domain are not very sensitive to the exact form of the extrapolation. As long as knowledge of the pressure at infinity is used in the extrapolation. The differences in the solutions appear as phase differences in the structures formed in the various calculations. In the closed ramjet problem, the outflow boundary condition forces the flow velocity to become sonic at the exit nozzle. Perhaps the most important boundary condition to do correctly is the inflow algorithm. The algorithm we use allows the incoming gas to respond to pressure pulses coming back toward the splitter plate or nozzle from downstream events such as vortex merging. We specify inflow density and velocity and then use a zero slope condition on the pressure to derive the energy. This choice of boundary conditions eliminated problems in our preliminary calculations in which mass, momentum and energy were specified and thus the pressure was effectively held constant in time.

In the calculations the grid spacing was set up initially and held fixed in time. For the planar calculations used to model the splitter plate experiments, finely spaced cells were clustered around the centerline where the instability first occurs and the coherent structures form. For the axisymmetric calculations used to model the gas jet the grid was finely spaced in the jet and through the region of the shear. The ramjet combustor calculations used fine zones in both directions near the inlet rim of the combustion chamber. Calculations performed used computational grids ranging in size from 20 x 50 to 150 x 250 cells.

Summary of Research to Date

1. Splitter-plate calculations

* Studies of mixing asymmetries in the flow
  * Effects of the velocity ratio of the two streams on mixing
  * Effects of the presence of bounding walls on the mixing
* Studies of the mechanism of reinitiating instabilities
  * Simulation and theory to evaluate the effects of downstream structures on upstream stability
* Future Studies
  * Effects on mixing of density differences in the flow
  * Effects on mixing of energy release in the flow
  * Effects of random inflow velocity perturbations
  * Supersonic flow: stability and structure
  * Effects of absolute velocity on the mixing properties
  * Effects of boundary layers on the splitter plate
  * Three-dimensional calculations

2. Axisymmetric jet

* Studies of the presence of mixing asymmetries in the early parts of the jet flow
* Studies of the effects of perturbation (noise) in the inflowing gas
* Studies of the effects of energy release and expansion on the jet transition region
* Future studies
  * Effects of density differences
  * Three-dimensional transition

3. Idealized ramjet combustor

* Interaction between acoustic waves and large scale structures
* Effects of acoustic forcing on vortex shedding and merging
* Future studies
  * Effects of energy release anc acoustic-vortex-chemical coupling

Selected Results

Figure 1 shows the development of the planar splitter-plate flow in which the velocity ratio of two air streams is 5:1. The fast fluid is on the bottom layer and comes in from the left. The velocity of the faster fluid is 100 m/s, about a third of the speed of sound in the material. The edge of the splitter-plate is indicated by an 'x' along the centerline. To emphasize the mixing processes in the visualization, we have contoured values of the ratio of the number density of fluid from the faster stream to the total number density in the range 0.3 - 0.7. The transition from a uniform shear flow first appears as a pair of vortices just ahead of the tip of the splitter-plate. As the original vortex pair grows and moves downstream, small vortices are still shed at the same approximate location. These vortices grow and merge. By the last panel, a spectrum of modes is seen, suggesting a snapshot from an experimental flow visualization. There is more faster than slower moving fluid in the mixing layer, and this mixing asymmetry increases as the velocity ratio increases.

Another case we have considered is the reactive axisymmetric jet in which a high speed (100 m/s) mixture of molecular hydrogen and nitrogen emerge into a background of molecular oxygen and nitrogen (air). Figure 2 shows results from a calculation in which a jet flows through a hole in a wall on the bottom left into a quiescent background. Contours of R, the ratio of the number density of hydrogen to the total number density in a volume element, are shown on the left hand side and indicate the mixing. As with the splitter plate, structures develop at a fixed distance from the nozzle edge, move along the interface, merge and grow. The graphs on the right hand side show the location of the reaction zone, as determined by the induction parameter describing where the energy is being released. The reaction zones move progressively outward, and the reactions cease in the centers when the oxidant is completely consumed. The material remaining there is hot and consists of hydrogen, from the high speed stream, and product, water.

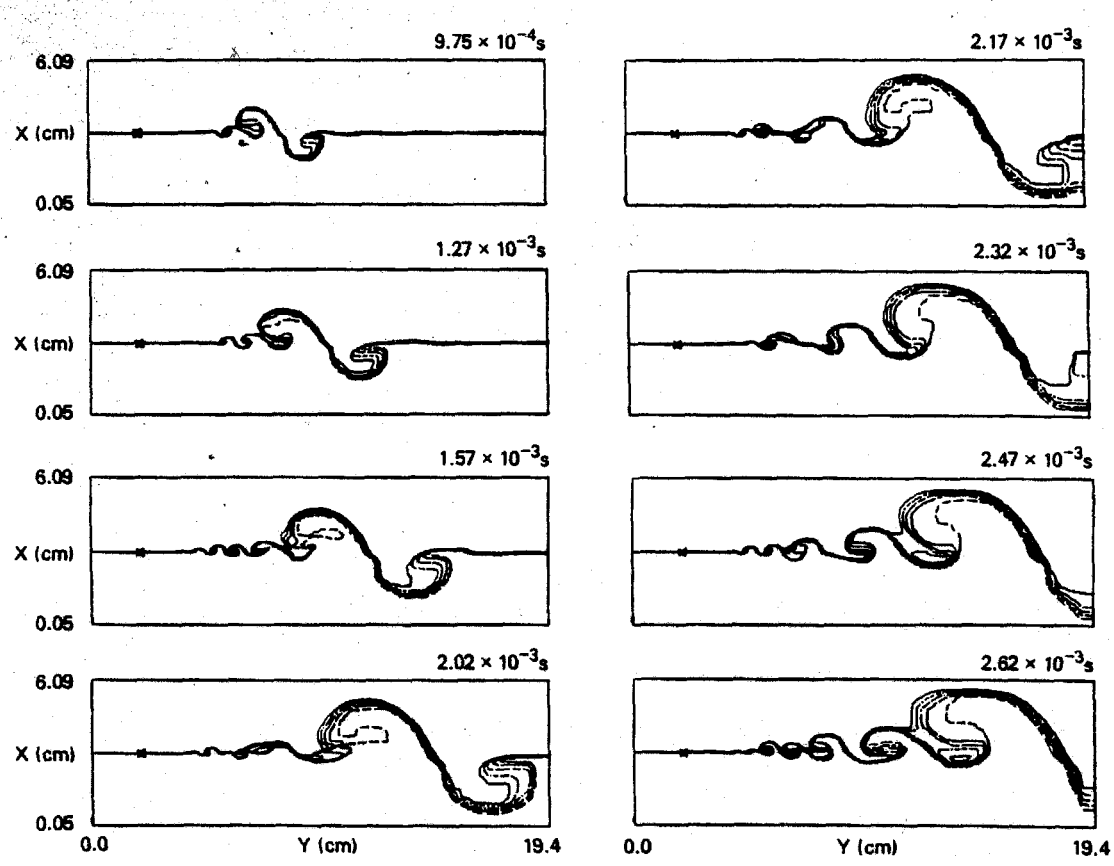

Figure 1

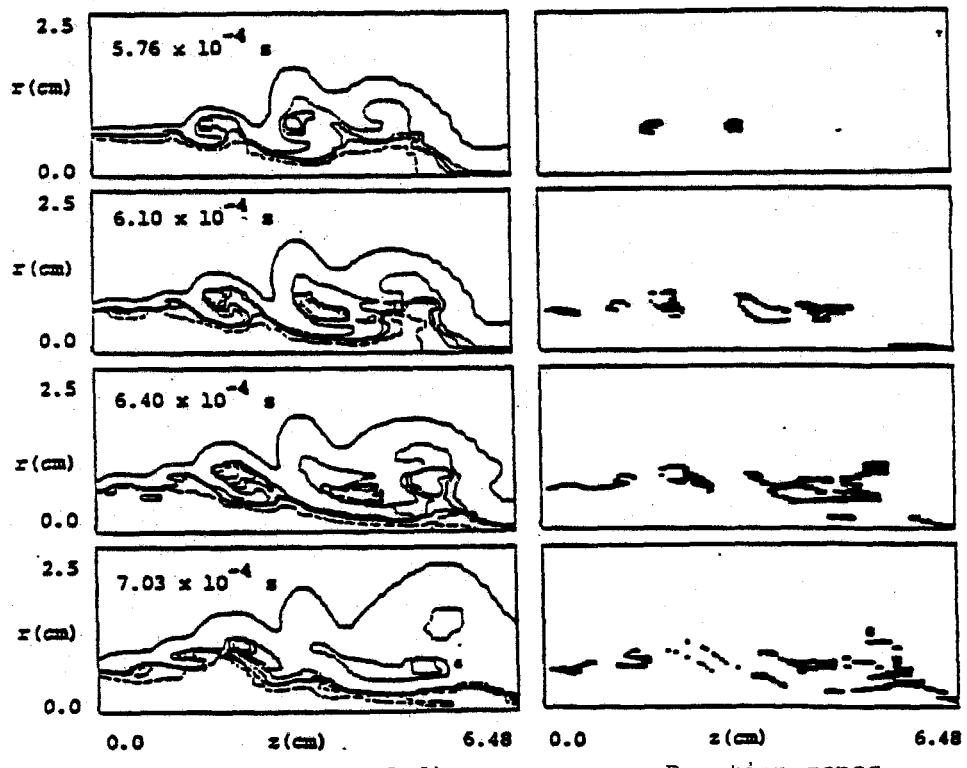

Figure 2 R (range 0.0-1.0) Reaction zones

MONODISPERSE FUEL SPRAY EVAPORATION STUDIES

AFOSR Contract No. F49620-83-K-0027

Principal Investigators: James E. Peters, Herman Krier, Kevin Kim

University of Illinois at Urbana-Champaign
Urbana, IL 61801

SUMMARY:

The goal of this program is to provide detailed information on the evaporation and combustion characteristics of fuel sprays at simulated gas turbine inlet conditions. In particular, evaporation rates in monodisperse sprays are currently being measured as a function of inlet temperature. The monodisperse sprays are generated with an acoustic excitation technique which has provided drops from 70 to 150 μm in diameter and with droplet to droplet separation distances from 2 to 15 diameters. Preliminary results obtained under relatively dilute spray conditions are satisfactorily explained by single droplet evaporation rate expressions. A theoretical effort consisting of an Eulerian solution to the gas phase using the k-ε turbulence model and a Lagrangian calculation for the droplets is also under way.

TECHNICAL DISCUSSION:

Fuel spray evaporation characteristics can strongly influence the combustion process in gas turbines. Consequently, a research program was initiated to study the evaporation and burning rates of fuels at simulated gas turbine combustor conditions. The major thrust of this program is to determine spray, rather than single drop, evaporation rates with a specially designed spray generation technique. With this technique monodisperse sprays are produced with independent control of the drop size, spacing and velocity. Thus the inlet conditions of the spray are well controlled and known which eliminates the uncertainty of the initial spray conditions, a current problem in most spray studies.

Detailed descriptions of the facility appear elsewhere [1]; only a brief discussion of the experimental system is given here. The system features a high pressure (100 to 900 kPa) and temperature (300 to 900 K) air supply (up to 1 kg/sec). As indicated in Figure 1, the liquid fuel spray is injected into the test section with a concentrically mounted fuel injector. Experimental techniques that are being applied to this spray study include a 1-D Laser Doppler Velocimeter (LDV), forward scattering drop sizing, high speed photomicrography and gas sampling with a phase discriminating probe. These systems will provide independent determination of the fuel spray evaporation rates in the test section through the measurement of drop size variations as a function of time (and position) and vapor phase fuel to air ratios.

The droplet injection system was specifically designed and built for this experimental study. The injector operates on the acoustic excitation technique where a vibrating plate at the rear of the injector launches a wave

through a small reservoir of fuel. The waves cause the fuel jets that exit through 40 μm holes in the face of the injector to break up into regularly spaced monosized droplets when the injector controls are tuned to an appropriate amplitude, frequency and pressure. With our "second generation" injector we can achieve a much wider variation in droplet size (70 - 150 μm) and spacing (2 - 15 droplet diameters) than previously thought possible. Figure 2 illustrates the quality of droplets and variable spacing that can be obtained. Note that these droplets were formed from an injector which produced 61 fuel streams and although only one stream is visible (due to the small depth of field of the photograph), the others are of similar quality.

Preliminary tests conducted with our "first generation" fuel injector indicated that the maximum droplet spacing obtainable was approximately 6 droplet diameters. With that spacing, droplets often "caught up" with their predecessors and collided, apparently due to an aerodynamic drag effect. While droplet interactions with collisions is an important area of research, the collisions were undesirable in this case because they disrupted the monodisperse nature of the spray and made the data interpretation much more difficult. The number of droplet collisions was also increased due to the reverse flow of the gas phase in the recirculation zone behind the injector. These problems led to the development of the "second generation" injector with its capability of increased droplet spacings as previously mentioned. The primary difference in the two injection systems is the excitation amplitude; the amplitude of the "second generation" injector's wave launcher is much larger. With the new injector and increased separation distances of the drops, collisions were virtually eliminated when the drops were injected into stagnant air. However, with flowing air the recirculation zone still created enough disturbances to cause a significant amount of collisions. This problem was eliminated by placing a cylinder or shroud around the end of the injector. The shroud extends 6 cm downstream of the injector and has sixteen 1/8" holes drilled approximately 30° off axis radially inward to introduce near axially flowing air. This minimizes (and perhaps eliminates) the recirculating flowfield and the fuel droplets now proceed downstream with minimal collisions. LDV measurements are currently underway to determine the details of the air flow patterns.

Some typical evaporation rate data obtained from our facility are shown in Figure 3. These data were taken by examining photomicrographs of droplets at different axial locations downstream of the fuel injector. No data are available at less than 6 cm because of the fuel injector shroud and data beyond 14 cm are currently limited due to window dimensions (although this limitation on maximum distance is soon to be relaxed). In looking at the data one notes that the evaporation rates roughly approximate a d^2 law behavior modified with droplet heating (assuming a constant drop velocity, which is a reasonable assumption for the particular test conditions used to obtain these data). Following a d^2 law approach, the evaporation coefficient obtained by fitting a straight line through each data set is twice what one would expect for a single drop evaporating in a quiescent atmosphere. The factor of two increase is attributed to forced convection and, in fact, estimates of forced convection corrections to the d^2 law for the test conditions of Figure 3 are approximately equal to 2. Thus the trends exhibited here are explainable with simple single drop expressions. This will most likely <u>not</u> be the case as more nondilute spray behavior is investigated.

Computationally, we have modified a single phase, constant density k-ε turbulence model (a version of the TEACH code) to accommodate compressible, two phase turbulent flow. The Eulerian gas phase equations are solved without the droplets present, and then Lagrangian equations which yield droplet histories are solved. Source terms for mass, momentum and energy obtained from the Lagrangian equations are added to the gas phase equations which are again solved and the process is repeated until convergence is achieved. Both deterministic and stochastic droplet behavior is modeled. Additional details of both the experimental and computation procedures and results can be found in reference [2].

Current and future work includes the continued measurement of evaporation rates with variations in temperature, pressure and fuel type and the comparison of the experimental and the modeling results.

REFERENCES:

1. Peters, J. E., Krier, H., Kim, K. K., Coverdill, R. E., Kirwan, J. E., Meisner, S. C., and Kim, K. W. (1984), "Research Test Facility for Evaporation and Combustion of Alternative Jet Fuels," Tech. Rep. UILU ENG-84-4001.
2. Peters, J. E., Coverdill, R. E., Kirwan, J. E., and Krier, H. (1985), "Monodisperse Fuel Spray Studies in High Temperature Flowing Air," presented at the AIAA/ASME/SAE 21st Joint Propulsion Conference, AIAA Paper No. 85-1319.

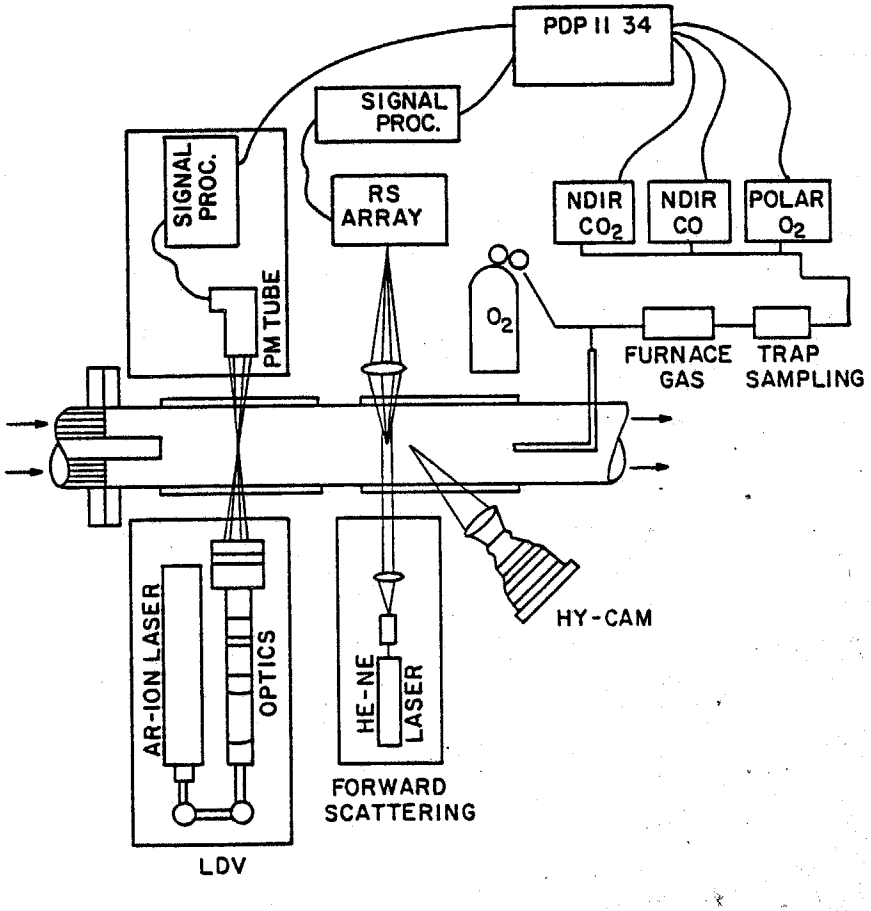

Figure 1. Test facility schematic showing measurement systems.

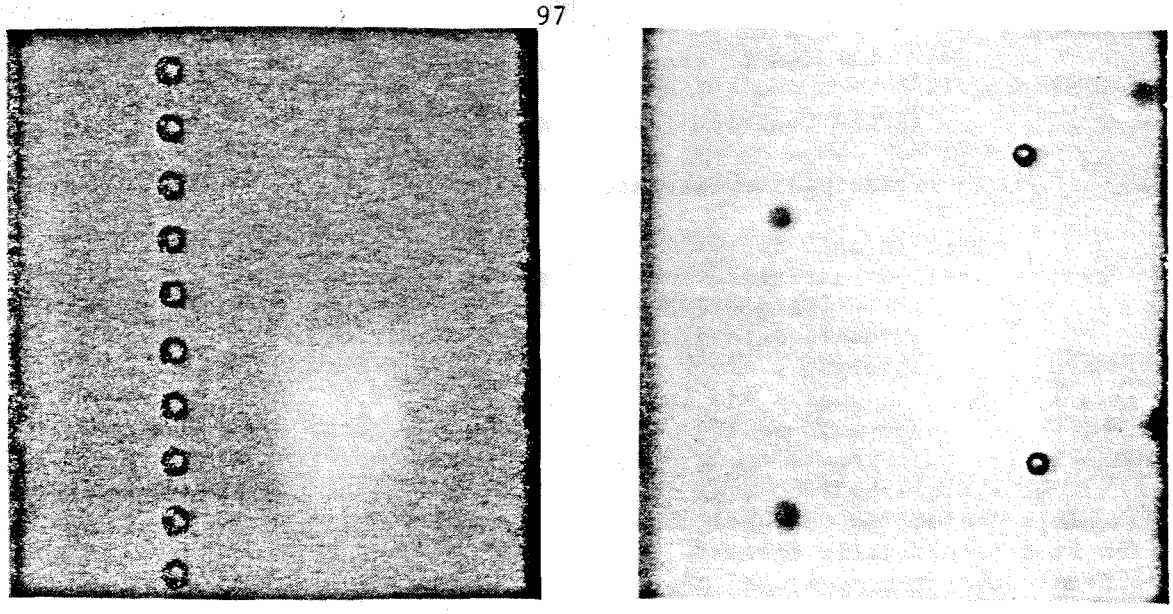

Figure 2. Photomicrographs of droplets illustrating the range of droplet spacings that can be achieved. Droplet sizes are approximately 100 μm.

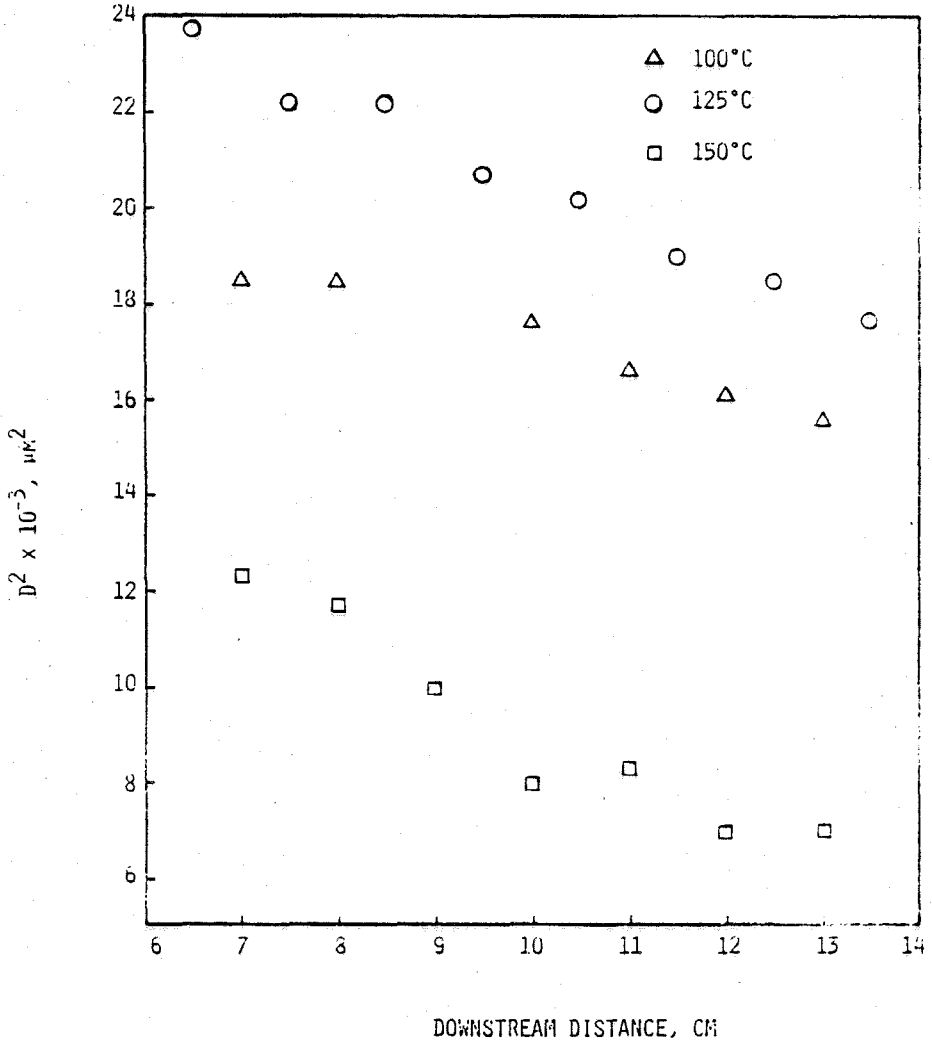

Figure 3. Variation of d^2 with distance downstream of the fuel injector for heptane droplets.

CHEMICALLY REACTING TURBULENT FLOW

(AFOSR Contract No. AFOSR--ISSA 85-00012)

Principle Investigators: William M. Pitts
Taskashi Kashiwagi

Center for Fire Research
National Bureau of Standards
Gaithersburg, MD 20899

SUMMARY:

This project is designed to study chemically reacting turbulent flow by systematically investigating the effects of density differences, temperature differences, and heat release on turbulent mixing. The discussion covers work performed during the period (20 months) since our last report to this group. Studies of the mixing behavior of variable density axisymmetric jets and the development of new diagnostics designed especially for, but not limited, to the study of this problem are emphasized. This work is yielding important clues as to the nature of density effects on turbulent mixing. Characterizing and predicting such effects is a necessary first step toward the goal of understanding and controlling chemically reacting turbulent flow with its concomitant heat release and density variations.

TECHNICAL DISCUSSION:

Introduction

This research program is a long term, systematic study of chemically reacting turbulent flow. This is the third year that this project has been supported by the Air Force Office of Scientific Research.

Previous reports of the development of Rayleigh light scattering as a real-time, spatially resolved probe of concentration fluctuations in turbulent binary gas mixtures [1,2] as well as its combination with hot-wire anemometry for simultaneous concentration and velocity measurements [3] are available.

During the current reporting period, work on the development of flow diagnostics has continued. A detailed investigation [4] of the response of hot-wires and films to flows of different gases has been completed in collaboration with Dr. Bernard McCaffrey of the Center for Fire Research. The Rayleigh light scattering technique for concentration measurement has been extended from point to line measurements by the development of a digital linear camera having the sensitivity and time response necessary for Rayleigh light scattering measurements in gases. Preliminary results indicate these line measurements offer the possibility of a greatly enhanced understanding of entrainment in variable density turbulent flows.

An investigation of density effects on turbulent mixing behavior in an axisymmetric jet has been extended to include the gas pairs CF_4/air, SF_6/air, and SF_6/He. Centerline concentration data is now available for jet/coflow density ratios covering the range from 0.14 to 37. Flow visualization using shadowgraphy for the various jets has also been employed to gain further insight into the effects of global density differences on turbulent mixing.

Short summaries of results and major conclusions of the diagnostic as well as the density effect studies follow.

Hot-wire and Film Behavior in Different Gases and Mixtures

The response of hot-wires and films to flows of nine different gases have been investigated. Attempts to correlate the results in terms of commonly used expressions for heat transfer from cylinders were unsuccessful. In particular, use of the Prandtl number correction usually employed in the literature failed to yield a correlation of the experimental results. However, by considering the effect of and correcting for end heat losses, Knudson number effects, surface accommodation effects, and especially temperature variation of molecular properties, the correlation shown in fig. 1 is obtained. Work on the response of these detectors to mixtures of gases is continuing. In this case, thermal diffusion effects may be important. Howard Baum of the Center for Fire Research is investigating this problem theoretically. Our findings concerning the responses of hot-wires and films to flows of different gases are not only very important for hot-wire anemometry, but have significant implications for the more general field of heat transfer.

Development of a Digital Line Camera

In the past, the use of laser-induced Rayleigh light scattering for real-time, spatially resolved concentration measurements has been limited to a single point. Recent developments in electronic image multipliers and solid state line detectors have opened up the possibility of extending these measurements to a line.

At NBS, a digital line camera has been designed and constructed which has the sensitivity and time resolution to allow real-time (2 kHz), spatially resolved (0.2mm) measurements of concentration in a turbulent flow of propane into a slow coflow of air. The camera incorporates a fast lens, two stage generation I image intensifier with P47 phosphor, 4:1 fiber optic taper, and a 128 pixel Reticon solid state line scanner. The configuration of the camera is shown in fig. 2.

Preliminary tests have demonstrated that the camera is capable of resolving temporal and spatial concentration fluctuations for the propane/air jet. The importance of large scale structures in this flow is obvious from these initial studies.

Concentration Effects on the Mixing Behavior of an Axisymmetric Jet

Rayleigh light scattering [5] has been used to measure the average, RMS, skewness, and kurtosis of centerline concentration fluctuations in turbulent jet/coflow combinations of He/air, CH_4/air, C_3H_8/CO_2, C_3H_8/air, CF_4/air, SF_6/air, and SF_6/He. Most measurements have been made for Reynolds numbers (Re) of approximately 4000. However, some results have been obtained at higher Re in order to elucidate effects of Re on the mixing behavior.

Figure 3 shows the results of measurements of the unmixedness (defined as the RMS of the concentration fluctuations divided by the average concentration) in terms of mass fraction as a function of nondimensionalized downstream distances. Two major conclusions can be inferred from this figure:

1. The value of unmixedness approaches an asymtote of $\sim$0.23 for all of the different jet/coflow combinations as the downstream distance increases.

2. The higher density ratio jet/coflow gas pair combinations approach the asymtotic value more slowly as a function of downstream distance.

The identification and characterization of global density effects such as these are necessary for the development of empirical relations and detailed theories of turbulent mixing in the presence of density fluctuations.

Flow visualization using time-resolved (FWHM of light pulse = 165 μs) shadowgraphy has been performed for the different jet/coflow gas combinations used in this study. These photographs reveal that the potential core lengths and initial spreading rates of these jets have a strong dependence on the density ratio. The empirical findings of the flow visualization study are in agreement with conclusions 1 and 2 above. The effects of density are especially evident for the low Re jets of SF_6 into air and He which demonstrate "fountain"-like behavior in which jet fluid actually falls through the coflow gases.

REFERENCES:
1. W. M. Pitts and T. Kashiwagi, NBSIR 83-2641 (1983).
2. W. M. Pitts and T. Kashiwagi, J. Fluid Mech. 141 (1984) 391.
3. W. M. Pitts, B. J. McCaffrey, and T. Kashiwagi, paper presented at the Fourth Symposium on Turbulent Shear Flows, Karlsruhe, FDR, September 12-14, 1983.
4. W. M. Pitts and B. J. McCaffrey, submitted for publication.
5. W. M. Pitts, manuscript in preparation.

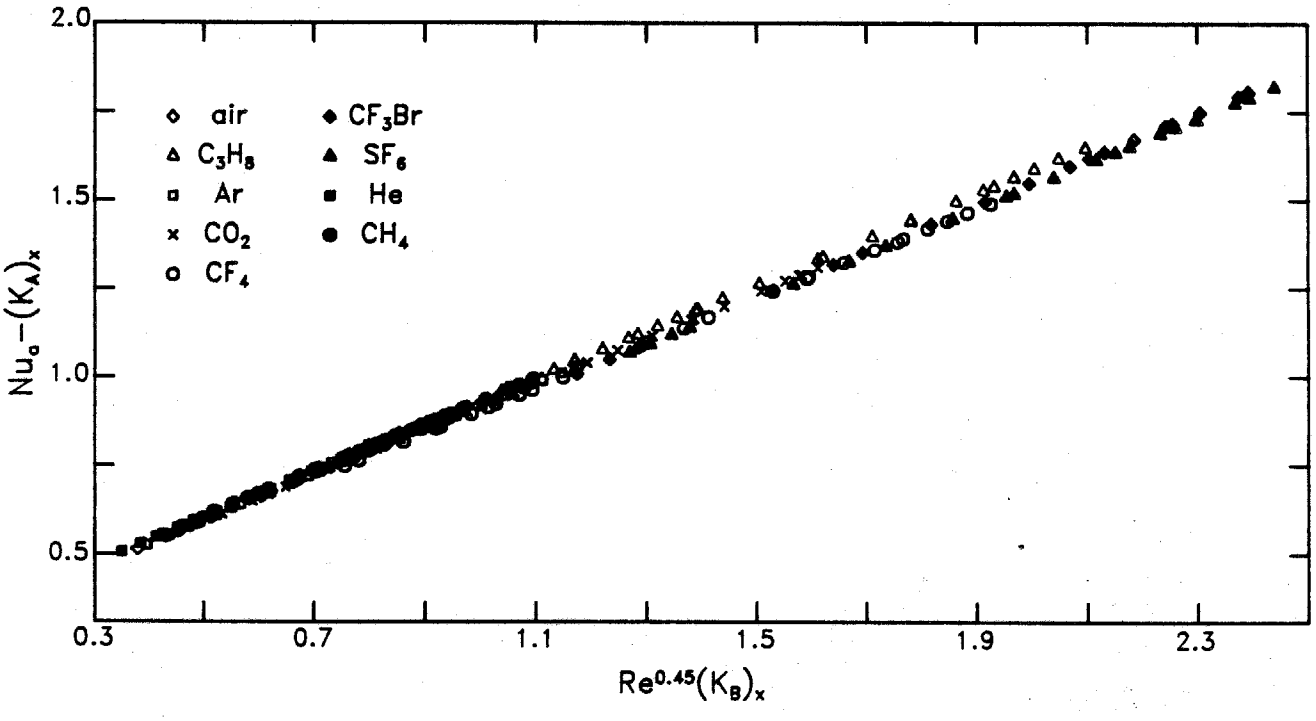

Figure 1. The measured responses of a hot-wire to flows of nine different gases are shown in terms of the Nusselt number (Nu_a) and Re. The values of Nu_a are corrected for heat losses at the end of the probe, flow slip effects, and surface thermal accomodation. $(K_B)_x$ and $(K_A)_x$ are corrections which are dependent on the molecular properties of the gases. All of the corrections are necessary to obtain the degree of correlation shown.

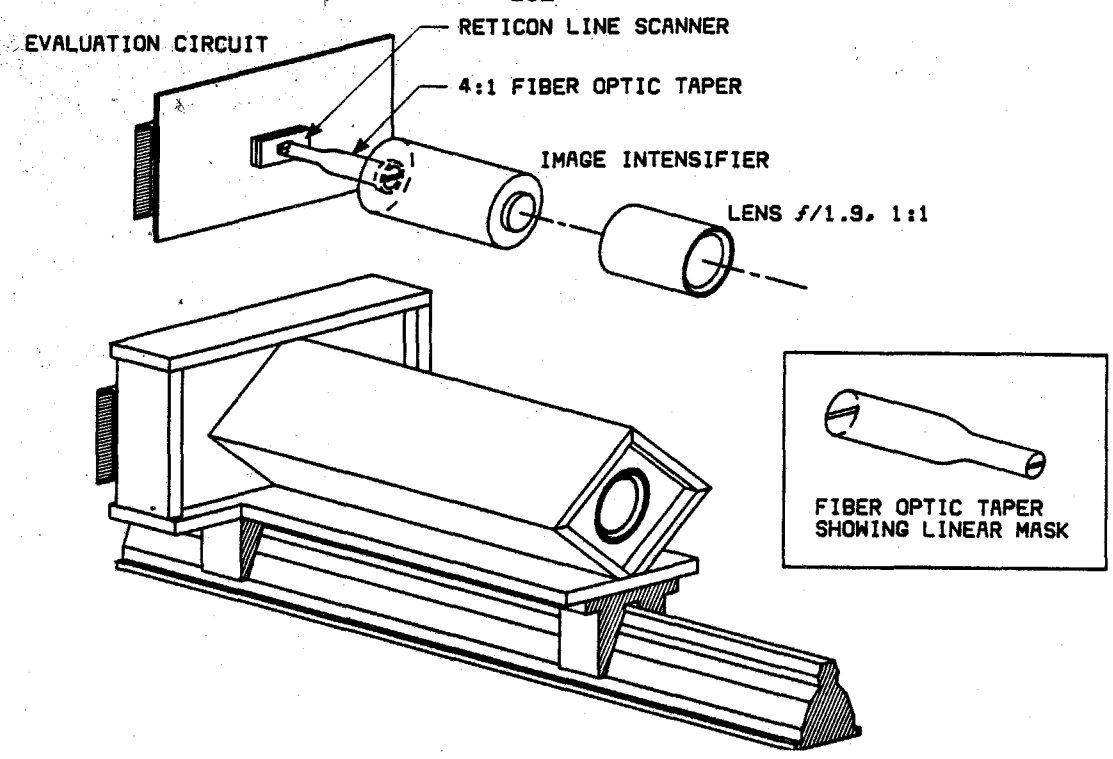

Figure 2. The experimental configuration for the camera used in the digital line camera system is shown. The fiber optic taper (shown Blown-up) is coated on its small end with aluminum and scribed with a 0.2 mm line to reduce parasitic light reaching the line scanner.

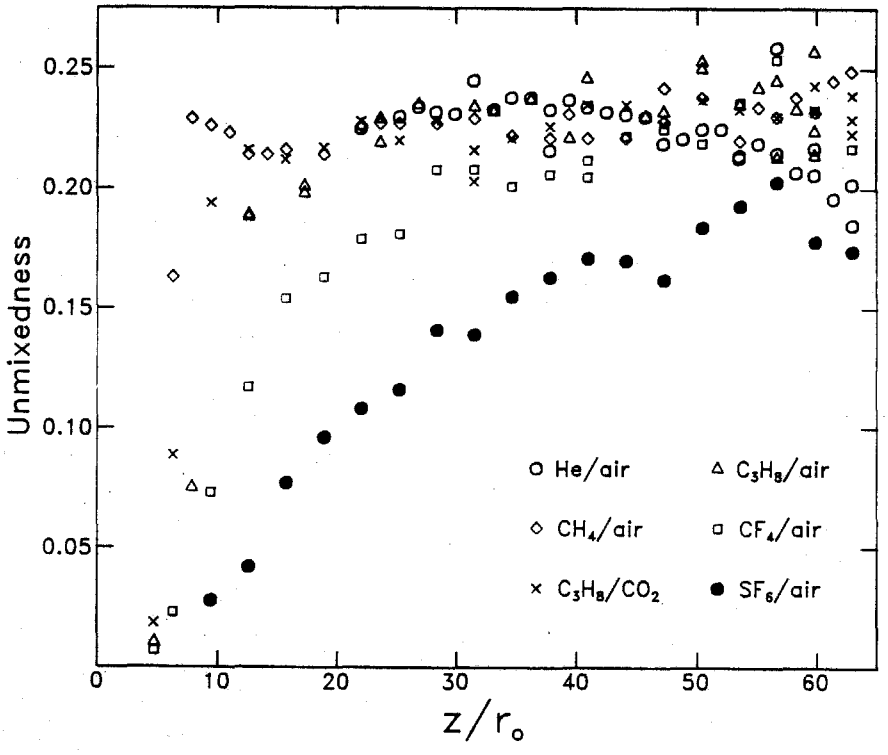

Figure 3. Values of unmixedness are plotted as a function of nondimensionalized downstream distance for the listed jet/coflow combinations. All of the measurements were taken at Re $\sim$ 4000 except the SF_6/air results for which Re $\sim$ 8000.

NUMERICAL EXPERIMENTS ON TURBULENT MIXING

(AFOSR Grant/Contract No. 85-0083)

Principal Investigator: S.B. Pope

Sibley School of Mechanical and Aerospace
Engineering, Cornell University, Ithaca, NY 14853

SUMMARY

In turbulent combustion, mixing by molecular transport is an essential process that is not well understood. Because mixing occurs on the smallest length and time scales it is difficult to study experimentally. Instead, we are starting a study based on the direct numerical simulation of turbulence, initially for a conserved passive scalar in homogeneous isotropic turbulence. The Eulerian velocity and scalar fields are calculated from the exact evolution equations, and both Eulerian and Lagrangian statistics are deduced from the computed fields.

INTRODUCTION

Nearly all flows of technological importance are turbulent. In most combustion devices, turbulence plays a vital role in promoting fluid mixing and hence accelerating combustion rates. While experimental techniques are making significant progress, there are unanswered fundamental questions concerning turbulent mixing that remain beyond the reach of experimentalists. These unanswered questions are an obstacle to the development and testing of statistical models of turbulence. Answers are needed so that these models can be developed into reliable design tools.

The objective of this work is to answer fundamental questions concerning turbulent mixing, through numerical simulations of turbulent flows.

The details of the mixing process are difficult to study experimentally because the smallest length and time scales must be resolved. Further, it is not sufficient just to measure the value of the scalar (e.g. composition or temperature) at a point: rather its first two derivatives in each direction are the prime quantities of interest. That mixing is a microscale process compounds experimental difficulties, but it provides grounds to hope for universality. That is (according to classical theory, Monin & Yaglom 1971), at high Reynolds number, the details of the mixing process are determined by a few macroscale quantities, but are otherwise independent of the large scale of the flow.

These considerations show that the direct numerical simulation of turbulence provides a good means of studying turbulent mixing. All scales are resolved, and any quantity of interest can be determined since the fields are known for all positions and times. In view of the universality of the small scales, it is sufficient to simulate just a few flows—the most easily computed being homogeneous turbulence.

The statistical information about turbulent mixing that can be obtained from direct numerical simulations is of general interest and importance. I am also strongly motivated to obtain a better understanding of the mixing process in order

to improve statistical models of mixing. In the last decade, PDF methods have been developed and demonstrated for a wide range of inhomogeneous reacting and non-reacting flows. They hold great promise as a practicable means of calculating the properties of turbulent reactive flows of engineering interest. The velocity-composition joint PDF method has the advantage of being able to treat reaction and convection without approximation. But a major unknown that has to be modelled is the molecular mixing term. Qualitative and quantitative information about the term is needed to improve and generalize its modelling. This information can be obtained from direct numerical simulations.

Since the governing equations of fluid flow (i.e. the Navier-Stokes equations) are known, it is in principle possible to solve them with boundary and initial conditions appropriate to the flow of interest. In practice, because numerical solutions are required, computational capabilities impose a limit on the complexity of the flows that can be studied and on the Reynolds number that can be attained. But for statistically-homogeneous turbulent flows - which are ideal for studying turbulent mixing - it is now possible to solve the flow equations at Reynolds numbers as high as are attained in laboratory wind tunnels.

PROGRESS

We have obtained from Dr. Rogallo (NASA Ames) a copy of the code he developed to simulate homogeneous turbulence. We have translated the code into FORTRAN and checked the results in detail against Rogallo's calculations. With this code we will be able to simulate turbulence with a Reynolds number R_λ in the range 50-80.

The Lagrangian approach offers a different--possibly better--perspective on turbulent mixing. In the numerical simulation, for each time step the Eulerian fields at the forward time are deduced from those at the current time. We will also track the positions ($\underline{x}^{(n)}$, n=1,2,•••,N) of a large number (N=50,000, say) of fluid particles. Then the Lagrangian velocity and scalar time series can be obtained (e.g. $\underline{U}^{(n)}(t) = \underline{U}(\underline{x}^{(n)}[t],t)$). We have coded and tested the algorithm that tracks the fluid particle positions.

TITLE: STRUCTURE AND MIXING IN TURBULENT SHEAR FLOWS

ONR Contract No. N00014-76-C-0260 Task No. NR 062, 431

Principal Investigator: Anatol Roshko

Graduate Aeronautical Laboratories
California Institute of Technology
Pasadena, California 91125

SUMMARY/OVERVIEW:

The broad problem being addressed in our research is to identify and describe the primary vortical ("coherent", "organized") large structures in various turbulent shear flows; to determine how they contribute to the mixing processes; and to make use of them in modelling and in possibly controlling or modifying those flows. Accumulating experimental evidence suggests that these primary vortical structures are different in different shear flows. Conclusions which follow from these views are that (i) there cannot be a universal turbulence model for these different flows; and (ii) existence of such structures implies the possibility of their manipulation or control and thus modification of the flow itself. These organized structures (and their response to excitation) are manifestations of instability response to natural or imposed disturbances and thus may be important in cooperation with other, physical processes, e.g., acoustic coupling, rate controlled chemistry, etc., in problems like combustion chamber instability.

TECHNICAL DISCUSSION

A variety of problems, using several different shear flows, have been investigated during the past three or four years. These include the following: (i) nature of the large organized structure in plane wakes; (ii) effects of a periodic disturbance on mixing in a plane mixing layer; (iii) effects of a periodic disturbance on organized structure in the shear layer of a separation bubble and the corresponding effects on bubble pressure coefficient; (iv) effect of curvature on free-shear-layer structure and mixing; (v) structure and mixing in transverse jets.

A significant result from the plane-wake experiments (Refs. 1, 2) is that the initial, quasi two-dimensional structures, which result from vortex shedding, rapidly decay; the structures that appear further downstream (e.g., observed by Taneda many years ago) are uncoupled from the initial ones. Porous cylinders which do not shed vortices eventually also develop the far-wake structures, which are a consequence of the hydrodynamic instability of the developing wake profile. A further result is that the far wake structures are three dimensional, in contrast to the quasi-two-dimensionality of the large structure in the initial vortex street and in mixing layers. This is consistent with the fact that, in wakes,

streamwise and spanwise instabilities have comparable growth rates, as computed for example by Robinson and Saffman (Ref. 2).

When a perturbation of about 1% was added to the free-stream velocity of a turbulent mixing layer in water (Refs. 4, 5), the effects reported by Oster and Wygnanski and Oster were observed: enhanced growth rate in the first part of the layer I; followed by zero growth rate in a portion of the layer (II) which scales with the forcing wave length; finally relaxation to unperturbed growth rate (III). The effect of all this on mixing (chemical reaction) was studied. By and large, at high Reynolds number, the chemical production rate (i.e., mixing rate) follows the variation in growth rate; in fact, it is rather astonishing that in region II the mixing is reduced to zero! At lower Reynolds numbers, effects of periodic disturbance are complicated by the effects of the "mixing transition".

In the case of a separation bubble, originating at the shoulder of an axisymmetric, blunt faced cylinder aligned with a free stream, periodic excitation at appropriate frequencies also accelerates the initial growth of the shear layer; this shortens the bubble, reduces the pressure coefficient at separation and reduces the average pressure (drag) on the face (Ref. 6). In the reattachment region of such bubbles, the quasi two dimensional vortex structures in the shear layer develop a strong spanwise instability as they approach reattachment. Alternate segments of the resulting spanwise wave are pulled upstream and downstream, respectively; their joining segments stretch out to form a pattern of streamwise vortices which bridge the reattachment zone. In the reattached flow, the convecting wave vertex and its pair of vortex legs form a large loop, which becomes part of the resulting boundary layer structure.

For curved mixing layers with uniform density the sense of the curvature has a large effect, which can be attributed to Taylor-Gortler instability. When the faster stream is on the inside three dimensionality is enhanced and the pairing events so common in plane mixing layers is much less evident; growth rate is faster than in the plane layer. On the other hand, when the faster stream is on the outside the growth rate is lower. For curved mixing layers between streams of different densities, Rayleigh-Taylor instability becomes an important sometimes dominant mechanism. Three dimensionality is greatly inhibited if the heavier gas is on the outside and enhanced when the heavier gas is on the inside. Growth rates are enhanced in the latter case.

The experiments on jets transverse to a stream are done mainly in water, making use of the various available visualization and chemical-reaction measurement techniques. Results obtained include data on jet trajectories, "flame length", large structures and mixing/concentration distributions. In addition, a curious structure in the "wake" of the jet, suggestive of a vortex street, has been observed. Most of the work outlined above has concentrated on regions many diameters from the jet exit; in the continuing work the early part of the flow will also be addressed.

1. References

Cimbala, John M. 1984 Large-structure in the far wakes of two-dimensional bluff bodies. Ph.D. Thesis, California Institute of Technology.

Cimbala, John M. 1985 An experimental study of large structure in the far wakes of two-dimensional bluff bodies. To be presented at the Fifth Symp. on Turbulent Shear Flows, 7-9 August, Cornell University.

Robinson, A.C. and Saffman, P.G. 1982 Three dimensional stability of vortex arrays. J. of Fluid Mech. 125, 411-427.

Roberts, Frederick A. 1984 Effects of a periodic disturbance on structure and mixing in turbulent shear layers and wakes. Ph.D. Thesis, California Institute of Technology.

Roberts, Frederick A. 1985 Effects of periodic forcing on mixing in turbulent shear layers and wakes. AIAA-85-0570 paper, AIAA Shear Flow Control Conference, 12-14 March, Boulder, Colorado.

Sigurdson, Lorenz W. 1985 Controlled excitation of a reattaching flow. AIAA-85-0552 paper, AIAA Shear Flow Control Conference, 12-14 March, Boulder, Colorado.

PARTICLE AND VAPOR MASS TRANSPORT THROUGH NON-ISOTHERMAL COMBUSTION GASES

Grant No. AFOSR-84-0034

Principal Investigator: Daniel E. Rosner

High Temperature Chemical Reaction Engineering Laboratory
Yale University, P.O. 2159 Yale Station, New Haven, CT 06520 USA

SUMMARY/OVERVIEW*:

The performance of ramjets burning slurry fuels (leading to condensed oxide aerosols and liquid film deposits), gas turbine (GT) engines in dusty atmospheres, or when using fuels from non-traditional sources (e.g., shale, or coal-derived), will depend upon the formation and transport of small particles across non-isothermal combustion gas boundary layers (BLs). Moreover, even engines burning "clean" hydrocarbon fuels can experience soot formation/deposition problems (e.g., combustor liner burnout, accelerated turbine blade erosion and "hot" corrosion). Accordingly, our research is directed toward providing propulsion systems design engineers with quantitative information on important particle and vapor mass transport mechanisms and rates.

An interactive experimental/theoretical approach is being used to gain an understanding of performance-limiting chemical, and mass/energy transfer phenomena at or near interfaces. This includes the development and exploitation of laboratory flat flame burners and cooled deposition targets (see, e.g., Fig. 1), flow-reactors, and new optical diagnostic techniques. Resulting experimental rate data, together with the predictions of comprehensive asymptotic theories, are then used as the basis for proposing and verifying simple viewpoints and effective engineering correlations for future design/optimization studies.

TECHNICAL DISCUSSION

1. Seeded Flame Experiments on Submicron Particulate Transport Rates Small particle transport through non-isothermal gases can easily be dominated by thermophoresis, as was confirmed in our recent optical experiments (1) on submicron MgO-particle deposition from ($MgSO_4$-seeded) propane/air flames. Relative deposition rates, measured on-line via the loss in Pt-target reflectivity, were obtained at various target and gas temperatures, and found to agree with the predictions of thermophoretic laminar boundary layer (LBL) theory (2,3). Moreover, for the same seed level, particle deposition rates at $T_w/T_g \approx 0.7$ were estimated to be over 1000-times larger than the corresponding rate of convective (Brownian) diffusion. These experiments have recently been extended to include carbonaceous soot deposition from fuel-rich premixed flat flames (4,5). Our data indicate that soot particle transport to gas-cooled targets (Fig. 1) or thermocouples is described by the abovementioned laws of particle thermophoresis. In the case of the gas-cooled stagnation point probe (Fig. 1), on which the rate of deposition is monitored via real-time laser light extinction by the deposit itself, the fact that Fig. 2 yields a straight line demonstrates (5) the dominance of thermophoresis (over Brownian diffusion).

2. Boundary Layer Mass Transfer Predictions and Rational Correlations We have formulated and solved numerically the BL conservation equations governing laminar self-similar variable property BLs (3) and law-of-the-wall fully-developed turbulent BLs (6) for a large number of low particle mass-loading cases (wall temperature ratio, particle Schmidt number, viscous dissipation (7), wall

* 1985 AFOSR/ONR Contractors Meeting on Airbreathing Combustion Dynamics, 22-25 July, 1985, California Inst. Technology, Pasadena, CA.

transpiration...) to obtain mass transfer Stanton numbers, St_m, in the presence (and absence) of thermophoresis, and to provide a means of testing the abovementioned "thermophoretic suction" correlation scheme. The success of the correlation scheme in the "cold-wall" cases was demonstrated in Ref. 2, which included solid wall cases in which the thermophoretic enhancement is about 10^3-fold. Recent calculations for hot-wall cases (8) (up to 6-times the mainstream temperature) reveal that thermophoretic reductions of greater than 10^{-10}-fold are possible (see Fig. 3 for TBLs, including the predictions of our simple "thermophoretic blowing" correlation scheme). Of course, in many practical high enthalpy gas situations, wall heating would not be a feasible means of reducing dust deposition rates*. Then, wall transpiration of a cool, dust-free gas is able to cool the surface and yet dramatically reduce dust deposition rates. While this reduction is not nearly so great as it would have been in the absence of thermophoresis (6,9), transpiration is probably the only practical method to simultaneously accomplish the goals of wall cooling and reduced submicron particle deposition rate.

3. Interactions Between Particle Deposition (PD) and Vapor Deposition (VD); BL Condensation

Because aerosol particles are often present along with other condensible vapors in combustion products, we have initiated experimental and theoretical studies of deposition rates in such PD-and VD-systems, exploiting our "flash evaporation" technique (for alkali compunds) described in Ref. 10 (see Fig. 4). An interesting and commonly occurring limiting case occurs when, presumably, VD is being studied, but in the unavoidable presence of condensation nucleii. Then, even if the mainstream is undersaturated, appreciable condensation can occur within the BL adjacent to the cooled surface. Since the resulting droplets are presumably less mobile than their parent vapors, this phenomenon (encountered at surface temperatures sufficiently below the prevailing dew point temperature) has been expected to dramatically reduce total deposition ratees. Reductions have often been observed (see, e.g., the Na_2SO_4 deposition rate data points (11) shown in Fig. 5 (12)) but, until now, there has been no tractable theory for calculating such rates. Based on the LBL physical model sketched in Fig. 6 (assuming local vapor/liquid equilibrium within the "fog-sublayer", and droplet drift toward the wall due to thermophoresis) we have predicted deposition rate trends for a number of eligible values of the thermophoretic diffusivity parameter. As shown in Fig. 5, the available data, while scattered, is well-described by the present theory on the assumption that the thermophoretic diffusivity of the $Na_2SO_4(\ell)$ condensate is about 1-decade smaller than the momentum diffusivity of the combustion products. We hope to make more detailed comparisons of this type once we extend the Na_2SO_4 deposition rate data presented in Ref. 10 to lower surface temperatures and lower mainstream undersaturation levels.

CONCLUSIONS, FUTURE RESEARCH

We have illustrated some important effects of temperature gradients on convective-diffusional mass transport rates in combustion systems. As discussed in Ref. 13, this class of phenomena destroys the widely used "analogy" between mass and heat transfer and would cause intolerable errors if mass transfer coefficients were estimated from St_h-values by merely replacing the Prandtl number, Pr, by the Schmidt number, Sc. In general, light vapor species tend to drift toward hot regions/surfaces, and heavy species/particles tend to drift toward cold regions/surfaces. The latter effect is particularly strong, and is found to dominate small particle capture rates in a number of propulsion-oriented applications. In the OSR-sponsored work briefly described here we have shown that new laser-based experimental techniques for rapidly measuring vapor and particle mass transfer rates (1,5,14), combined with recent advances in what might be called "thermophoretic boundary layer theories" (2,3,6-9), are providing useful means to incorporate these phenomena in many propulsion engineering design/optimization calculations. In the future we hope to extend this work to include, among other things, the potentially important effects of highly nonspherical particles (or molecules) (15).

---

* Yet, in hot substrate/cold wall chemical vapor deposition reactors used in the semiconductor industry, the resulting thermophoretic "rejection" of unwanted dust particles is a very desirable feature.

REFERENCES

1. Rosner, D.E. and Kim, S.S., "Optical Experiments on Thermophoretically Augmented Submicron Particle Deposition from 'Dusty' High Temperature Gas Flows," The Chem. Engrg. J. 29, No. 3, 147-157 (1985).
2. Gokoglu, S.A. and Rosner, D.E., "Correlation of Thermophoretically-Modified Small Particle Diffusional Deposition Rates in Forced Convection Systems with Variable Properties, Transpiration Cooling and/or Viscous Dissipation, Int. J. Heat & Mass Transfer 27, 639-645 (1984).
3. Gokoglu, S.A. and Rosner, D.E., "Thermophoretically-Augmented Forced Convection Mass Transfer Rates to Solid Walls Across Non-Isothermal Laminar Boundary Layers, AIAA J. (in press, 1985).
4. Eisner, A.D. and Rosner, D.E., "Experimental Studies of Soot Particle Thermophoresis in Non-Isothermal Combustion Gases Using Thermocouple Response Techniques," Combustion & Flame (in press, 1985).
5. Eisner, A.D. and Rosner, D.E., "Experimental and Theoretical Studies of Submicron Particle Thermophoresis in Combustion Gases," presented at the 5th Int. Symposium on PhysicoChemical Hydrodynamics, Tel-Aviv, Israel, Dec., 1984, J. PhysicoChemical Hydrodynamics (in press, 1985).
6. Gokoglu, S.A. and Rosner, D.E., "Thermophoretically Enhanced Mass Transport Rates to Solid and Transpiration-Cooled Walls Across Turbulent (Law-of-the-Wall) Boundary Layers," I/EC Fundamentals 24, No. 2, 208-214 (1985).
7. Gokoglu, S.A. and Rosner, D.E., "Viscous Dissipation Effects on Thermophoretically-Augmented Particle Transport Acros Laminary Boundary Layers," Int. J. Heat & Fluid Flow (in press, 1985).
8. Gokoglu, S.A. and Rosner, D.E., "Prediction and Rational Correlation of Thermophoretically Reduced Particle Mass Transfer to Hot Surfaces Across Laminar or Turbulent Forced-Convection Gas Boundary Layers," (submitted, 1985).
9. Gokoglu, S.A. and Rosner, D.E., "Effect of Particulate Thermophoresis in Reducing the Fouling Rate Advantages of Effusion-Cooling," Int. J. Heat & Fluid Flow 5, No. 1, 37-41 (1984).
10. Rosner, D.E. and Liang, B., "Laboratory Studies of the Deposition of Alkali Sulfate Vapors from Combustion Gases Using a Flash-Evaporation Technique," Chem. Engrg. Commun. (in press, 1985).
11. Santoro, G.J., Gokoglu, S.A., Kohl, F.J., Stearns, C.A. and Rosner, D.E., "Deposition of Na_2SO_4 from Salt-Seeded Combsution Gases of a High Velocity Burner Rig," NASA TM 83751 (1984).
12. Castillo, J.L. and Rosner, D.E., "Theory of Surface Deposition from a Unary Dilute Vapor-Containing Stream, Allowing for Condensation Within the Laminar Boundary Layer," Chem. Engrg. Sci. (submitted, 1985).
13. Rosner, D.E., Transport Processes in Chemically Reacting Flow Systems, Butterworths Publishers (to appear, Spring, 1986).
14. Seshadri, K. and Rosner, D.E., "Polarization (Ellipsometric) Measurement of Condensate Deposition and Evaporation Rates and Dew Points in Salt/Ash Containing Combustion Gases," Combustion & Flame (in press, 1985).
15. Garcia-Ybarra, P., Eisner, A.D. and Rosner, D.E., "Thermophoretic Proeprties of Small Nonspherical Particles and Large Nonspherical Molecules," to be presented at the Amer. Assoc. for Aerosol Research Conference, Nov. 18-22, 1985, Albuquerque, NM.

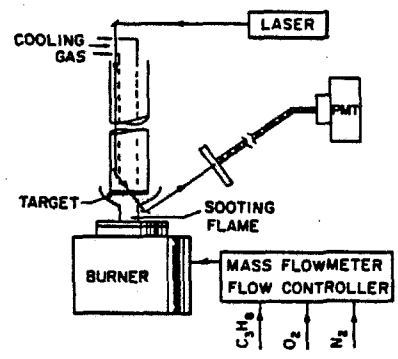

Fig. 1: Laser-light extinction through the surface deposit (LESD) technique (schematic) (5).

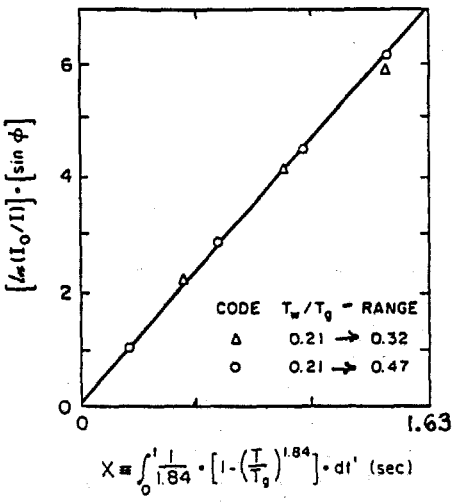

Fig. 2: Straight-line test of thermophoretically dominated soot transport postulate. Ordinate calculated from transmitted laser light intensity measurements (see Fig. 1 and Ref. 5).

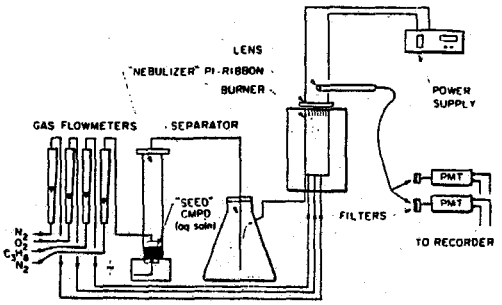

Fig. 4: Experimental arrangement (schematic) for laboratory studies of multicomponent alkali compound deposition rate processes (undersaturated and saturated) using the "flash evaporation technique" (10).

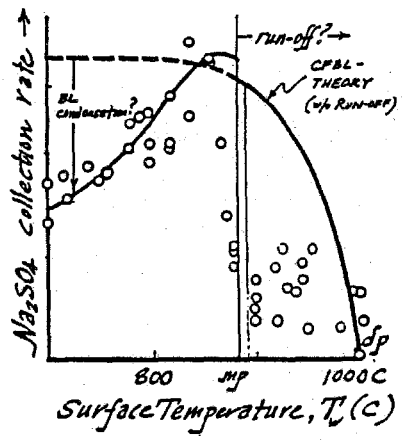

Fig. 5 Comparison of experimental and predicted surface temperature dependence of Na_2SO_4 deposition rate from an undersaturated stream of combustion products; conditions: T_∞ = 1713K, T_{dp} = 1273K, 2 dim (planar) stagnation line (m=1), $\alpha(\equiv \alpha_T D_c/\nu)$ = 0.1 (12).

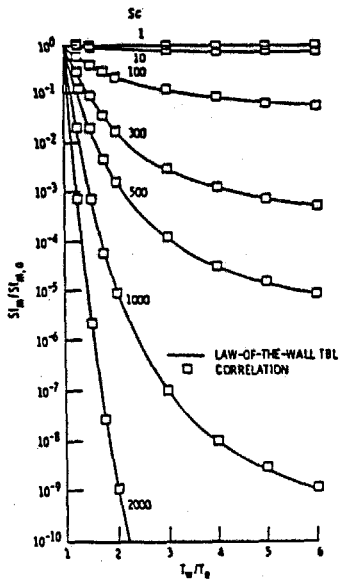

Fig.3 Comparison of correlations and numerical law-of-the-wall turbulent BL calculations for predicting thermophoretic reduction in deposition rate with respect to T_w/T_e and particle size (via Sc): α_TLe = 0.4; Re = 5.8 x 10^5 (8).

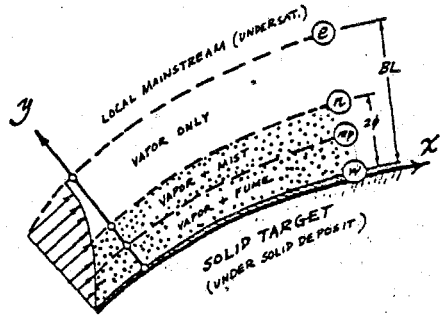

Fig.6 Schematic of structure of laminar boundary layer near deposition surface showing inner zone(s) of two-phase (aerosol condensate) flow; primary condensate deposition mechanism is thermophoresis toward cooled surface (12).

TURBULENCE SCALES AND THEIR EFFECT ON TURBULENT PREMIXED FLAME STRUCTURE

(AFOSR Grant No. 84-0224)

Principal Investigator: D. A. Santavicca

Department of Mechanical Engineering
The Pennsylvania State University
University Park, PA

SUMMARY/OVERVIEW:

Despite the importance of turbulence length scales in the formulation of mathematical models of turbulent premixed combustion, in hypotheses regarding the structure of turbulent premixed flames, in models of turbulent transport coefficients, and in turbulent to laminar flame speed correlations, relatively few length scale measurements have been made in studies of turbulent premixed flames. Experiments are planned which will be conducted in a high pressure, turbulent flow reactor using premixed propane and air. A turbulent flame will be stabilized in a diverging test section where the turbulence intensity, length scale and time scale will be measured using laser Doppler velocimetry and the turbulent flame structure will be measured using 2-D flow visualization. The experiments will address fundamental questions regarding the role of turbulence length scales in turbulent premixed flames including, i) the relationship between turbulence length scales and flame structure, ii) the effect of combustion on turbulence length scales, iii) the relationship between turbulence length and time scales and iv) the effect of density on turbulence scales and flame structure.

TECHNICAL DISCUSSION

The performance, efficiency, and emissions characteristics of gas turbine combustors are controlled by the complex coupling of numerous subprocesses including fuel spray atomization, fuel spray vaporization, turbulent mixing, and turbulent combustion, both premixed and non-premixed. Detailed mathematical models are valuable for understanding the relative importance of these subprocesses and the basic controlling mechanisms. Formulation of such models however requires fundamental understanding of the individual subprocesses. The motivation for the planned research is the need for such fundamental knowledge regarding the interaction of turbulence and combustion in turbulent premixed flames under conditions typical of those found in gas turbine combustors where

high pressures, large turbulence intensities, and both large and small scales of turbulence must be considered.

Models of turbulent premixed combustion are generally based on specific hypotheses regarding the structure of turbulent premixed flames and the relationship of that structure to such parameters as the turbulence Reynolds number, the ratio of the laminar flame thickness to the turbulence length scale and the ratio of the laminar flame speed to the turbulence intensity. These models also include assumptions regarding the effect of combustion on turbulence scales and intensity. In addition, turbulence length scales are used in turbulent transport coefficient models, as well as in turbulent to laminar flame speed correlations. Despite the importance of turbulence length scales in the formulation, validation and use of such models and correlations, there have been very few direct measurements of turbulence length scales made in studies of turbulent premixed flames. The planned research will address fundamental questions regarding the role of turbulence length scales in turbulent premixed flames including, i) the relationship between turbulence length scales and flame structure, ii) the effect of combustion on turbulence length scales, iii) the relationship between turbulence length and time scales, and iv) the effect of density on turbulence scales and flame structure.

A high pressure, turbulent flow reactor will be designed and built to simulate typical pressures, turbulence intensities and turbulence scales found in practical gas turbine combustors. A schematic drawing of the planned high pressure, turbulent flow reactor is shown in Figure 1. An important feature of the flow reactor is that the turbulence is generated upstream of the test section. The turbulence intensity and scales are controlled by the characteristics of the turbulent gas jets of premixed fuel and air that are injected into the plenum upstream of the test section. The test section will be a diverging nozzle in which the flame will be stabilized. The measurements will be made near the certerline outside of the wall boundary layer. Measurements will be made of the turbulence intensity, the turbulence time and length scales and the turbulent flame structure.

The turbulence intensity measurements will be obtained using laser Doppler velocimetry at sufficiently high data rates in order to separate the high and low frequency turbulence components.

The time and length scales of velocity fluctuations will be obtained directly from temporal and spatial correlation measurements, respectively. The two-point velocity measurements from which the spatial correlation will be determined will be made using a recently developed optical fiber detector [1].

The basic idea being to use a very long focal length lens on the probe beams to generate a long, narrow probe volume, e.g., 1 cm long x 300 micron diameter. This elongated probe volume is then imaged onto a slit aperture. On the other side of the slit aperture are the input ends of two optical fibers, one fixed and the other traversable. Therefore scattered light is collected from two distinct volumes within the elongated probe volume and the distance between the two measurement points is adjusted by moving the traversable optical fiber. The output ends of the two optical fibers go to photomultiplier tubes, the outputs of which go to two LDV counter processors. A schematic drawing of the two-point detector is shown in Figure 2. This detector has a spatial resolution of 300 micron and a traversing range of 1 cm.

Two-dimensional flow visualization will be used to make 2-D maps of the gas density within the turbulent flame [2]. The 2-D measurements are single-shot measurements made by focusing the output of a Nd:YAG laser into a planar sheet, e.g., 5 mm wide by 200 micron high, from which light is scattered, by Mie scattering from titanium dioxide particles, and then imaged onto a 2-D matrix camera. The output of the camera is transferred with a high speed A to D to an IBM PC for storage, of what is in effect a "snap-shot" of the 2-D density profile within the flame.

The measurements made in this study will provide valuable information about the relationship between turbulence intensity and scales and turbulent flame structure which will potentially lead to improved phenomenological models of premixed turbulent combustion.

REFERENCES

1. Fraser, R., Pack, C. and Santavicca, D. A., "An LDV System for Turbulence Length Scale Measurements," Experimental Measurements and Techniques in Turbulent Reactive and Non-Reactive Flows, edited by So, Whitelaw and Lapp. The American Society of Mechanical Engineers, AMD-Vol. 66, 1984.

2. zur Loye, A. O., Santavicca, D. A. and Bracco, F. V., "Preliminary Study of Flame Structure in an Engine using 2-D Flow Visualization," to be presented at the International Symposium on Diagnostics and Modelling of Combustion in Reciprocating Engines, Tokyo, Japan, September 1985.

HIGH PRESSURE TURBULENT FLOW REACTOR

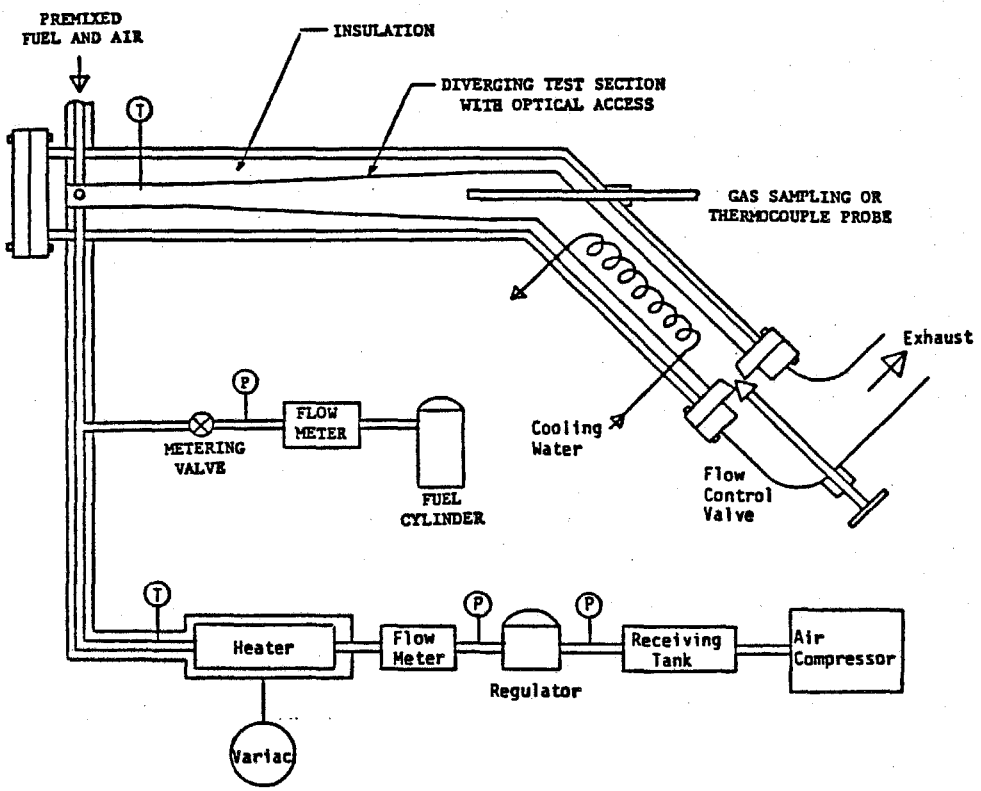

FIGURE 1

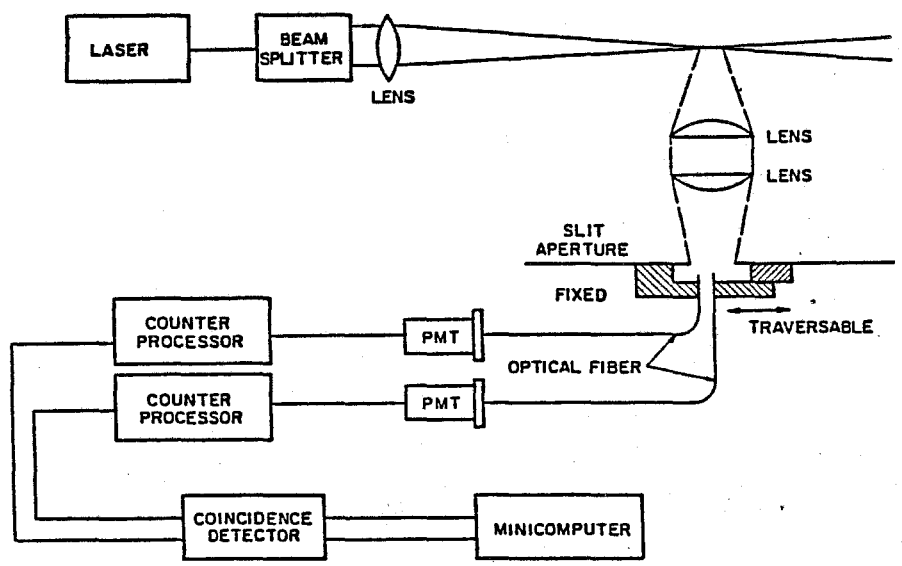

FIGURE 2

LDV SYSTEM FOR TURBULENT LENGTH SCALE MEASUREMENT

SOOT FORMATION IN DIFFUSION FLAMES: EFFECTS OF FUEL STRUCTURE, TEMPERATURE AND PRESSURE

(AFOSR Contract No. AFOSR-ISSA85-0025)

Principal Investigators: R.J. Santoro and H.G. Semerjian

Center for Chemical Engineering
National Bureau of Standards
Gaithersburg, MD 20899

SUMMARY/OVERVIEW:

Soot formation is now well recognized to be a major challenge for the next generation of gas turbine engines which will operate with broader specification fuels at higher operating pressures and under stricter emission standards. However, the present understanding of the fundamental processes leading to soot particle formation, growth and subsequent oxidation is insufficient to allow a reliable evaluation of the impact that soot formation is likely to have on future engine technology. In order to gain a better understanding of these processes, a detailed study of the formation, growth and burnout of soot particles has been initiated. Specific attention is given to the effects of fuel structure, temperature and pressure on the soot formation processes. Detailed measurements of the particle, velocity and temperature fields are used to investigate the dependencies of the underlying processes. These results are expected to provide an understanding of the fundamental processes involved in soot formation under conditions which are characteristic of practical combustion systems.

TECHNICAL DISCUSSION

Recent interest in the formation of soot in combustion processes has been motivated by several related developments. It is now well recognized that future combustion systems will operate with broader specification fuels under conditions of higher operating pressures and stricter emissions standards. Each of these developments require appropriate optimization of combustion processes and system performance capabilities; increased soot formation represents a major challenge in this process. Since soot production has been shown to have strong sensitivity to fuel properties and operating conditions (temperature and pressure) [1, 2], it would be desirable to have an understanding of the fundamental processes governing formation and subsequent oxidation. However, such understanding must also be developed under conditions which can be directly extended to processes occurring in practical combustion systems. The objective of the present effort is to investigate the effects of fuel composition, temperature and pressure on the rates of soot formation, particle growth and burnout in a well characterized flow field. During the first year of this program, emphasis has been given to the study of the effects of fuel flow rate and fuel species on the soot formation process.

The experiments have been conducted using a coannular diffusion flame burner in which gaseous hydrocarbon fuels burning in air are studied. Laser-based

techniques such as laser scattering/extinction for particle measurements and laser velocimetry for flow field characterization have been utilized. Presently, fine wire thermocouple techniques are being used to obtain temperature measurements in these flames. Non-intrusive temperature measurement techniques are presently under development. As these techniques are proven reliable for particle laden environments, they will be applied to these studies.

The effect of fuel structure is being investigated by adding selected fuel constituents to an ethene diffusion flame. To establish a well defined baseline, initial efforts have focussed on detailed characterization of the ethene/air flame. Previous studies have concentrated on the particle field measurements as a function of fuel flow rate [3]. Thus, recent work has emphasized the velocity and temperature measurements [4,5]. Figure 1 shows radial profiles of the axial and radial velocity components as a function of axial position for one of the ethene diffusion flames studied. These measurements can then be used to construct the particle paths (streak lines) which the soot particles follow (see Fig. 2). From such measurements, the time temperature history can also be resolved. A series of measurements to characterize the particle, velocity and temperature fields have been carried out as a function of fuel flow rate. It is well known that, for sufficiently small fuel flow rates, the soot particles formed in the lower part of the diffusion flame are totally oxidized before leaving the flame zone. However, there is a characteristic fuel flow rate for which soot particle emission is observed from the flame tip. In order to understand this process, a series of ethene/air diffusion flames have been studied in which the fuel flow rate has been systematically varied to examine this characteristic transition. The combined particle, velocity and temperature measurements have revealed that the dominant controlling feature in these flames is the residence time available for particle growth. Figure 3 shows the soot volume fraction, particle size and number concentration as a function of time for the three flow rate conditions along a particle path located in the annular region of the flame. This region is identified in Fig. 2 by dashed lines. As the fuel flow rate increases, Fig. 3 indicates that the particle residence time increases, thus allowing a larger amount of particle growth to occur. In addition, by following individual particle paths for the same flow rate condition, comparisons can be made between different regions of the flame. Examination of the annular and center line regions of the flame reveal that processes occurring near the flame reaction zone (but on the fuel rich side) are controlling the transition from nonsooting to soot emitting conditions. From temperature and radiation measurements, it appears that radiative transfer from soot particles plays an important role in controlling the temperature of the oxidation zone, and thus on the transition from nonsooting to sooting flames.

Recent studies have examined the effect of fuel species on the soot formation process [6]. In these studies, a constant amount of carbon is introduced into a well characterized ethene diffusion flame in the form of different fuel species. Detailed measurements of the evolution of the soot particle field are obtained throughout the flame region. Results have been obtained for methane, ethane, ethene, acetylene, propene and butene. Since the flame temperature is affected by the variation of the fuel species, a similar series of experiments have been conducted in which nitrogen dilution of the fuel flow has been used to achieve constant adiabatic flame temperatures. Analysis of these experiments is presently underway. The results to date indicate strong fuel structure effects particularly in the early formation zone of the flame. In addition, the experiments in which the temperature is controlled indicate a significant temperature

sensitivity which must be included if a proper understanding of the fuel structure effect is to be obtained.

Future efforts will include more detailed studies of the effect of fuel structure and temperature. In the more heavily sooting flames, the particle sizes are found to be near the upper limit of the size range where the simple Lorenz-Mie theory is appropriate for interpretation of laser scattering/extinction measurements [7]. Other diagnostic techniques will be investigated, which may be more suitable for the larger particle size range. During the next year, design and assembly of a high pressure flame facility will also be undertaken.

REFERENCES

1. Jackson, T.A., "Fuel Property Effects on Air Force Gas Turbine Engines - Program Genesis", J. Energy, 6, pp. 376-383 (1982).

2. Blazowski, W.S., Sarofim, A.F., and Keck, J.C., "The Interrelation Between Soot and Fuel NO_x Control in Gas Turbines Combustors", J. of Eng. Power, 103, p. 43 (1981).

3. Santoro, R.J., Semerjian, H.G., and Dobbins, R.A., "Soot Particle Measurements in Diffusion Flames", Combustion and Flame, 51, pp. 208-218 (1983).

4. Santoro, R.J. and Semerjian, H.G., "Soot Formation in Diffusion Flames: Flow Rate, Fuel Species and Temperature Effects", 20th Symposium (International) on Combustion (in press).

5. Santoro, R.J., Yeh, T.T., and Semerjian, H.G., "The Transport and Growth of Soot Particles in Laminar Diffusion Flames", accepted for presentation at the 23rd ASME/AIChE National Heat Transfer Conference, August 4-7, 1985, Denver, Co.

6. Santoro, R.J. and Semerjian, H.G., "Laser Light Scattering Measurements of Soot Particles in Flames", 16th Annual Meeting of the Fine Particle Society, April 25, 1985, Miami, Fl.

7. Dobbins, R.A., Santoro, R.J., and Semerjian, H.G., "Interpretation of Optical Measurements of Soot in Flames", Advancements in Non-Intrusive Diagnostics for Combustion Research, Ed. T.D. McCay and J.A. Roux, Progress in Astronautics and Aeronautics, Vol. 92, p. 208 (1984).

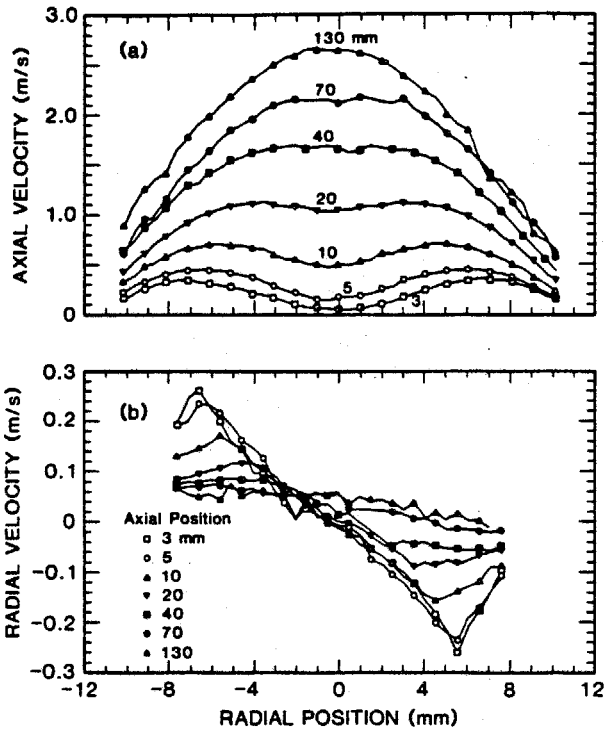

Fig. 1 Radial velocity profiles in an ethene/air diffusion flame; a) axial velocity component, b) radial velocity component.

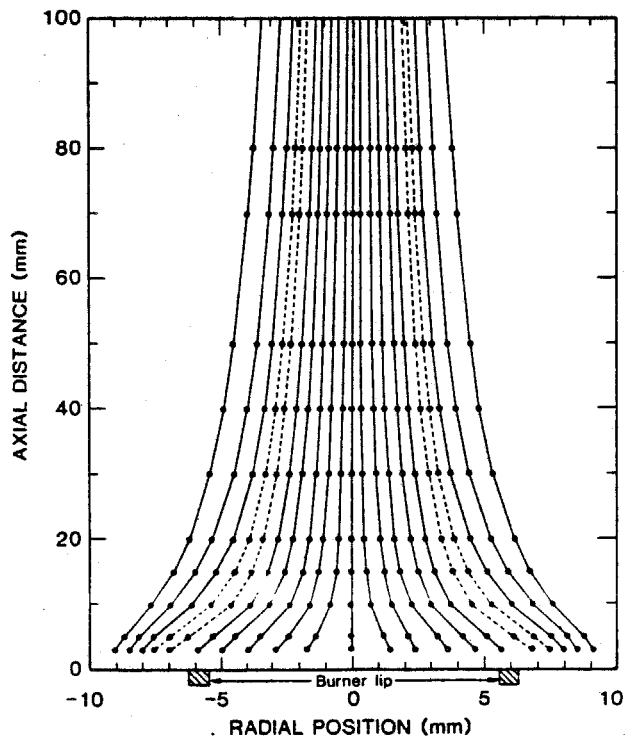

Fig. 2 Particle paths (streak lines) calculated from the velocity measurements for an ethene/air diffusion flame. Every third streak line is shown and the dotted lines indicate the region enclosing the streak line exhibiting the maximum f_v value for this flame.

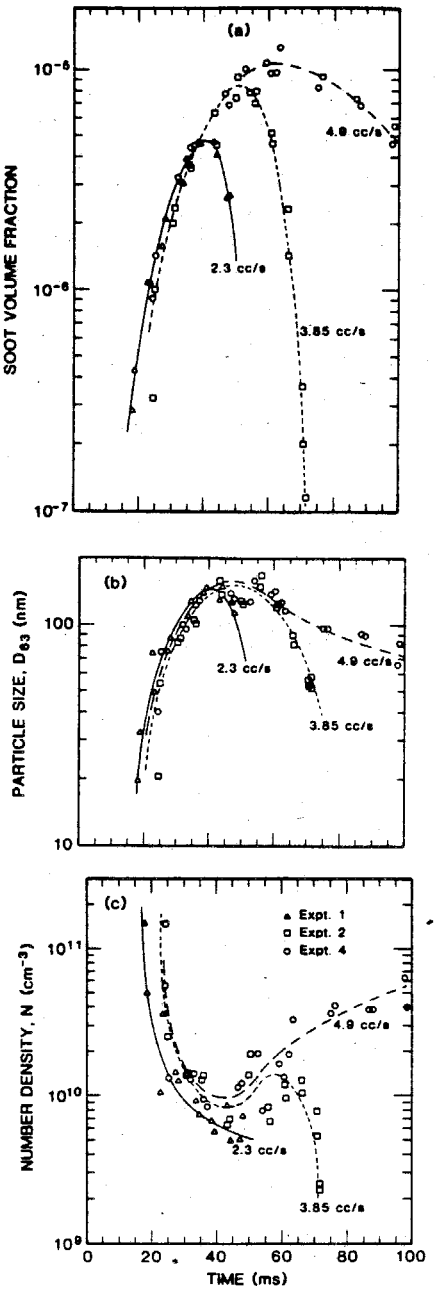

Fig. 3 Comparison of soot volume fraction, f_v, particle size, D_{63}, and number density, N, along streak lines exhibiting the maximum f_v value.

LASER TOMOGRAPHY FOR INVESTIGATION OF TURBULENT FLAMES

(AFOSR Contract No. AFOSR-ISSA84-00061)

Principal Investigators: H.G. Semerjian and S.R. Ray

Center for Chemical Engineering
National Bureau of Standards
Gaithersburg, MD 20899

SUMMARY/OVERVIEW:

Laser tomography, an optical diagnostic technique based upon multiangular absorption spectroscopy, is being developed for investigation of turbulent flames. This technique allows the rapid measurement of both species concentration and temperature throughout a two- or three-dimensional non-uniform flow field. Measurements of OH concentration and temperature have been made in an axisymmetric premixed methane flame. The technique is currently being extended to non-uniform fields; extinction measurements have been carried out in a sooting diffusion flame, using a six-angle optical system. The maximum repetition rate that can be achieved with the present system is 10 KHz.

TECHNICAL DISCUSSION

New requirements to improve the efficiency and performance of combustion systems, to reduce pollutant emissions and to enable utilization of fuels with broad specifications, have necessitated the development of a number of sophisticated optical diagnostic techniques, which can provide measurements with high spatial and temporal resolution. However, in general, these techniques provide single point measurements with low repetition rates. In addition, they require statistical methods to interpret data obtained in fluctuating fields, and are difficult to directly relate to the observed physical phenomena.

This work involves the development and application of laser tomography to non-uniform, fluctuating combustion fields to provide simultaneous measurements of temperature and concentration throughout a two-dimensional "slice" of a flame zone. This is accomplished by measuring absorption along M equally spaced parallel beams and N equally spaced angles, forming an MxN data set from which the property field (temperature and/or concentration) is retrieved or "reconstructed". Early work in this laboratory included feasibility studies measuring the absorption field of a non-reacting turbulent jet of methane [1,2], the measurement of the methane concentration in an axisymmetric diffusion flame [3], and the rapid measurement of sodium distribution in a seeded flame using an array detector [4]. More recently, the OH concentration and translational temperature was measured in an axisymmetric premixed methane flame, using a single measurement angle [5]. The method was then extended to a six angle system which was used to measure non-symmetric extinction fields at repetition rates up to 10 KHz. As a parallel effort, alternatives to the widely used convolution reconstruction technique are being investigated, which show promise of yielding superior reconstructions in situations where only a few measurement angles are possible.

Brief summaries of the activities in each of these three areas are given below:

a) Measurement of OH Concentration and Temperature in a Flame: The goal of this experiment was to investigate the performance of high speed simultaneous measurements of both temperature and OH concentration distribution throughout an axisymmetric premixed methane/oxygen/diluent flame. An ultraviolet laser beam was generated by frequency-doubling the output of a dye laser at 612 nm. This beam was spatially scanned through the flame while the frequency of the laser was simultaneously modulated across the $R_1(5)$ line of the (0,0) $A^2\Sigma$-$X^2\Pi$ transition of the OH molecule. In this way, a series of projections was generated at different wavelengths across the absorption line (see Figure 1). By taking advantage of the axisymmetry, each projection could be used to reconstruct the local values of absorption coefficient throughout the plane of measurement, at a particular wavelength. In this manner, the local absorption coefficient was measured at several wavelengths. These values were fitted to a theoretical Voigt profile which is uniquely related to temperature, assuming the pressure is known. Once the temperature distribution is known, the OH concentration can be readily calculated from the measured absorption coefficient field. Results using this approach are shown in Figure 2. Although the OH concentration was not independently verified, the temperature field was consistent with corrected thermocouple scans.

b) Measurement of Non-Symmetric Extinction Fields: To extend the technique to high speed measurements in non-uniform flowfields, a tomography system providing measurements at six equally spaced angles has been designed and assembled (Figure 3). For the sake of simplicity at this stage, a fixed frequency (argon ion) laser system was used, and the more straightforward phenomenon of extinction was measured, rather than spectral absorption by a molecular species. A sooting butene diffusion flame was used as the measurement field. Several designs of burners were used to generate flames in a variety of shapes. A reconstructed extinction field using a circular burner is shown in Figure 4. Note that while the flame is circular, it is not located in the center of the field; no symmetry properties were assumed in performing the reconstruction. Preliminary experiments were also performed with a burner which was physically oscillated from side to side to generate a fluctuating extinction field.

c) Investigation into Reconstruction Methods: As a parallel effort to the experimental program, a computer based study is continuing to identify the reconstruction approach best suited to the particular experimental configurations in use. It is common practice to use the convolution reconstruction method in situations where many measurement angles are provided. This was the approach used in the axisymmetric flows, where a single projection can be duplicated to mimic as many measurement angles as desired. However, when only six projections are provided, the convolution method exhibits severe effects of aliasing due to undersampling, which is manifested by large amplitude oscillations emanating from regions of strong signal. In the search for viable alternative reconstruction methods, it has been found that a technique based on the maximum entropy method shows great promise in the undersampled case. Using this technique, aliasing ripples are completely eliminated, as can be seen in Figure 5. It appears that the method is not as precise in estimating the magnitude of the reconstructed field, but this should improve with the addition of appropriate constraints in the algorithm. This is currently under investigation.

In summary, experimental tomography systems have been designed and built to address a systematic progression of technical challenges. High speed systems have been demonstrated in both axisymmetric (single angle) and non-symmetric (six angle) versions, capable of repetition rates up to 10 KHz. Future plans include upgrading the six angle system to a full frequency scanning capability to allow the rapid imaging of species concentration and temperature in non-uniform flows. Emphasis will be placed on maximizing the temporal resolution of the system to allow the study of rapidly fluctuating, turbulent flows.

References

1. Emmerman, P.J., Goulard, R., Santoro, R.J. and Semerjian, H.G.; "Multiangular Absorption Diagnostics of a Turbulent Argon-Methane Jet", Journal of Energy, 4, 70 (1980).

2. Santoro, R.J., Semerjian, H.G., Emmerman, P.J. and Goulard, R.; "Optical Tomography for Flow Field Diagnostics", Int. J. Heat Mass Transfer, 24, 1139 (1981).

3. Semerjian, H.G., Santoro, R.J., Goulard, R. and Emmerman, P.J.; "Optical Tomography for Diagnostics in Combusting Flows", p. 119 in "Fluid Mechanics of Combustion Systems", Eds. Morel, T., Lohman, R.P. and Rackley, J.M.; ASME, New York (1981).

4. Ray, S.R. and Semerjian, H.G.; "Laser Tomography for Simultaneous Concentration and Temperature Measurement in Reacting Flows", p. 300 in "Combustion Diagnostics by Nonintrusive Methods", Eds. McCay, T.D. and Roux, J.A.; AIAA, New York (1984).

5. Goulard, R. and Ray, S.R., "Optical Tomography in Combustion", Proceedings of the Interactive Workshop on Advances in Remote Sensing Retrieval Methods, Williamsburg, VA (1984); in press.

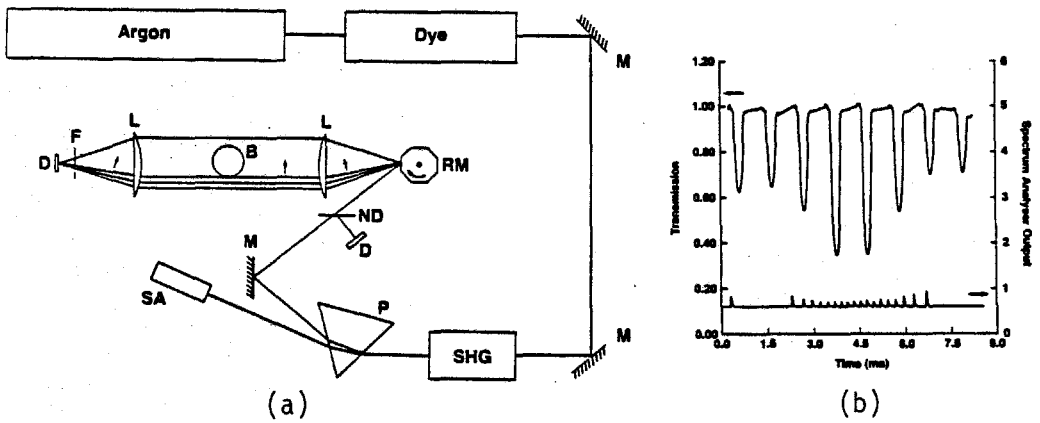

Figure 1. a) Schematic diagram of the axisymmetric scanning beam tomography experiment; b) Transmission data through a premixed methane flame.

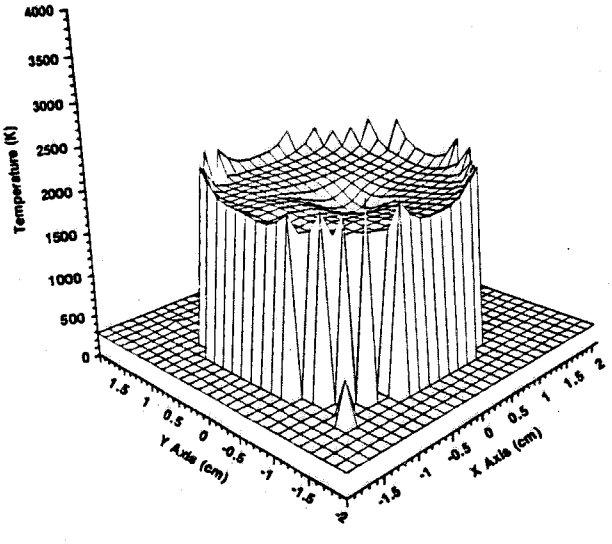

(a)

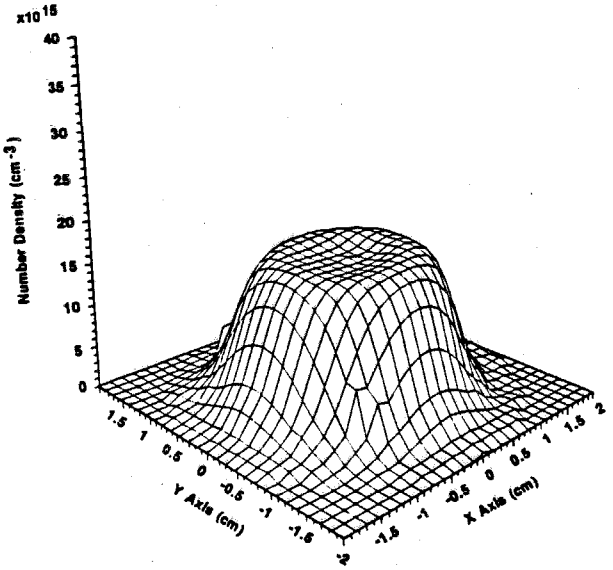

(b)

Figure 2. a) Reconstructed temperature field from the data of Figure 1b; b) Reconstructed OH concentration field.

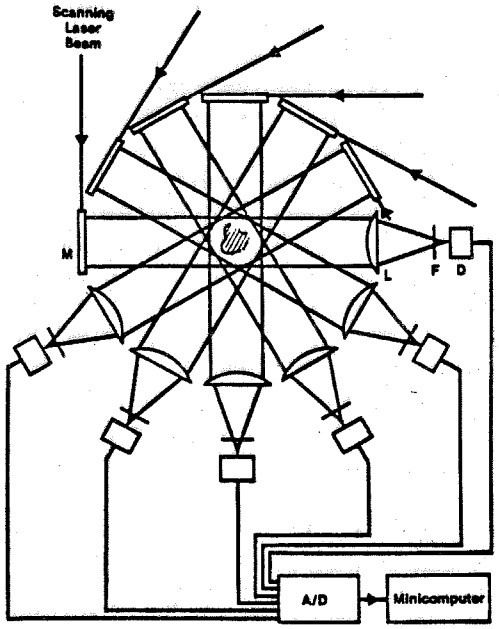

Figure 3. Schematic of the six angle tomography system.

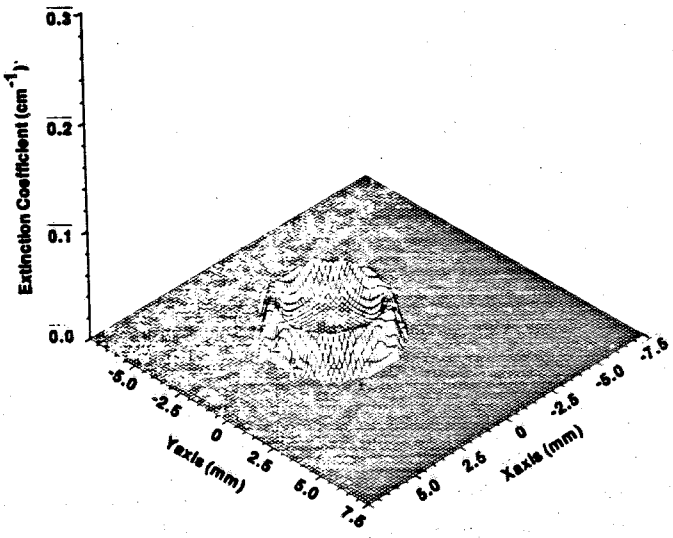

Figure 4. Reconstructed extinction field for a butene diffusion flame, using the six angle tomography system.

Ignition of Fuel Sprays

W.A. Sirignano, Univ. of California, Irvine, S.K. Aggarwal, Univ. of Illinois, Chicago, and H.T. Sommer, Carnegie-Mellon Univ., Pittsburgh.

A theoretical-experimental program has been initiated at Carnegie-Mellon University with emphasis on the ignition of combustible sprays. Although the principal investigator and an associate investigator have relocated recently, the program has continued as a cooperative effort. This program has involved the examination of a broad range of phenomena but this abstract will discuss primarily the recent progress on the study of a stream of droplets moving past a heated flat plate. The purpose of the program is to understand the mechanisms that are dominant, in various portions of the parameter range, in the ignition of hydrocarbon fuel sprays. The phenomenon is studied on the fine scale (smaller than the average spacing between droplets) and the random variation of some key parameters will be taken into account.

The starting point for the theoretical study is the set of equations for a chemically reacting flow in unsteady compressible boundary layer. The source terms are due to the chemical reaction and due to the vaporization of droplets. Self similar solutions of the steady-state form of these equations are used as the initial conditions for calculating the vaporization and trajectories of droplets. A Howarth transformation is employed to reduce the steady-state compressible b.l. equations to the incompressible form. The result is the Blasius equation and the corresponding energy equation. The solution of the energy equation is easily found for unity Prandtl number as a function of the solution of the Blasius equation.

The Blasius equation is solved by a fourth order Runge-Kutta scheme in conjunction with a shooting method. This yields U, Θ and ρ (as given by)

$$U = U_o f'$$

$$Q = 1 - f' = \frac{T - T_o}{T_p - T_o}$$

$$\rho = S_o T_o / T$$

T_o = Free stream temperature

T_p = Hot plate temperature.

Hyperbolic liquid-phase equations for a droplet (or a group of droplets) can be solved. Initial values are specified. The value of the Blasius coordinate is obtained giving droplet location. The gas-phase properties are then calculated at this location by an interpolation method. The droplet equations are solved by a second-order Runge-Kutta method. The droplet surface temperature is obtained by using a conduction-limit transient heating model. This yields new values of the droplet properties. At the new location, the gas-phase properties are calculated, which are then employed to advance the droplet properties. This procedure is repeated for a specified time period.

For the purpose of debugging the numerical code, the problem of droplet ignition in the thermal boundary of a hot plate has been solved. The ignition criterion is based on the critical Damkohler number. The ignition length (the axial length traversed by the droplet) is calculated as a function of plate temperature and the initial droplet location with respect to the plate. A few representative results are shown below:

Dynamics, vaporization and ignition of a single droplet in a b.l.

Effect of Y_{IN} (distance of droplet from plate) - $T_p = 1500^o$ K

Y_{IN}	X_{ig} (length to ignite)
.03 cm	.346 cm
.05	.381
.08	.489
.01	.618
.115	.793
.12	does not ignite

Effect of Tp (plate temperature) - Y_{IN} = .05 cm

T_p	X_{ig}
1200° K	Fails to ignite
1300	.53 cm
1400	.437
1500	.381
1700	.319

These results are preliminary and do not show that a minimum occurs in ignition delay as distance from the ignition source varies. In non-flowing spray calculations already published in the Proceedings of the Twentieth Symposium (International) on Combustion, it has been shown that in a certain parameter range, a minimum occurs in ignition delay as distance from the ignition source varies. Also, a minimum can be found as initial size varies. Since the basic physics of the flowing and non-flowing systems are identical, we expect to find a minimum can occur in the flowing system as we extend the parameter survey.

Based on the theoretical considerations an experiment was designed to determine the dependency of fuel droplet ignition on each major system variable enhancing or reducing a particular physical effect. The droplet size was identified as one of the important variables of the process. The following experiments have been conducted to identify the influence of the above quantities on fuel ignition experiment. An electrically heated flat plate was positioned in front of a single droplet stream of Toluene generated by a TDI model 3450 vibrating orifice aerosol generator. The distance between the hot plate and the droplet stream was measured through a microscope. The droplet generator produces a single stream of droplets of uniform size when tuned appropriately. Droplet velocity and spacing of droplets were determined through double-flash photography. The following quantitative results were observed: the event of ignition is strongly affected by the temperature of the hot surface, the distance of the droplet to the wall, and the residence time of the droplet in front of the hot surface.

It was observed that with increasing wall temperature the ignition delay time (residence time in front of hot surface) reduced. Due to enhanced radiative and conductive heat transfer evaporation of the fuel is stimulated and a vapor-air mixture of optimum ignition condition was reached earlier For constant wall temperature, a minimal ignition time delay was observed for a specific distance from the hot surface. During this experiment the wall

temperature was kept constant the stream of 110 μm diameter droplets was brought closer to the surface and the location of ignition relative to the leading edge of the hot surface was measured. It was observed that once a flame had developed after ignition of the first droplet, the point of ignition moved further down the droplet stream indicating that radiative and conductive heat transfer from the flame enhanced the ignition of approaching droplets. For very small droplets (below 30 μm diameter) a stable flame remained even after the hot surface was removed.

Currently, we only can compare the experimental and theoretical results on a qualitative basis. It is observed in experiments that ignition occurs earlier than the model predicts. The reason for this may be that the radiation heat transfer is not included in the model. A comparison of predicted Decane ignition delay times and Toluene delay times calculated from experimental data indicates a qualitative agreement considering the difference in material properties.

SINGLE PARTICLE SIZING BY MEASUREMENT OF BROWNIAN MOTION

(AFOSR Contract No. F49620-83-C-0154)

Principal Investigators: Alan C. Stanton and Wai K. Cheng*

Aerodyne Research, Inc.
45 Manning Road
Billerica, Massachusetts 01821

*Department of Mechanical Engineering
Massachusetts Institute of Technology
Cambridge, Massachusetts 02139

SUMMARY

Few nonintrusive techniques are available for particle measurements in the submicron size range (< 0.1 μm diameter), yet measurement of these particles is basic to an understanding of important processes in combustion, such as soot formation and oxidation. The objective of the present research is the development and application of a technique for measurement of individual submicron particles in a gas stream. The approach is to measure the inertial relaxation time of individual particles in Brownian motion, by statistical analysis of the time-resolved (100 MHz) heterodyne signal obtained in an interferometer system resembling a more conventional laser Doppler velocimeter. Progress to date has included the development of an optical system and fast data acquisition for conducting the experimental studies as well as the preliminary measurement of time-resolved interferometer signals from particles suspended in water. A detailed Monte Carlo numerical simulation of the Brownian motion of isolated particles has been developed and applied to the calculation of the time dependent signals. These simulated signals have been analyzed for correlations between the particle size and statistical properties of the signal. The mean time between signal extrema has been found to be proportional to the square root of the product of the particle relaxation time, a quantity which is proportional to the particle diameter, and the data sampling interval.

TECHNICAL DISCUSSION

Existing optical techniques for measurement of submicron particles do not yield direct information on the particle size distribution. Our studies are aimed at development of a technique for measurement of individual submicron particles, based on the statistics of Brownian motion of the particles. Progress on the program to date has included the preliminary demonstration of an experimental system implementing this approach, combined with detailed numerical simulations of the time-dependent experimental signals. The simulations have been used to devise an approach for signal analysis.

The optical and data acquisition instrumentation developed for this study are shown in Figure 1. The output from a 2-watt argon ion laser is expanded and split into two collimated beams, which are focused to a spot size (beam waist) of approximately 30 μm. Light scattered from the two beams by a (single) particle in the probe volume is collected and mixed at a photomultiplier, as in the usual fringe-Doppler laser velocimeter. In order to resolve statistical behavior arising from Brownian motion, fast (10 ns) time resolution of the signal is required. A transient digitizer is used to record the data, which are transferred to a

microcomputer. In preliminary measurements, the time-resolved interference signals from single particles of known size suspended in water have been recorded, and statistical analyses are continuing with the aid of our numerical simulations.

In considering the technical approach, it is important to realize that the mean particle excursion due to Brownian motion is much smaller than the wavelength of visible light and is therefore smaller than the LDV fringe spacing for the system shown in Figure 1. The Brownian modulation amplitude of the signal is thus dependent on the spatial location of the particle within the probe volume, and only time (not Brownian velocity) information may be derived from analysis of signal fluctuations. It is also important to realize that signal fluctuations, which are resolved in 10-ns time increments, represent the statistics of Brownian motion (the superposition of many random velocity changes), but do not represent individual collision events between the particle and fluid molecules. These observations suggest a strategy in which the time-statistics of the "velocimeter" signal are analyzed to determine a characteristic time for the Brownian motion. This characteristic time is the relaxation time, or the time scale for the particle velocity distribution to approach a Maxwellian distribution at the temperature of the surrounding fluid.

Based on Monte Carlo numerical simulations of the experimental signals, we have developed an approach for statistical analysis of the signal time histories. The signals are analyzed to obtain the mean time between local extrema (derivative zero crossings). This statistical parameter may be thought of as a measure of the inertia of the particle and is longer for more massive particles. A correlation between this parameter and the particle relaxation time is therefore anticipated. Such a correlation is evident in Figure 2, where this statistical mean time is plotted versus $(\Delta t/\beta)^{1/2}$, where Δt is the sampling interval and $1/\beta$ is the relaxation time. In the free flow limit, the relaxation time is proportional to particle diameter. Thus, the size of individual submicron particles may be determined from such statistical analyses. Our present efforts are directed at confirmation of the correlation represented by Figure 2.

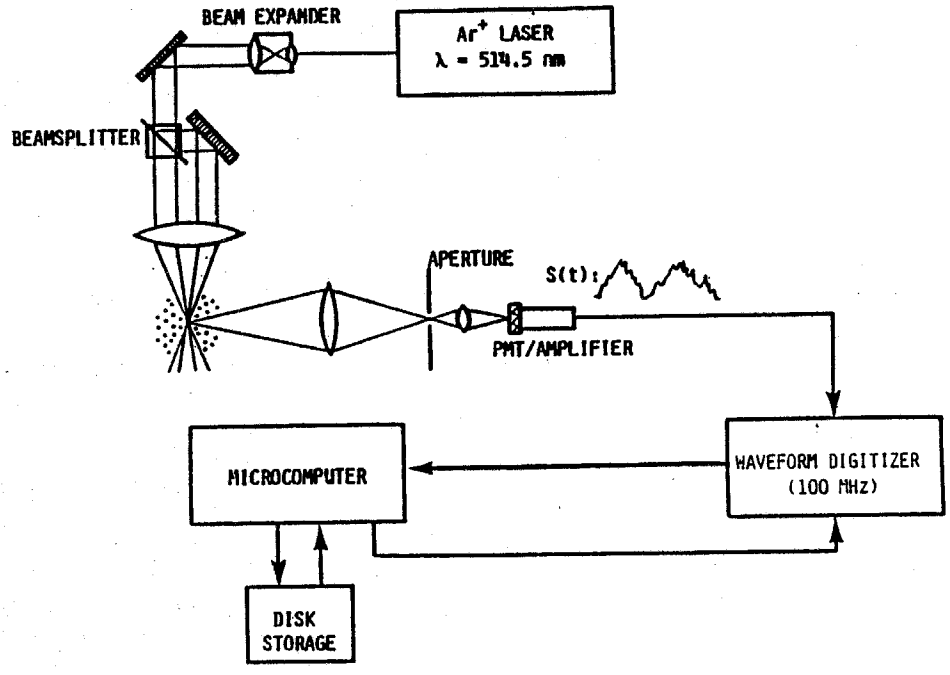

Figure 1. Schematic of Experimental Optical System for the Study of Brownian Motion Measurement Techniques.

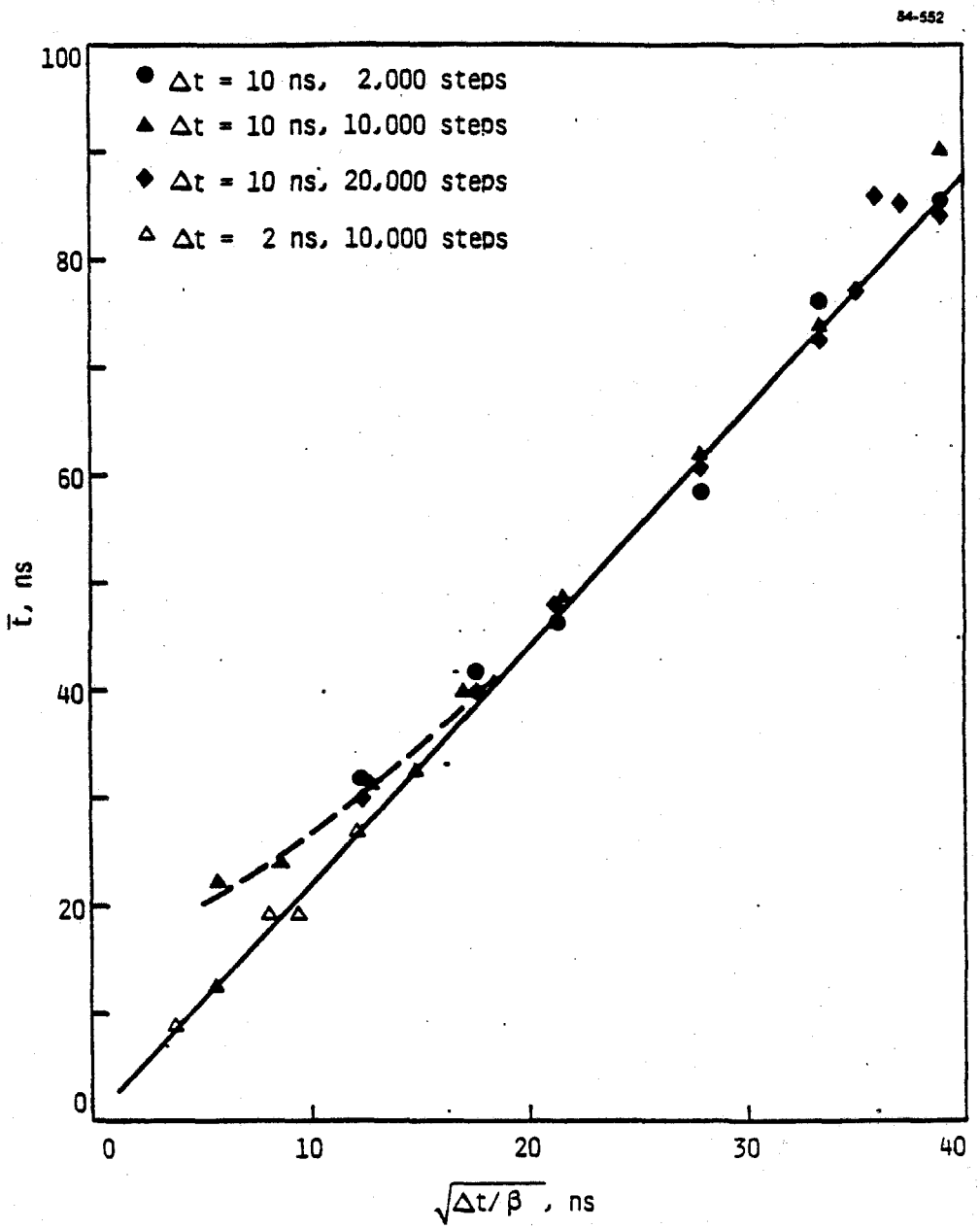

Figure 2. Correlation Between the Mean Time Between Signal Extrema and the Particle Relaxation Time, β^{-1}.

EVALUATION OF EXPERIMENTAL DATA FOR VALIDATION OF NUMERICAL PREDICTIONS FOR TURBULENT COMBUSTION

AFOSR Grant No. 83-0356

Principal Investigator: Warren C. Strahle

School of Aerospace Engineering
Georgia Institute of Technology
Atlanta, GA 30332

SUMMARY/OVERVIEW

By committee, the available data bases in turbulent reacting flows that could be treated analytically by a parabolic method have been reviewed. The original objection was to catalogue the "best" data bases for a test of computational methods. For several reasons the output will be a document containing data bases, but no computational test is recommended at this time.

TECHNICAL DISCUSSION:

Over the period July 1983 to the present an effort has been ongoing, and is currently being concluded, to analyse existing data bases in turbulent reacting flows. An Organization Committee was formed to plan and execute this effort. At a meeting in Reno, Nevada in January, 1984 it was decided that only flows which could be treated analytically by parabolic methods would be considered. At the meeting data base analysers were assigned and the flows categorized. The categories and personnel follow:

Variable density nonreacting flows	Sheridan C. Johnston Frederick C. Gouldin
Fast reaction non-premixed flows	Gerard M. Faeth G. S. Samuelson
Slow reaction non-premixed flows	Wolfgang Kollman Michael C. Drake
Premixed flows	Paul A. Libby James H. Whitelaw

Other members of the Organization Committee are Spyridon G. Lekoudis, Edward J. Mularz and Warren C. Strahle (Chairman). The dominant charge to the analyzers was to determine and catalogue those data bases which were suitable for computational test in a manner similar to the Stanford conference for turbulent boundary layers in 1968.

Two meetings followed. One was held in August, 1984 in Ann Arbor and a last one in Atlanta in December, 1984. For several reasons which will be outlined at this meeting, it was decided to not have a computational test effort. However, the "best" data bases are being compiled and a document will be made available to the community containing recommended data bases.

COMBUSTION RESEARCH USING LASER SHEET LIGHTING

AFOSR SUMMER FACULTY RESEARCH PROGRAM AT APL

R. S. TANKIN: NORTHWESTERN UNIVERSITY

H. H. CHIU AND S. A. LOTTES: UNIVERSITY OF CHICAGO

W. M. ROQUEMORE: AERO PROPULSION LABORATORY

SUMMARY/OVERVIEW:

The objective of this research is to demonstrate the flow visualization capabilities of a new laser sheet lighting technique for studying reacting flows without and with heat release. The fuel, which is seeded with titanium tetrachloride vapor, is ejected from a jet located in the center of a vertically mounted bluff body (see Fig.1). The $TiCl_4$ in the dry fuel reacts spontaneously and nearly isothermally with the water in the annulus air to form titanium dioxide particles. In combusting flows, soot and TiO_2 are used as scattering media. High speed movies and visual observations of vertically and horizontally located sheets of laser light (via Mie scattering) clearly demonstrate the effects of unmixedness and how vortex shedding can occur in cold flows and not in combusting flows because of a decrease in local Reynolds number due to an increase in kinematic viscosity.

TECHNICAL DISCUSSION

Visualizating the product of a chemical reaction using Mie scattering and laser sheet lighting has proven to be very valuable techniques for studying a bluff-body combustor.[1] In contrast to seeding the upstream flow with particles for visualization, sheet-lighting the product of a fast chemical reaction provides a view of where molecule to molecule mixing is occurring and how the product and air species are transported. The $TiCl_4$ water vapor reaction proved to be an excellent choice for this type of study.

Visual observations of the sheet-lit reacting cold flow field in the near-wake of the bluff body tend to provide a time averaged view. In general, one observes a large recirculation zone which is bound to the bluff body and is driven by the annular jet. The central jet flow extends into the center of the recirculation zone. A second recirculation zone, which is driven by the central jet as it entraines fluid, appears narrow and is stretched along the stem of the central jet. In an attempt to

characterize the visually observed flow fields, the three flow conditions shown in Fig. 2 were identified. The first condition is characterized by the domination of the annular jet. The second is where neither jet dominates and the third is where the central jet dominates. This description is consistent with that obtained by studying a large, confined centerbody combustor at APL.[2]

The laser sheet lighting technique provides an amazingly detailed visualization of the dynamic processes occurring in the flow field. By chopping the laser beam at different frequencies, vortices of different length scale and frequency can be observed visually. High speed movies also provide an excellent view of the vortex dynamics associated with the mixing process. Studies of such movies shows that the cold flow fields are not axisymmetric and steady, but rather, highly three-dimensional and unsteady in terms of the dynamic evolution of large scale vortices shed from the bluff body. The shed vortices have a toroidal shape (as determined by horizontal sheet lighting) and appear to provide a primary mechanism of mass exchange between the recirculation zone, annular jet and the downstream region. Some of the vortices are captured in the photographs in Fig. 3.

In combusting flows, a strong laminarization effect due to heat release with consequent increase in kinematic viscosity was observed. This effect appears to prevent vortex shedding from the bluff body for the flow rates studied (cold flow inlet Reynolds numbers based on bluff body diameter up to 10,000). The first photograph in Fig. 4 shows a laminar flame stablized on the face. The second photograph shows a laser sheet-lit view of the same flame taken with an optical filter to eliminate light from sources other than the laser. The Mie scattering from the soot and TiO_2 particles clearly shows the laminar structure of the flame. The dark region on the right hand side between the central jet and the vortex shows an air entrainment path that extends deep into the recirculation zone without being mixed (unmixedness). The third photograph shows the non-combusting flow with propane and $TiCl_4$ in the central jet and the same inlet conditions as the combusting case. In contrast to the exothermic flow, the cold reacting flow is in a transition state with active vortex shedding from the bluff body. Comparison of the cold flow structure with that of the hot flow confirms that the latter flow is strongly affected by combustion laminarization due to the large increase in kinematic viscosity at high temperatures (approximately a factor of 8).

The success of this sheet-lighting visualization technique combined with high speed photography opens up a wide range of possibilities for future studies. A few of these possibilities include: the study of effect of blockage ratio on combustor operating modes and flow field dynamics, the study of ducted versus unducted flows, and a study correlating the

visualization of vortex dynamics recorded in high speed movies with the results of simultaneous measurements made with advanced diagnostic techniques. The prospects of acoustically driving the flow and using a sheet-lit laser strobe for conditional sampling seems another attractive possibility as well as a means of studying instabilities in cold and combusting flows.

REFERENCES

Roquemore, W. M., et al., "The Role of Vortex Shedding in a Bluff-Body Combustor," Presented at The Winter Annual Meeting of the ASME, Dec. 1984.

Roquemore, W. M., et al., "Utilization of Laser Diagnostics to Evaluate Combustion Models," AGARD No. 353, 19, 1151 (1983).

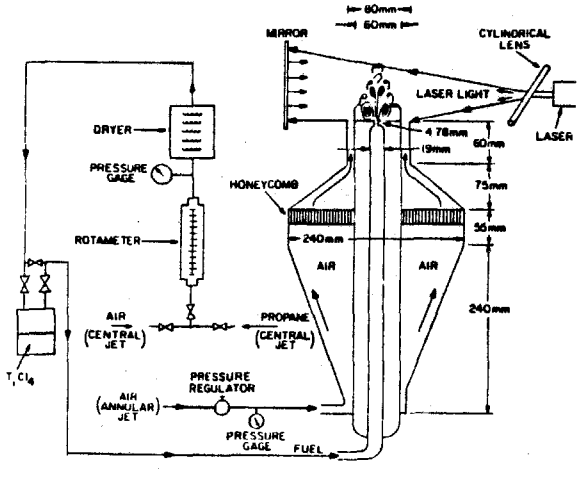

Figure 1. Illustration of experimental set-up.

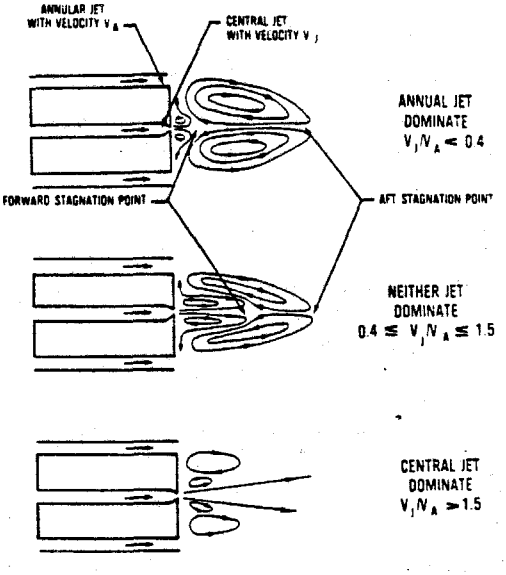

Figure 2. Illustration of the time-averaged flow fields.

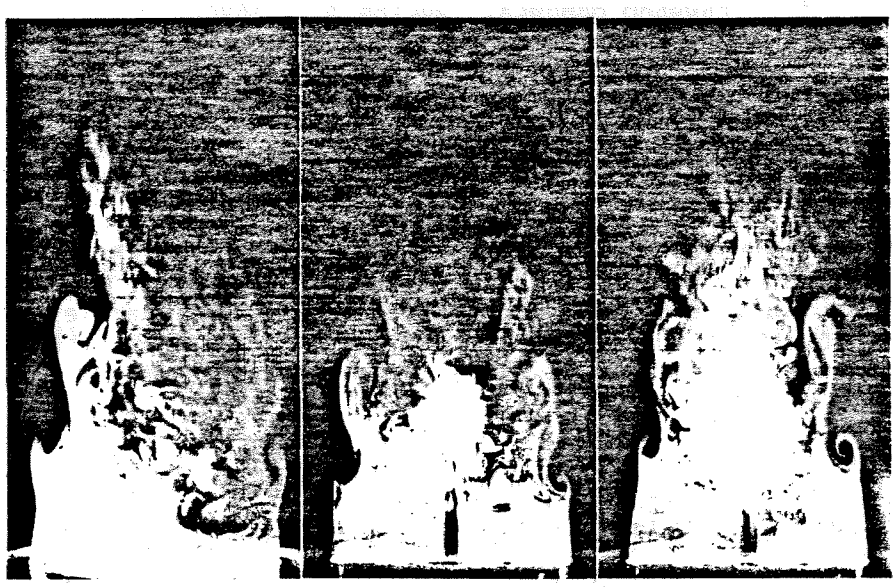

Figure 3. Photographs for a fixed annulus velocity of 4 m/s and central jet ($TiCl_4$ vapor and dry air) velocities of: 1, 3, and 6 m/s from left to right.

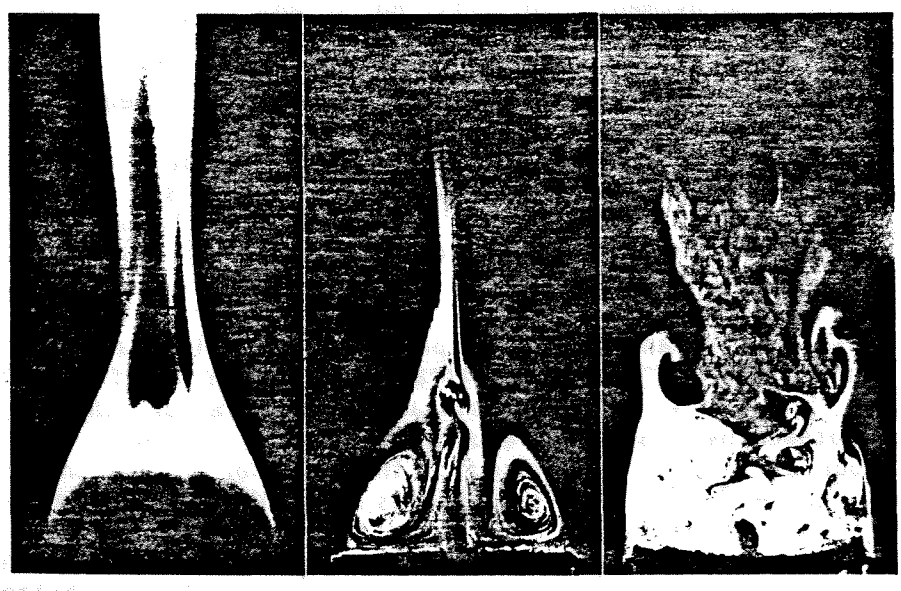

Figure 4. Photographs for an annulus velocity of 2 m/s and a central jet (C_3H_8 +$TiCl_4$) velocity of 0.5 m/s. Left to right: flame, sheet-lit flame with blocking filter and sheet-lit non-combusting flow.

AFOSR SPONSORED RESEARCH IN AIRBREATHING COMBUSTION

PROGRAM MANAGER: JULIAN M TISHKOFF

AFOSR/NA
BOLLING AFB, DC 20332-6448

SUMMARY/OVERVIEW: The Air Force Office of Scientific Research (AFOSR) program in airbreathing combustion is currently focused on seven areas of study: turbulent mixing, turbulent combustion, soot, sprays and slurries, combustion instability, combustion enhancement and supersonic combustion. An assessment of major research needs in each of these areas and new interests in combustion chemistry is presented.

TECHNICAL DISCUSSION

AFOSR is the single manager for Air Force fundamental research, including programs based on external proposals and in-house work at Air Force Laboratories. Airbreathing combustion is assigned to the AFOSR Directorate of Aerospace Sciences along with programs in rocket propulsion, diagnostics in reacting flow, fluid and solid mechanics, and civil engineering.

Current interests of the AFOSR airbreathing combustion program are given in the SUMMARY section above. Many achievements can be cited for these interests, yet imposing fundamental research challenges remain. The objective of the program is publications in the refereed scientific literature describing significant new understanding of multiphase turbulent reacting flow. Incremental improvements to existing scientific approaches, hardware development and computer codes are not considered to be valid research goals.

Decisions on support for research proposals are based on scientific opportunities and technology needs. Current AFOSR perceptions of scientific opportunities appear in Figure 1. Large uncertainties exist about the availability of financial support for the next two years. However, current projections indicate only modest growth for airbreathing combustion research. Research relevant to supersonic combustion and boron fuel utilization will be emphasized.

In FY85 a $1.2 M enhancement was provided for airbreathing combustion through the Gas Turbine Hot Section Initiative. Figure 1 reflects both AFOSR and Air Force laboratory programs as a consequence of this initiative. Particularly noteworthy is the addition of six efforts in numerical simulation. Four of these efforts predict the behavior of gas-phase turbulent reacting flow, while the other two efforts describe primary and secondary liquid atomization behavior. Other initiative growth areas include experimental studies of turbulent combustion and soot formation. The level of support for each of the aforementioned areas of research is substantial, and new research efforts will be added through program turnover.

In FY86 a new laboratory task will be formally included with combustion activities - Laser Fluid Mechanics conducted by personnel at the Air Force Weapons Laboratory (AFWL). Dr Leroy Wilson is the task manager. The role of fluid transport processes delimiting the rate of energy release through mixing and chemical reaction within chemical lasers is generically similar to the physico-chemical behavior of airbreathing combustion systems. AFOSR contractors and grantees are encouraged to interact with AFWL personnel.

The purpose of this abstract has been to communicate AFOSR perceptions of research trends to the research community. However, communication from that community back to AFOSR also is desirable and essential for creating new research opportunities. Therefore, all proposals and inquiries for fundamental research are encouraged even if the content is inconsistent with areas of emphasis described herein. Comments and criticisms of current AFOSR programs are also welcome.

Air Force Basic Research
Aerospace Sciences

Airbreathing Combustion — $5360 K

Science Area	Trend	Decrease	Increase	FY 85 $K
Turbulent Mixing	↘	Uniform Density	Simulations Variable Density	360
Turbulent Combustion	↗	Time-Averaged Models, Stable Flames	Simulations, Flame Limits, Ignition	1985
Soot	→	Global Behavior, Laboratory Flames	Fluid Transport Effects, Turbulent Flames, Radiation, Pressure	1018
Sprays and Slurries	↗	Dilute Sprays, Time-Averaged Models	Dense Sprays, Drop Interactions, Simulations, Atomization	1244
Combustion Instability	→	Combustor Experiments and Models	Flame/Flow Interactions, Active Control	495
Combustion Enhancement	→	Catalytic Combustion	UV and IR Techniques Pulsed Combustion	162
Supersonic Combustion	↗	Combustor Development	Flame Holding, Flame Structure	96
Combustion Chemistry	↗		Sensitivity Theory, Metal Combustion	—

TURBULENCE-COMBUSTION INTERACTIONS — THEORY AND EXPERIMENTS

(AFOSR Grant No. 83-0373)

Principal Investigator: Tau-Yi Toong

Massachusetts Institute of Technology
Cambridge, Massachusetts 02139

SUMMARY/OVERVIEW:

Despite recent important advance in the study of turbulent combustion, physical understanding of turbulence-combustion interactions is still obscure. The main objective of this research is to determine and elucidate the mechanisms governing these interactions in different spectral regimes. Both theoretical and experimental investigations are conducted. It is hopeful that this coordinated study will help to advance our understanding of the physics of turbulence-combustion interactions and to provide sound guidelines for improving combustion efficiency and reducing emissions.

TECHNICAL DISCUSSION

Examination of the thermal structure of premixed, rod-stabilized, lean methane-air V-flames has shown possible role of chemical kinetics in augmenting the temperature fluctuations. In order to shed light on this mechanism, both theoretical and experimental studies are conducted. The theoretical study shows the importance of a "wrinkling-like" effect as well as the effect of the chemical reaction rate while the experimental study shows the effect of adding various amounts of ethane to methane-air mixtures at the same overall equivalence ratio.

(1) Theory

In order to understand the origin, nature and governing mechanisms in turbulence-combustion interactions, the stability of a chemically reacting shear layer with streamwise-velocity, concentration and temperature gradients in the transverse direction under the influence of a longitudinal (or streamwise) pressure disturbance is examined. In this two-dimensional model (cf. Fig. 1), it is expected that the interactions between the pressure and density or entropy fluctuations would lead to the generation of vorticity, which is one of the three basic modes of fluctuations in turbulence.

The governing equations show clearly the following:

(a) The propagation of the pressure disturbance is affected by the presence of the mean transverse streamwise-velocity and temperature gradients as well as the fluctuations in the chemical reaction rate.

(b) The streamwise-velocity fluctuations are affected mainly by the mean transverse velocity gradient while the temperature fluctuations are affected mainly by the mean transverse temperature gradient and the fluctuations in the reaction rate. The effects of pressure fluctuations are comparatively small for low Mach numbers and for relatively long wavelength of the pressure disturbance with respect to the shear-layer thickness.

(c) The concentration fluctuations are affected by the mean transverse concentration gradient and the fluctuations in the reaction rate.

(d) The transverse velocity fluctuations are induced by non-uniform distribution of the pressure fluctuations in the transverse direction.

(e) In conjunction with the mean transverse streamwise-velocity, concentration and temperature gradients, the transverse velocity fluctuations induce fluctuations in the streamwise-velocity, concentration and temperature, respectively, through a "wrinkling-like" effect.

(f) In addition to the "wrinkling-like" effect, there is the direct rate-augmentation effect on the concentration and temperature fluctuations due to chemical reaction.

(g) The direct chemical effects depend on the activation energy, order and enthalpy of reaction as well as the Damköhler's first and third parameters.

Numerical solutions of the governing equations for the case of small shear-layer thickness relative to the wavelength of the pressure disturbance show that the flow is always unstable, leading to amplification of all fluctuations. The case of a non-reacting shear layer with no transverse temperature gradient is found to be the most unstable. In the presence of the transverse temperature gradient, with or without chemical reaction, the flow becomes less unstable. Nevertheless, the flow is more unstable with chemical reaction, with increasing amplification rate for higher activation energy and faster chemical reaction rate. Also, with increasing wave number or decreasing wavelength of the pressure disturbance, the amplification rate per second increases while the amplification rate per cycle decreases.

Figure 2a shows a comparison of the complex eigen-functions for the temperature fluctuations $\hat{T}/\pi_o$ in the phase plane at different positions within the shear layer with and without chemical reaction. For case 2, with no chemical reaction, $\hat{T}/\pi_o$ remains in the first quadrant with rather small change in the phase angles at different positions. On the other hand, for case 4 with chemical reaction, the phase angles change rather drastically within the shear layer from $\eta = 0.01$ (near the unreacted region) to $\eta = 0.98$ (near the completely reacted region). Thus, the main effect of chemical reaction is to cause large changes in the phase angles, thus leading to rather complex coupling between different fluctuations.

Figure 2b shows a comparison of the normalized cross-correlation of the temperature and the transverse-velocity fluctuations within the shear layer with and without chemical reaction. For non-reacting flows (case 2), the correlation remains negative, thus indicating that the turbulent energy transport may be related to the mean transverse temperature gradient on the basis of a "eddy-diffusivity" model. On the other hand, with chemical reaction (case 4), the correlation is positive in that part of the shear layer nearer the unreacted region, thus indicating the inappropriateness of the gradient model.

(2) Experiments

Errors due to the use of frequency-compensated fine-wire thermocouples have been analyzed and found to lead to a possible 10 to 15% attenuation of the signals over the frequency range of interest (of less than 1000 Hz). Reasonably good agreement is also observed between our temperature meansurements and the density measurements by Rayleigh scattering reported in the literature for comparable experiments, thus lending further support to the validity of our measurements.

Earlier results on the effects of the equivalence ratio and turbulence scale and intensity showed possible coupling between chemical kinetics and turbulence in the augmentation of the higher-frequency temperature fluctuations. Such coupling is also indicated in the theoretical investigation summarized above. In order to further elucidate the role of chemical kinetics, experiments are conducted to examine the effects of adding various amounts of ethane to methane-air mixtures. Figure 3 shows a comparison of the RMS temperature fluctuations within the high-frequency region at different "instantaneous" mean temperatures (pertaining to a time interval of 25 ms) for different compositions of methane-ethane-air mixtures. Again, it is noted that the presence of a 10-mesh turbulence grid leads to larger RMS values than those for quasi-laminar flames (without grid-generated turbulence). The effect of ethane addition, however, is not monotonic. For both quasi-laminar and turbulent flames, the RMS values are the highest for 10%-ethane addition and become lower for 12 and 100% ethane.

Similar differences are observed in the spectral density distributions and the probability density functions for different compositions of methane-ethane-air mixtures. Possible coupling between chemical kinetics and turbulence is again suggested.

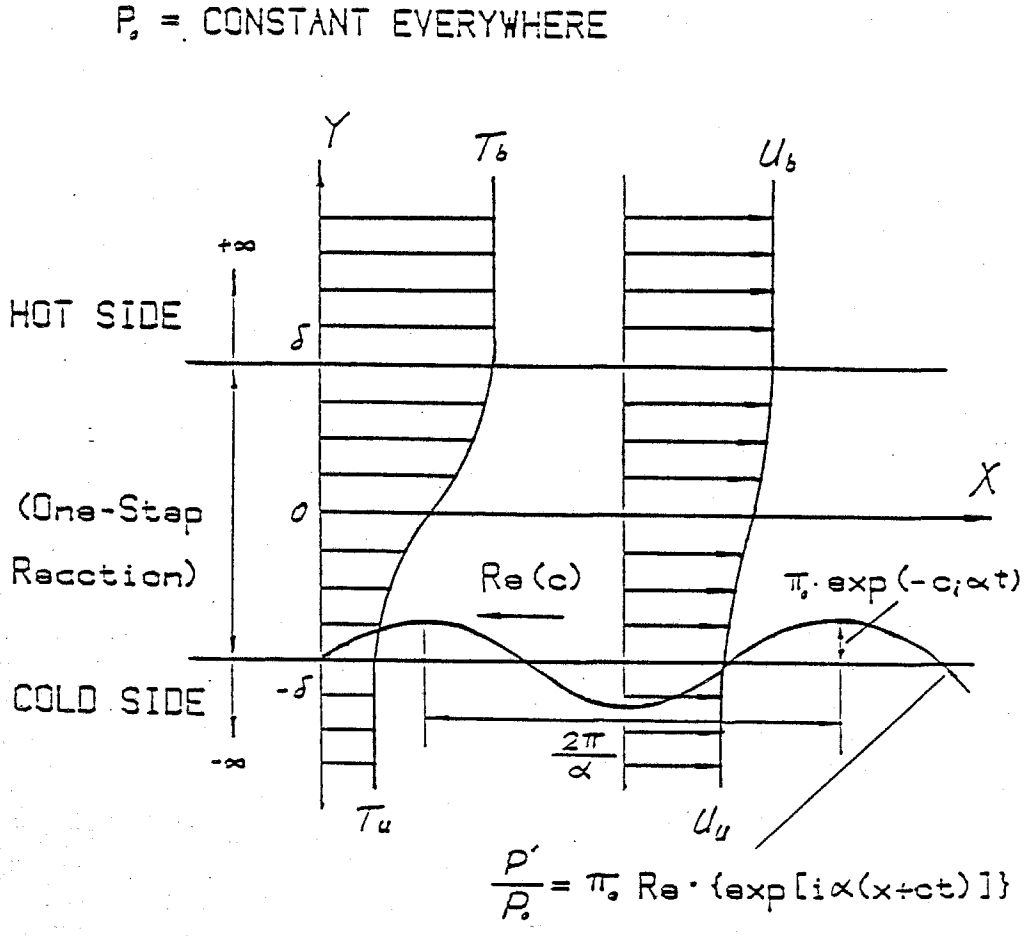

Figure 1 Model

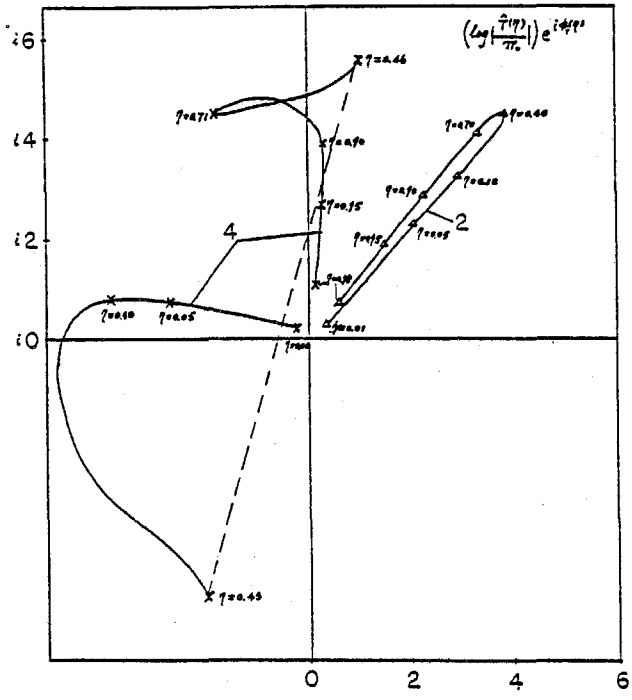

Figure 2a Comparison of temperature fluctuations in the phase plane at different positions within the shear layer. Case 2: no chemical reaction. Case 4: with reaction. Amplitudes in logarithmic scale.

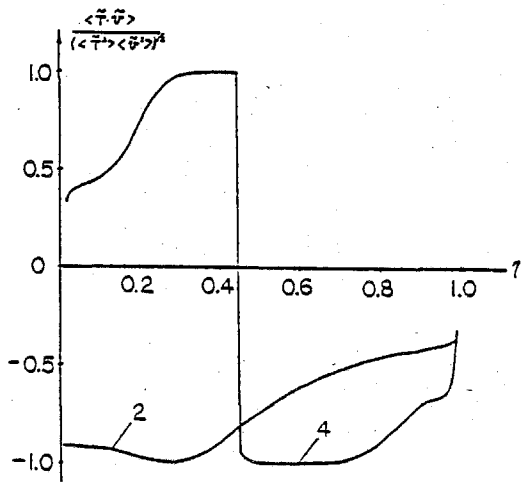

Figure 2b Comparison of normalized cross-correlation of temperature and transverse-velocity fluctuations. Case 2: no chemical reaction. Case 4: with reaction.

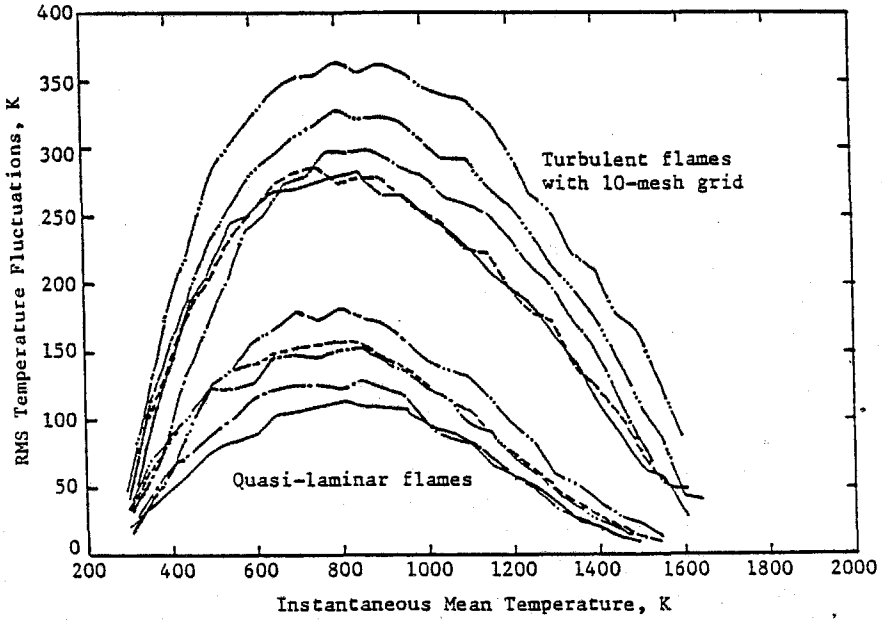

Figure 3 Comparison of RMS temperature fluctuations within high-frequency region at different "instantaneous" mean temperatures for different compositions of methane-ethane-air mixtures: —— 0% ethane, — • — 5% ethane, — •• — 10% ethane, — ••• — 12% ethane, ---- 100% ethane. Top curves, with 10-mesh turbulence grid, bottom curves, no turbulence grid; equivalence ratio, 0.75; mean mixture velocity, 2.4 m/s; 35 mm downstream of 2.1 mm-diameter flameholder.

List of Attendees

Alfano, Angelo	Rockwell International Science Center
Andersen, Blaine	Garrett
Ball, Irven	Garrett
Baughcum, Steven L.	Los Alamos National Laboratory
Baum, Howard R.	National Bureau of Standards
Bellan, Josette	Jet Propulsion Laboratory
Bonczyk, Paul A.	United Technologies Research Center
Bowman, Craig T.	Stanford University
Broadwell, James E.	California Institute of Technology
Butler, T. Daniel	Los Alamos National Laboratory
Calcote, H. F.	Aero Chem Research Laboratories, Inc.
Cantwell, Brian	Stanford University
Cheen, Kang	Northrop
Cheng, R. K.	University of California, Berkeley
Cheng, Wai	Aerodyne Research, Inc.
Colket III, Meredith B.	United Technologies Research Center
Correa, S. M.	G.E. Corp. Research & Development
Culick, Fred E. C.	California Institute of Technology
Daily, John W.	University of California, Berkeley
Dibble, Robert W.	Sandia National Laboratories
Dimotakis, Paul E.	California Institute of Technology
Dobbs, Gregory M.	United Technologies Research Center
Donaldson, Coleman duP.	Aero. Res. Assoc. of Princeton, Inc.
Drake, Michael	G.E. Corp. Research & Development

Edelman, Ray B.	Science Applications Int'l. Corp.
Ghoniem, Ahmed F.	Massachusetts Institute of Technology
Givi, Peyman	Flow Industries, Inc.
Hansen, Elmer C.	University of Florida
Hanson, Ronald K.	Stanford University
Harsha, P. Tom	Lockheed Advanced Aeronautics Co.
Hertzberg, J.	University of California, Berkeley
Hubele, Norm	Garrett
Johnston, Sheridan C.	Sandia National Laboratories
Jou, Wen-Huei	Flow Industries, Inc.
Karagozian, Ann	University of California, Los Angeles
Kelly, John	Acurex Corp.
Kerch, Paul	Air Force Engineering & Services Center
Kertamus, N. J.	Southern California Edison
Kezerle, James A.	Gas Research Institute
King, Galen B.	Purdue University
Kliegel, James R.	TRW Inc.
Koochesfahani, Manooch	California Institute of Technology
Krier, Herman	University of Illinois
Krueger, Eric	Naval Air Propulsion Center
Lang, Daniel B.	California Institute of Technology
Lavid, Moshe	M L Energia, Inc.
Law, Chung K.	University of California, Davis
Lear, William E.	University of Florida
Lefebvre, Arthur H.	Purdue University
Libby, Paul A.	University of California, San Diego

Lick, Wilbert	University of California, Santa Barbara
Liepmann, Hans W.	California Institute of Technology
Malmuth, N. D.	Rockwell Science Center
Manuccia, Tom	Naval Research Laboratory
Marble, Frank E.	California Institute of Technology
McMichael, James M.	AFOSR
Miake-Lye, Richard C.	California Institute of Technology
Mongia, Hukam C.	General Motors Corporation
Mularz, Edward J.	NASA Lewis Research Center
Mungal, M. Godfrey	California Institute of Technology
Namazian, Mehdi	Acurex Corp.
Oldenborg, Richard C.	Los Alamos National Laboratory
Oran, Elaine S.	Naval Research Laboratory
Peters, Jim E.	University of Illinois
Pitts, William M.	National Bureau of Standards
Pope, Stephen B.	Cornell University
Pritt, C.	Rockwell Science Center
Ray, Steven R.	National Bureau of Standards
Rehm, Ronald G.	National Bureau of Standards
Roquemore, W. M.	Aero Propulsion Lab, US Air Force
Roshko, Anatol	California Institute of Technology
Rosner, Daniel E.	Yale University
Salkind, Michael	AFOSR
Santavicca, Domenic A.	Pennsylvania State University
Santoro, Robert J.	National Bureau of Standards
Shepherd, I. G.	University of California, Berkeley
Shih, Tom I. P.	University of Florida

Lick, Wilbert	University of California, Santa Barbara
Liepmann, Hans W.	California Institute of Technology
Malmuth, N. D.	Rockwell Science Center
Manuccia, Tom	Naval Research Laboratory
Marble, Frank E.	California Institute of Technology
McMichael, James M.	AFOSR
Miake-Lye, Richard C.	California Institute of Technology
Mongia, Hukam C.	General Motors Corporation
Mularz, Edward J.	NASA Lewis Research Center
Mungal, M. Godfrey	California Institute of Technology
Namazian, Mehdi	Acurex Corp.
Oldenborg, Richard C.	Los Alamos National Laboratory
Oran, Elaine S.	Naval Research Laboratory
Peters, Jim E.	University of Illinois
Pitts, William M.	National Bureau of Standards
Pope, Stephen B.	Cornell University
Pritt, C.	Rockwell Science Center
Ray, Steven R.	National Bureau of Standards
Rehm, Ronald G.	National Bureau of Standards
Roquemore, W. M.	Aero Propulsion Lab, US Air Force
Roshko, Anatol	California Institute of Technology
Rosner, Daniel E.	Yale University
Salkind, Michael	AFOSR
Santavicca, Domenic A.	Pennsylvania State University
Santoro, Robert J.	National Bureau of Standards
Shepherd, I. G.	University of California, Berkeley
Shih, Tom I. P.	University of Florida

Sirignano, William A.	University of California, Irvine
Sojka, Paul E.	Purdue University
Sokolowski, Daniel E.	NASA Lewis Research Center
Stanton, Alan C.	Aerodyne Research, Inc.
Strahle, Warren C.	Georgia Institute of Technology
Stutrud, Jeffrey S.	Aero Propulsion Lab, US Air Force
Sullins, Gary A.	Johns Hopkins University
Talbot, Larry	University of California, Berkeley
Tishkoff, Julian M.	AFOSR
Toong, T-Y.	Massachusetts Institute of Technology
Vranos, Alexander	United Technologies Research Center
Whitehead, R. E.	ONR
Williams, F. A.	Princeton University
Wilson, Leroy	AFWL/ARDC
Zidzik, James	Naval Air Propulsion Center
Zukoski, Edward E.	California Institute of Technology